NTNU – Trondheim
Norwegian University of
Science and Technology

Lithology detetection in real time

Jorge Garcia-Delgado

Earth Sciences and Petroleum Engineering
Submission date: February 2013
Supervisor: Pål Skalle, IPT

Norwegian University of Science and Technology
Department of Petroleum Engineering and Applied Geophysics

NTNU
Norwegian University of
Science and Technology

Lithology determination in real time

Master's Thesis

Department of Petroleum Engineering & Applied Geophysics
Student: Jorge García Delgado
Supervisor: Pål Skalle

i. Acknowledgement

To Pål Skalle, my thesis supervisor, for his guidance and patience in many difficulties which I faced; to Justko for invaluable help with my poor English; and to my parents for their support, without which nothing would be possible

Thank you!

ii. Abstract

The works published until today about lithological interpretation in drilling, use the ROP, rate of penetration, as the base for the diagnosis. These analyses are poorly detailed and often limited to distinction between hard and soft layers. This thesis establishes a direct relationship between lithology and drillability, using well data from Gullfaks 34/10 C-47. This relationship provides the basis for standardization of the parameter.

The model was made from the equation relating the ROP to WOB, weight on bit; RPM, revolutions per minute; and K, drillability at each point. The values for each drilling point were obtained from C-47 data and after being treated, they generated the graph which enabled numerical association between K and lithology.

The main difficulty which was presented was the standardization of K. The formula for the model does not account for the size and type of bit causing different values of the ratio K-lithology in each of the sections; additionally, in overpressured areas K values are unreliable. However, it is possible to establish a relationship between the K values from the different sections allowing the estimation of the theoretical value of K for a lithology which is not present in a section.

The parameter K enables better lithological interpretation than simply using ROP. The use of this new parameter only requires a software implementation in existing equipment, so it does not require a large investment in time and money for its operationalization. The next step for widespread application is the refinement in obtaining the parameter by using other factors which influence it.

Resumen

Los trabajos que hasta hoy existen sobre interpretación litológica en sondeos usan el ROP, velocidad de penetración como base interpretativa. Estos análisis están escasamente detallados y en ocasiones se limitan a distinguir entre capas duras y blandas. En la presente tesis se establece una relación directa entre la litología y su perforabilidad usando los datos del pozo Gullfaks 34/10 C-47. De esta manera se sienta la base para la estandarización del parámetro.

El modelo se realizó a partir la ecuación que relaciona el ROP con el WOB, peso en martillo; las RPM, revoluciones por minuto; y la K, drillability para cada punto. Los valores para cada punto de la perforación fueron obtenidos a partir de los datos de C-47 y después de ser tratados, generaron un grafico que facilitó la asociación numérica entre K y la litología.

El mayor problema que se presentó fue la estandarización de K. La fórmula del modelo no tiene en cuenta la talla y tipo de martillo provocando que los valores de la relación K – litología sean distintos en cada una de las secciones. Además en las zonas de sobrepresión los valores de K no son fiables. Sin embargo, es posible establecer una relación entre los valores de K de las distintas

secciones permitiendo la estimación del valor teórico de K para una litología que no está presente en una sección.

El parámetro K permite una mejor interpretación litológica que el simple uso del ROP. La utilización de este nuevo parámetro solo requiere una implementación informática a los equipos actúales, por lo que no se necesita una gran inversión en tiempo y dinero para su puesta en práctica. El siguiente paso para generalizar su aplicación es el refinamiento en la obtención del parámetro mediante el uso del resto de factores que lo influyen.

iii. Content

1. Introduction.

In recent decades the demand for underground resources such as industrial and energy minerals, hydrologic and ground-source energy has increased considerably. Drilling is a necessary requirement for extraction of some of these resources. But like any tool, the drill, as engineering process has a number of issues which are not well discussed and the more information should be provided. Thus drilling has become an important source of information in this work field. Slow drilling, damaged bit, stuck pipe, lost circulation or the need to clean the wellbore are some of them. The project will define and evaluate the formation lithology for the detection of these possible trouble spots; looking for significant savings in both time and money. The selected issues for present thesis is the concepts of slow drilling, formation, hardness and lithology boundaries. These concepts are related, in the context of drilling, to the challenges mentioned above. Improvement of these issues, eventually lead to the reduction of costs of non-productive time and repair time.

The main aim of this thesis is to establish a relationship between hardness and lithology, focusing on the understanding of how different materials have different answers when they are traversed in a drilling. In order to reach the goal, the study will seek to build up necessary knowledge and stepwise treat, and analyze such geological knowledge in an engineering approach.

The first step will be acquiring relevant previous knowledge on all the issues stated above, sort it methodically and in a meaningful manner. Study how hardness is related to Lithology, Mineralogy, Diagenesis, Compaction, will be the second step. Finishing with modelling hardness based on drilling parameters. This study will be based on different textbooks and published papers, as well as on log analysis of drilling parameters. Initial empirical knowledge is expressed through this equation:

$$\mathrm{ROP} = \mathrm{K} \cdot \mathrm{WOB} \cdot \mathrm{RPM}^{\mathrm{C}}$$

This project will join concepts from different fields related to engineering drilling and geological knowledge, seeking an explanation for hardness through geological causes such as mineral composition and formation of the layers. These causes combined with concepts such as bit type and drillability establish how apparently similar materials from the technical point of view may have different origins and therefore different behaviours during drilling.

2. Previous knowledge with respect to lithology and its detectability during drilling.

Herein shall is presented to bring both engineers and geologists to a common point where the development of the model and discussion can be understood. Using a holistic approach on the basis of the two disciplines and emphasizing those points are especially relevant to this work.

This chapter introduces the preliminary concepts concerning the real-time lithology determination. Three different perspectives: engineering, geological and petroleum are described following the order from general to specific concepts. Firstly, review of the processes which are involved in the drilling engineering; secondly, the process which sediment go through from its deposition until its transformation into rock; and finally, a brief reference to the Petroleum Geology and the Gullfaks field.

2.1. Engineering approach

Drilling is the action of placing a hole to a depth and location (King 2010). This section presents the initial situation and the mechanical properties of the rock which is perforated, the problems related to lithology during drilling, and the parameters measured.

2.1.1. Rock situation

Rocks are a naturally composed aggregate of minerals. The properties of rocks depend upon the amount of different minerals in their composition; e.g. quartz is very hard and glass-like mineral while mica is flaky and flexible. Size, shape and orientation have considerable influence. Rocks have geological names related to their origin and composition. They do not necessary reflect the strength or material properties interesting to engineers; e.g. a sandstone could be anything from very porous and friable to strong and non-porous material. The properties of in-situ rock mass are governed by the joints and discontinuities as well as weakness zones and faults (Nilsen and Thidemann 1993).

2.1.1.1. Porosity

The reservoir rocks as sandstones were originally individual particles of sand of different sizes which were buried and compacted during deposition. Some spaces remain between the grains enabling storage. This capacity is the porosity, Φ; and resulting from the expression pore volume (void space) divided by total volume (bulk volume). This is being calculated as a percentage. (Dandekar 2006)

$$\emptyset_T = \frac{pore\ volume}{total\ or\ bulk\ \ volume} \quad (1)$$

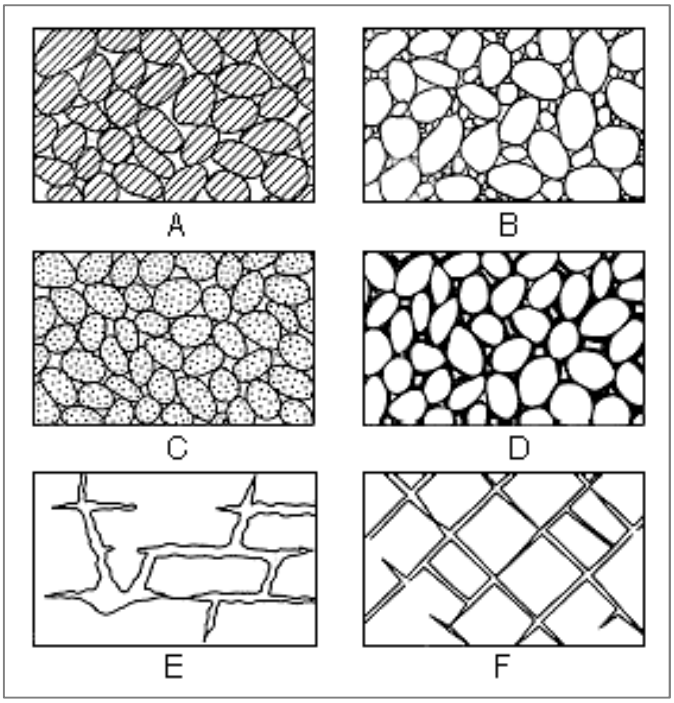

Figure 2-1: Several types of rock intensities and the relation between rock texture and porosity. A, Well-sorted sedimentary deposit having high porosity; B, poorly sorted sedimentary deposit having low porosity; C, Well-sorted sedimentary deposit consisting of pebbles that are porous themselves, so that the deposit as a whole has a very high porosity; D, well-sorted sedimentary deposit whose porosity has been diminished by the deposition of mineral matter in the interstices; E, rock rendered porous by solution; F, rock rendered porous by fracturing. (From Meinzer, 1923a)(Pawnee and Edwards Geology and Groundwater 2004)

There are three general types of pores interconnected, deadend, and isolated pores. The presence of one or other establishes the kind of porosity. The effective porosity is defined as ratio of volume of interconnected and deadend pores to the total or bulk volume. The ineffective porosity is defined as ratio of the volume isolate or completely disconnected pores to the total or bulk volume (Dandekar 2006). (Dandekar 2006)

$$\emptyset_{ef} = \frac{interconnected\ and\ deadend\ pores\ volume}{total\ or\ bulk\ volume} \quad (2)$$

$$\emptyset_{nef} = \frac{completely\ diconnected\ pore\ volume}{total\ or\ bulk\ \ volume} \quad (3)$$

Porosity presented in a rock can be primary, if kept from its deposition; or secondary if is a consequence of diagenetic processes.

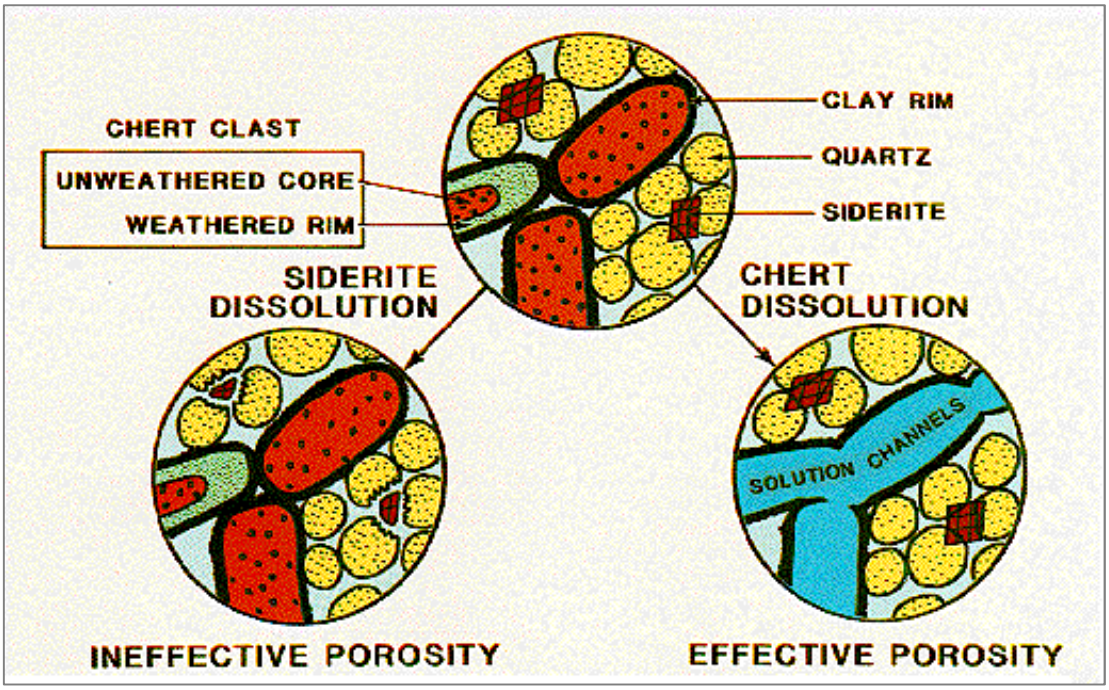

Figure 2-2: Hypothetical model of secondary porosity showing development of effective porosity (solution channels) from chert dissolution (bottom right) and ineffective porosity from siderite dissolution (bottom lef) (Shanmugam and Higgins 1988)

2.1.1.2. Permeability

Porosity is necessary but not sufficient condition so that rock would be considered reservoir. Permeability, *k*, is an intrinsic property of the reservoir which refers to how pore spaces are interconnected. Henry Darcy developed the mathematical expression known as Darcy's law, which is used for the calculation of this property.

$$Q = KA\frac{(h_1 - h_2)}{L} \quad (4)$$

Q is the volumetric flow or the amount of fluid which flows out of a given reservoir section, *A*, over a set amount of time. *K*, hydraulic conductivity, is a property of every material which indicates the speed any liquid moves through it. *K* is directly related to the porosity and permeability of the reservoir and the density of the fluid in question. $(h_1\text{-}h_2)/L$ is the hydraulic gradient representing the difference in fluid level between the two points of measurement (h_1,h_2) divided by the distance between them (*L*). Usually it is represented with the letter *i*.

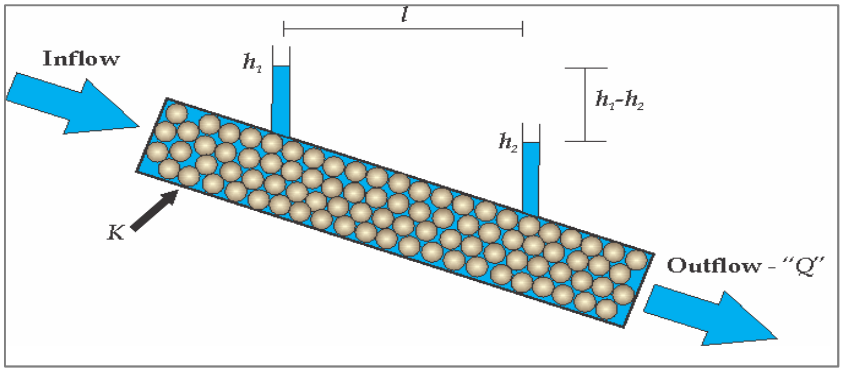

Figure 2-3: Graphical representation of Darcy's Law in a hypothetical porous medium with two points of measurement (h1 and h2) and a hydraulic conductivity of K. (Herod 2011)

K can also be expressed as k/μ where *k* is a permeability of the porous medium and μ la viscosity of a given fluid; and *i* in terms of pressure gradient as d*P* over d*L* allowing to write (4 in generalized expression as

$$Q = \frac{k}{\mu} A \frac{dP}{dL} \tag{5}$$

Permeability unit is darcy; a porous medium is said to have a permeability of one darcy when: a single phase fluid with a viscosity of one centipoise (cP) completely saturates the porous medium which flows through it at rate of 1cm^3/s under a viscous flow regime and a pressure gradient of 1 atm/s; through a cross-sectional area of 1 cm^2 (Dandekar 2006).

No direct relation exists between porosity and permeability because permeability depends on continuity of pore space whereas porosity means the availability of pore space. A reservoir rock must have a nonzero porosity to have nonzero permeability, however, it possible to have very high porosity without having any permeability.(Dandekar 2006).

2.1.1.3 Pressures

Three kinds of pressures are involved in drilling operations. The first is the hydrostatic pressure exerted by the weight of a static column of fluid as a function of height of the column and fluid density. Fluid column height is the distance between the measured point and the projection of the well onto the perpendicular for this point, the True Vertical Depth (Mouchet and Mitchell 1989).

$$P_h = \rho \cdot g \cdot h = 9{,}81 \cdot \rho \cdot h \tag{6}$$

In (6) P_h is the hydrostatic pressure (*Pa*); ρ is the average fluid density; g is the gravity acceleration; and h is vertical height of the column. The formula used in the practice is the following:

$$P_h = d \times \frac{h}{10}$$

(7)

Where P_h is the hydrostatic pressure $(kg \cdot cm^{-2})$; d is the average fluid density $(g \cdot cm^{-3})$; h is the vertical height of fluid column (*m*); and the coefficient 10 considers metric oilfield unit and gravity acceleration (Mouchet and Mitchell 1989).

The second pressure involved is overburden pressure at a given depth which is exerted by the weight of overlaying sediment. This is not a fluid pressure, so one can refer to it using the term overburden stress and it is expressed as

$$S = \rho_b \times \frac{Z}{10}$$

(8)

In this equation S is overburden stress $(kg \cdot cm^{-2})$; ρ_b is the formation average bulk density $(g \cdot cm^{-3})$; and Z is vertical thickness of overlying sediment (*m*). The bulk density of a sediment can be expressed as:

$$\rho_b = \emptyset \rho_f + (1 - \emptyset)\rho_m$$

(9)

Where Φ is the porosity (from 0 to 1); ρ_f is the formation fluid density $(g \cdot cm^{-3})$; and ρ_m is matrix density $(g \cdot cm^{-3})$ (Mouchet and Mitchell 1989).

Sediment porosity decreases with the compaction which is produced by burial and it is proportional to increase of overburden pressure.

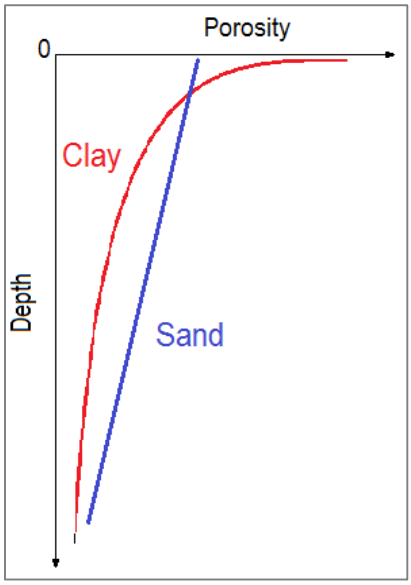

Figure 2-4: Diagram of porosity vs. depth relation for sand and clay. Clays reduction depends on weight of the sediment following a exponential function. Sands and carbonates reduction is a function of other parameter such as diagenesis, sorting or original composition; therefore a decrease in porosity is accompanied by increase in a bulk density. Modified form (Mouchet and Mitchell 1989)

The last type of pressure is the formation pressure which is due to the fluid contained in the pore space of sediments or rocks; it is also called pore pressure (P_p). If $P_p<P_h$ then there is a negative pressure anomaly or subnormal pressure; If $P_p>P_h$ then there is a positive pressure anomaly or overpressure; and If $P_p=P_h$ then there is a normal hydrostatic pressure which is a function of pore fluid density (Mouchet and Mitchell 1989).

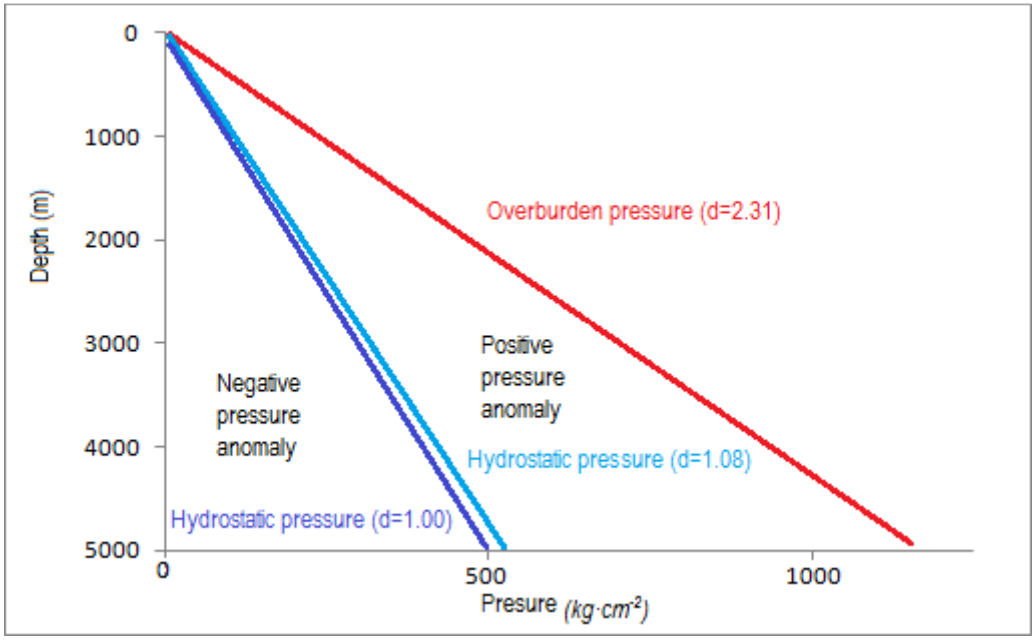

Figure 2-5: Pressure categories in a pressure vs. depth plot. In blue is shown the hydrostatic pressure in the range of average densities used for sedimentary basins (1.00-1.08). Pressures lower than P_h are a negative anomaly while higher

represents a positive anomaly. Red line shows the average bulk density at depth (2.31). Modified form (Mouchet and Mitchell 1989)

The reservoir outcropping at a lower altitude than the elevation at which it was penetrated during drilling is a common cause of negatives anomalies; higher altitude causes the positive anomaly. When impermeable rocks such as shales are formed and sediments are compacted, their pore fluids cannot always escape and must then support the total overlying rock column, leading to anomalously high formation pressures. Because reservoir pressure changes as fluids are produced from a reservoir, the pressure should be described as measured at a specific time, such as initial reservoir pressure (Gillis 2013).

2.1.1.4. Capillarity pressure

Capillary force arises due to the attraction between fluids and solids. In a very small passage (capillary), these attractive forces can cause the fluids to move along the passageway (Devereux 1999).In porous media, capillary pressure is the force which is necessary to squeeze a hydrocarbon droplet through a pore throat (works against the interfacial tension between oil and water phases) and it is higher for smaller pore diameter. The expression for the capillary pressure is the following

$$p_c = p_{\text{non\_wetting phase}} - p_{\text{wetting phase}} \tag{10}$$

In oil-water systems, water is typically the wetting phase, while for gas-oil systems; oil is typically the wetting phase. The quantities p_c, $p_{non\text{-}wetting\ phase}$ and $p_{wetting\ phase}$ are obtained by averaging these quantities within the pore space of porous media either statistically or using the volume averaging method (Bear 1972).

2.1.1.5. Mechanical properties of rock and rock masses

Reservoirs are dynamic systems in constant change during the production of reservoirs fluids. The reduction in the reservoir pore pressure causes an increment in net effective stress. The state of stress acting on a rock influences petrophysical properties mentioned above. The determination of mechanical properties of a reservoir rock, rocks mechanic, includes the study of strength of rocks (Dandekar 2006).

Stress (σ) refers to force applied to a rock (F) in an area (A) which tends to change its dimensions. This external force is normally referred as load. Usually stresses are in a range of megapascals.

$$\sigma = \frac{F}{A} \tag{11}$$

Three different stress conditions depend on how the implicated forces interact are identified: tensile stress where forces are in the same plane tending to pull apart the material; compressive stress where the forces are in the same plane tending to press the material; and shear stress where the forces are in two different planes in opposite directions.

Strain (ε) is the product of application of the stress generating a relative change in shape or size of a rock; i.e. strain is the measure of deformation when a load is applied. The axial strain is defined as the ratio of the increment of length (L) from the original length (L_0), to the original length (L_0)

$$\varepsilon = \frac{L - L_0}{L_0} \tag{12}$$

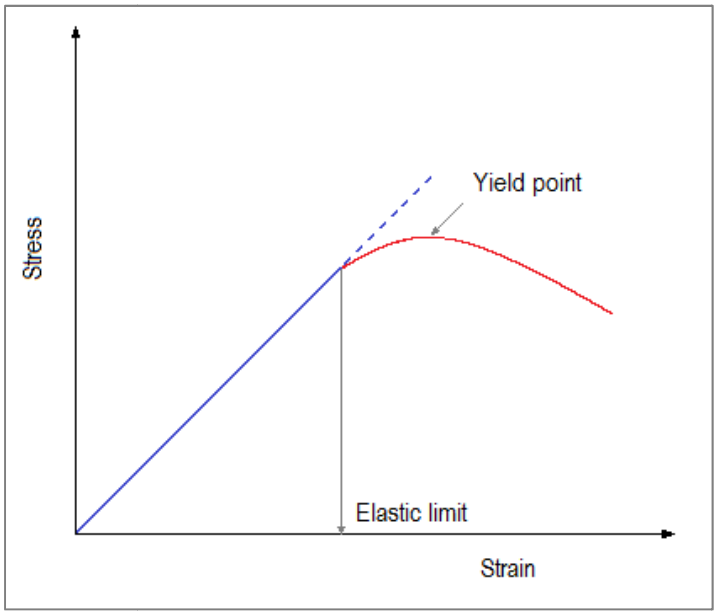

Figure 2-6: Stress-strain relationship. Blue line shows the elastic deformation suffering by a material with the increase of stress. Exceeded the elastic limit (red line) the deformation turns plastic.

In an elastic deformation, stress is proportional to strain, when an amount of stress is applied for a time the strain is incremented; if this is removed the strain comes back to zero. The plastic deformation is marked by the elastic limit from which removing the stress does not lead to strain going to zero. After the yield point, the stress increases again with increasing strain.

The factors which influence the relation stress-strain depending on mineralogy and fluid contained in rocks include: Confining pressure, temperature, time, ratio fluid-pore space, anisotropy, porosity, permeability, degree of cementation and cementing material. The study of these factors is done in the laboratory through recreations of in situ conditions (Dandekar 2006).

The strength of a material is its ability to resist the stress without yielding or to resist deformation. This is specified as tensile strength, compressive strength or shear strength depending on the type of stress acting. Compressive stress is crucial to understanding well-bore stability during drilling. Its determination is performed using laboratory test such as uniaxial or triaxial compressive strength tests which conclude the ultimate strength i.e. the maximum value of stress attained before failure.(Dandekar 2006)

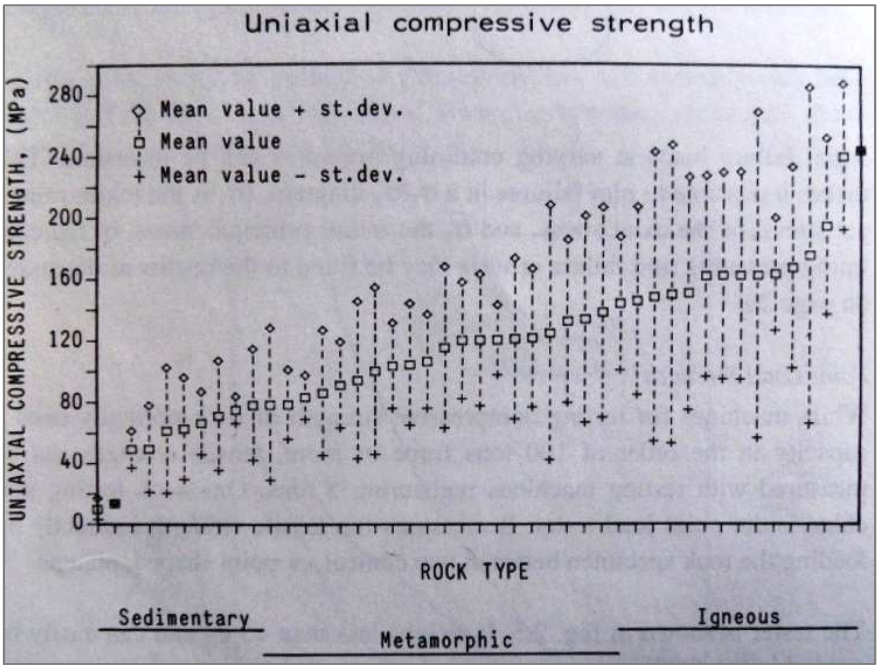

Figure 2-7: Summary of results from UCS rock testing made at Norwegian Institute of Technology as a function of the rock type. (Hannsen 1998)

2.1.2. Drilling problems related to lithology

The most common downhole problems are lost circulation and stuck pipe. When these problems occur; it is necessary to know which causes are in order to establish an efficient strategy to solve it.

2.1.2.1. Lost circulation

The loss of drilling fluid to a formation is usually caused when the hydrostatic head pressure of the column of drilling fluid exceeds the formation pressure. This loss of fluid may be loosely classified as seepage losses, usually caused by permeable formations; partial losses, caused by high permeable formations, an ineffective filter cake or non-sealing faults; serious losses, caused by non-sealing fracture systems; and total losses with non-return in surface, caused by non-sealing fracture systems or formations that contain large cavern (vugs). Those are handled differently depending on the risk to the rig and personnel and the economics of the drilling fluid and each possible solution (Singer 2013). The drilling fluid overbalances the formation and a path that allows the mud to flow into the formation away from the wellhole are the necessary conditions for losses to occur.

Losses in the surface have two common causes, very permeable formations (e.g. unconsolidated sands) which allow mud seep through the pore space; and fractures, where severe or total losses may occur. Losses into the permeable formations may be cured adding lost circulation material such as clay, sawdust, mica etc.; and in fractures pumping cement into the well.

Losses in normally pressured deeper formations may be caused by unconsolidated, normally fractured, fracturable by drilling, or high pore size consolidated formations. The loss zone can be anywhere in the open hole, not just in the drilling point. The identification of the loss zone and the mechanism causing is necessary to elaborate a strategy.

Losses in heavily fractured or cavernous formations which are typical in limestone can present abrupt total losses which are a good method to identification. One option can be to drill blind with water or foam far enough to give a reasonable column of cement above the shoe. (Devereux 1999)

2.1.2.2. Stuck pipe

Stuck pipe refers to the varying degrees of inability to move or remove the drillstring from the wellbore. At one extreme, it might be possible to rotate the pipe or lower it back into the wellbore; or it might refer to an inability to move the drillstring vertically in the well, though rotation might be possible. At the other extreme, it reflects the inability to move the drillstring in any manner. Usually, even if the stuck condition starts with the possibility of limited pipe rotation or vertical movement, it will still degrade the inability to move the pipe at all (Singer 2013).

When drilling through a section of soft or unconsolidated rock such as loosely compacted sand or gravel it is possible for the formation to break up and to collapse into the wellbore. This tends to fall a bridge which can gradually or in some circumstances suddenly jam the drill string.

Mobile formations such as flowing shales exist in a plastic condition. When drilled any restraining forces are removed and overburden from the adjacent formation causes the salt to flow or ooze into the wellbore. Continued invasion of this kind can result in contact with the drill string causing it to slowly jam as it is squeezed by the salt. Some clays and coal can also be plastic and will therefore have the same effect.

When drilling formations which are naturally fissile or in the vicinity of the fault zone such as limestones or shales pieces of rock may break off into the wellbore jamming the drill string immediately. These pieces can vary from quite small to very great size.

When drilling through geopressured formations it is possible that the rock may cave into the wellbore. The loose material may pack up as the drill string trips out causing it a jam.

Certain formations such as Gambo shales which contain a large amount of benthonic clay can react with a mud filtrate causing it to swell and subsequently invade the wellbore. Continued

invasion of this kind results in clay balls and mud rings which can build up and eventually make contact with the drill string causing it to jam. The potential risk for stuck pipe is increased as the pipe is tripped out and the bottom hole assembly becomes trapped by the mud rings (Statoil 1992).

2.1.3. Parameter identification

This section introduces the parameters which were measured during the drilling of well 34/10-C-47. Subsection "Other parameters" presents those which are not used in the model described in chapter 3. The use of drilling dynamics data along with downhole drilling parameters, measured and transmitted in real time proves to be effective for identifying drilling dysfunctions (J.Thomson and Mathur 2010).

2.1.3.1 ROP

Rate of Penetration (*ROP*) is the speed at which the drill bit can break the rock under it and thus deepen the wellbore (Ramsey and Associates 2013). This speed is usually reported in units of feet per hour or meters per hour but sometimes it is expressed in minutes per foot or meters. ROP is the most common way to evaluate the drilling efficiency and the characteristic of the formation such as lithology and hardness.

The drilling parameters which affect the ROP are weight on bit (*WOB*), the speed of the bit (*RPM*), the drillstring configuration, the type of bit and its conditions, bottom hole cleaning and hydraulic. (Moore 1986)

The interpretation of a ROP curve is more understandable using a simplified example which can illustrate the different kind of information presented on these logs. The Figure 2-8 is a sample of this.

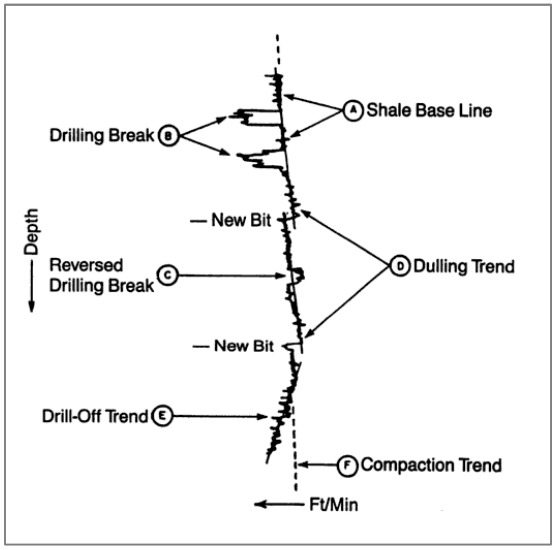

Figure 2-8: Simplification of a ROP curve. The *base line* (A) is the reference point used in the interpretations, usually the hardest lithology through in the drill. In the example formation is used shales and in carbonate sequences is often used limestone.

The deflections imply lithology changes or the result of crossing a fault, and they are noted as an abrupt increase of ROP. This *drilling break* (B) in the example is interpreted as a sand/shale sequences. The reverse drilling break (C) indicated by an abrupt decrease of ROP can imply changes into very dense formations called *caps,* denoted a shale/sand interface, or formations where production has depleted the formation pressure. The decrease in efficiency resulting bit wear out is reflected as changes in the slope of the baseline (D), the *dulling trend* can help to alert when a bit needs to be replaced. A *drill-off trend* (E) is a gradual increase in the ROP which indicates a transition to an increased pore pressure zone. Overburden pressure and diagenesis processes turn formation into more compact. *Compaction trend* (F) can be seen on log over long intervals (Johnson and Pile 2002).

Generally, ROP increases in fast drilling formation such as sandstone (positive drill break) and decreases in slow drilling formations such as shale (reverse break). ROP decreases in shale due to diagenesis and overburden stresses. Overpressured zones can give twice of ROP as expected which is an indicative of a well kick. The Figure 2-9 shows the normal responses of the ROP for different kind of lithologies.

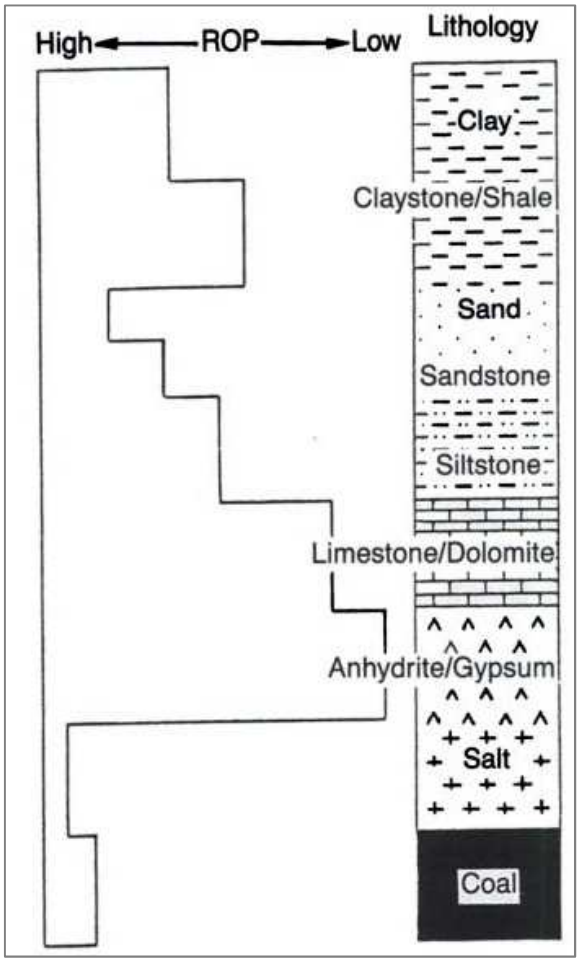

Figure 2-9: ROP response in common rock types

Previous publications in relation to lithology detection using ROP (Provost Jr. 1987)

Normalized Rate of Penetration (NROP) is normalization of the effects that different input drilling parameter has on penetration rate with a drilling equation. The result is a penetration rate plot that is not affected by how the driller changes bit weight, rotary speed, or hydraulic – which

can be significant in control or directional drilling. This formula, from Prentice, is simply the actual drilling parameters multiplied by a filter factor - the normal conditions.

$$NROP = ROP \cdot \frac{Wn - M}{Wo - M} \cdot \left(\frac{Nn}{No}\right)^{r} \cdot \frac{(Pbn \cdot Qn)}{(Pbo \cdot Qo)} \quad (13)$$

$$Pbn = \frac{MWn \cdot Qn^2}{10858 \cdot TFAn^2} \quad (14)$$

$$Pbo = \frac{MWo \cdot Qo^2}{10858 \cdot TFAo^2} \quad (15)$$

WHERE:

- ROP = Observed rate of penetration (ft. /hr.)
- Wn = Normal bit weight (lbs.)
- Wo = Observed bit weight
- M = Formation threshold weight (lbs.)
- Nn - Normal rotary speed (rpm)
- No - Observed rotary speed
- r = Rotary exponent (dimensionless)
- Pbn - Normal bit pressure drop (psi)
- Pbo - Observed pressure drop
- Qn= Normal circulation rate (gpm)
- Qo - Observed circulation rate
- MWn =Normal mud weight (ppg)
- NW = Observed mud weight
- TFAn = Normal bit nozzle area (in^2)
- TFAo - Observed bit nozzle area

"Normal" conditions are arbitrary variables used to drill the base formation (normally shale). They are changed every time the bit size is changed to avoid shifts in the plot. These values are totally arbitrary as long as the percent change NROP is used for lithology and pore pressure predictions.

Lithology Prediction

The NROP plot is very effective for lithology predictions based on the drillability of the formations. It is more sensitive than other penetration rate plots. In send-shale sequences the base formation (shale) should drill significantly slower than sand zones at the same depth. An abrupt change in penetration rate, while drilling the base formation, suggests that sandy formation is being drilled. Formation pressure changes are suggested when the penetration rate forms a continuous trend faster or slower. In continuous depositional basins, the pressure changes will occur in the base formations.

Pore Pressure Prediction

Pore pressure predictions, can also be made with the NROP plot using different methods. A method shown here is by comparison with the conductivity curve. This has worked on walls where of sets have NROP data. Wells using MWD conductivity, and wells with a logging run deep enough into competent shales. Comparison of the NROP to the conductivity curve is made over intervals of the hole where the salinities do not change. Obviously, if the salinities vary so that the conductivity is not an accurate means of predicting pore pressures, this assumption is not valid.

2.1.3.2. WOB

Weight on bit is a quantitative term used to express the amount of weight or force placed by the lowering of the drillstring and collars onto the bit. To cut rock, the drill bits used in these operations are forced against the bottom of the wellbore by the weight of the entire drillstring and, in particular, heavy tube sections known as drill collars. In deep drilling wells and boreholes, the drill bit is lowered to the bottom of the wellbore. There it is forced against the bottom face of the hole by steadily lowering weights onto it as it rotates. I.e. the amount of weight added to the drill bit section of the drillstring is known as WOB

Readings are typically taken from a drillstring weight indicator located on the drill platform, alternately, measurement while drilling (MWD) sensors located downhole just above the bit section can also be used to send more accurate weight-on-bit values to a surface readout interface(Scott 2013).

2.1.3.3. RPMB

Revolution per minute in bit (RPM) is the measure of rotational speed of the bit.

2.1. 3.4. DMEA and DBTM

Measured depth (MD or DMEA) is the depth measured from the depth reference point (defined as being zero) for the well. It is typically the top of the kelly bushing or the level of the drill floor on the rig that is used to drill the well. Even when the drilling rig has been removed, all subsequent measurements and operations in the well are still tied in to the same depth reference. However, for multiwell studies, the depths are normally shifted to the permanent datum. The depth reference and its elevation above the permanent datum are recorded on the log heading. In some contexts, the term may refer to any point from which depth is measured (Singer 2013).Bit Measured Depth (DBTM) is the depth measured from the reference point which the bit is located at.

2.1.3.5. Others parameter

Other parameters attached in the information provided by Statoil which were not used in the model to obtain K.

2.1.3.5.1. HKL

Hook Load (*HKL*) is the total force pulling down on the hook. This total force includes the weight of the drillstring in air, the drill collars and any ancillary equipment, reduced by any force that tends to reduce that weight. Some forces that might reduce the weight include friction along the wellbore wall (especially in deviated wells) and, importantly, buoyant forces on the drillstring caused by its immersion in drilling fluid. If the BOPs are closed, any pressure in the wellbore acting on the cross-sectional area of the drillstring in the BOPs will also exert an upward force (Ramsey and Associates 2013).

2.1.3.5.2. BPOS

Block Position (*BPOS*) is the position which is occupied by the block: A set of pulleys used to gain mechanical advantage in lifting or dragging heavy objects. There are two large blocks on a drilling rig, the crown block and the travelling block. Each has several sheaves that are rigged with steel drilling cable or line such that the travelling block may be raised (or lowered) by reeling in (or out) a spool of drilling line on the drawworks (Ramsey and Associates 2013).

2.1.3.5.3. SPP

Stand pipe pressure (*SPP*) is which is measured in stand pipe: A rigid metal conduit that provides the high-pressure pathway for drilling mud to travel approximately one-third of the way up the derrick, where it connects to a flexible high-pressure hose (kelly hose). Many large rigs are fitted with dual standpipes so that downtime is kept to a minimum if one standpipe requires repair (Ramsey and Associates 2013).

2.1.3.5.4. MFI

Mud Flow In (*MFI*) is the mud flowing into the well. The mud-in sample is taken from the suction pit (the last pit in the flow series) just before the mud goes into the pump and down the wellbore. The in sample is also called the suction-pit sample, or "mud in" on a drilling fluid report. This mud has been treated and properly weighted and is in good condition to encounter downhole pressures, temperatures and contamination. Comparisons are made between properties of this mud-in sample and the "out" or mud-out sample taken at surface prior to solids removal(Singer 2013).

Mud is a term that is generally synonymous with drilling fluid and that encompasses most fluids used in hydrocarbon drilling operations, especially fluids that contain significant amounts of suspended solids, emulsified water or oil. Mud includes all types of water-base, oil-base and synthetic-base drilling fluids. Drill-in, completion and workover fluids are sometimes called muds, although a fluid that is essentially free of solids is not strictly considered mud (Singer 2013).

2.1.3.5.5. TRQ

Torque (*TRQ*) is the amount of turning force which is applied to a shaft or rotary mechanism causing to rotate a bit and cutting a hole.

2.2. Geological approach

Rock types can be classified according to three different categories: first, igneous rocks which originate from direct solidification of magmatic fluid; second, the metamorphic rocks which are a transformation of pre-existing rocks under high pressure and temperature; and finally, sedimentary rocks which are composed of fragments of any type of rock weathered, transported and accumulated in sedimentary basins.

Most of the solid Earth consists of igneous and metamorphic rocks; about 90-95 percent of the outer 16 kilometres of Earth's crust. The 75 percent of all exposure rocks on surface are sedimentary rocks (Tarbuck y Lutgens 1993).

The sediments suffer processes from weathering, erosion and transportation until their deposition in diverse sedimentary environment. Lithification describes how these deposits become rocks. It is convenient to consider temperatures and pressures in the surface environment and the way they affect fluids that are involved in diagenesis.

2.2.1. Sedimentology

Sedimentology was defined as "the study of sediment" by Wadell (1932) and can be described as the study of the sediments and their formation. Sediment deposits are formed on the surface of the Earth and in the seabed in sedimentary basins.

The sediment formation depends in large parts on physical and chemical reactions present in rock-atmosphere and rock-water transitions. Sedimentological processes occur without the action of high pressures and temperatures. Sedimentary environment refers to the geographic place where sediments are accumulated; there are three types of sedimentary environments: continental, marine and transitional.

The Figure 2-10 gives a graphical explanation of how these three sedimentary environments fit within the Earth system and the eleven sub-environments which they are divided in. Rocks produced in each of these sub-environments may have similar mechanical or textural properties. Different origins lead to different diagenetic processes which result in different contents in both texture and organic matter. Sedimentological process knowledge is essential for the exploration of reservoirs.

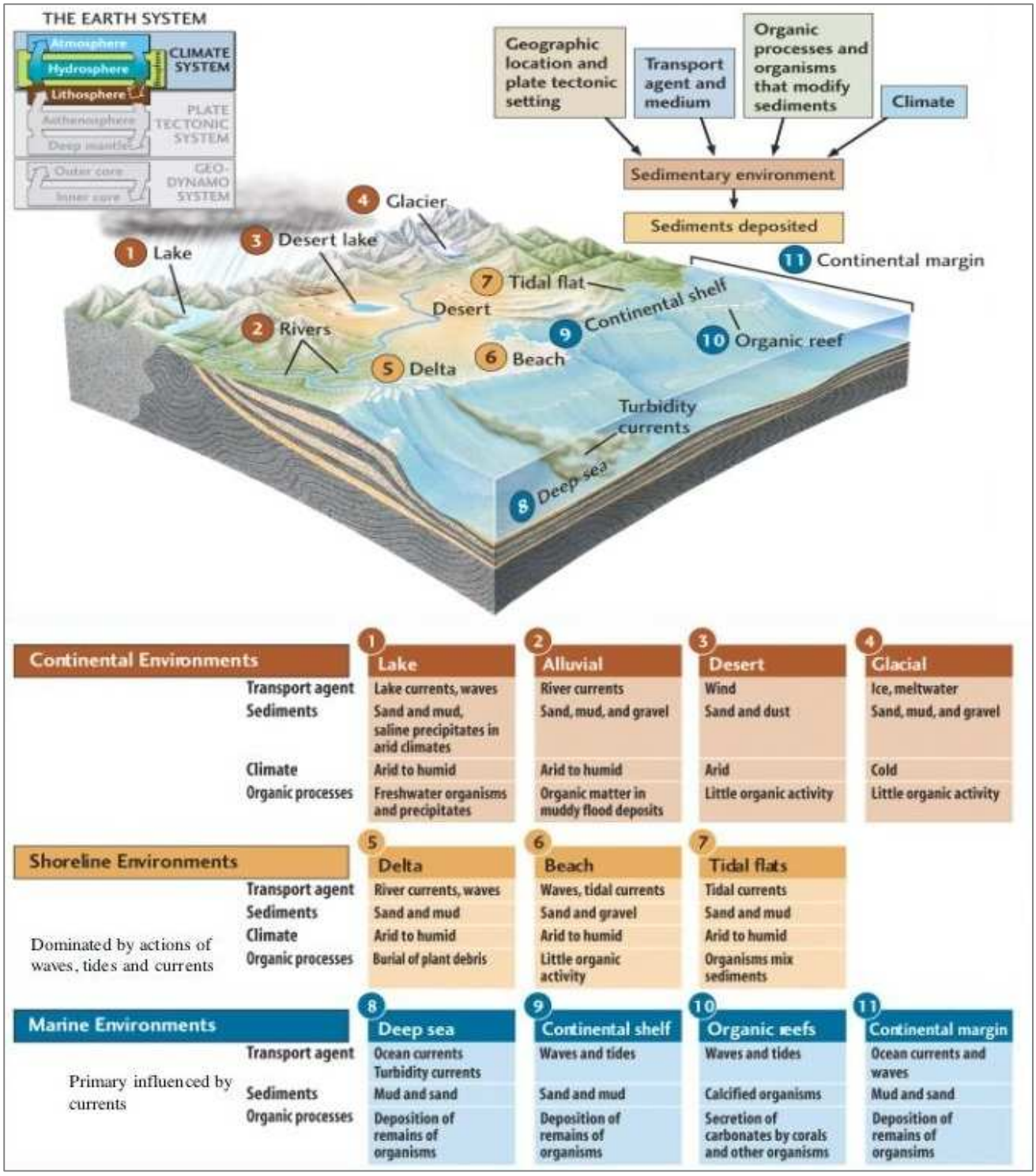

Figure 2-10: Interacting factors in the creation of sedimentary environments and sub-environment. Image from (FSU 2013)

2.2.2. Lithology types

Lithology refers to the physical character of a rock. It describes the rock based on its physical characteristics including: mineral composition, shape, color, size grain, and texture. The

constituents and textures of the rock are the key which helps to discover which conditions it was originated in.

Sedimentary rocks are the product of the lithification of accumulated sediment in the basins. Lithification is the process by which unconsolidated sediments are transformed into solid sedimentary rocks and includes compaction and cementation processes. Accumulated materials come from two main sources. First, the solid particles from other rocks which lead detrital sedimentary rocks; and second, soluble materials dissolved which result in chemical sedimentary rocks in case of precipitating. Organic matter is another source of materials in the form of skeletal components or as a rock itself (e.g. coal).

Major sedimentary rocks are shales, forming 75 percent of total, the sandstones making up about 11 percent, the carbonates comprising about 13 percent, and evaporites in the last place (Devereux 1999). Sedimentary rocks are the most important in terms of reservoirs.

2.2.2.1. Detrital rocks

The components of detrital rocks are present in all three groups, although in different proportions: rock fragments, quartz, feldspar and accessory minerals. The composition of the rock fragments and feldspars basically depends on the geology of the source area and the grain durability during transportation. The quartz remains resistant to chemical erosion. The compositional maturity is the relationship between the total grain quartz against feldspar and rock fragments. This is a useful index to compare different types of sandstones. Immature sandstones have many unstable rock fragments and feldspar, while mature sandstones have much quartz and feldspar (Zarza 2010). The accessory minerals more common are coarse micas (muscovite and biotite), pyroxenes, amphiboles and heavy mineral (zircon, tourmaline, hematite and opaques).

The sandstones occur in beds with a thickness ranging from centimetres to tens of meters. Sandstones are formed by the consolidation and compaction of the sand and held together by a natural cement such as silica. The particles consist of framework between 1/16 and 2 mm, and a smaller fraction called matrix.

Shales are fine grained rocks which are made from the compaction of silt and clay size mineral particles thus forming fissile and laminated layers; these clay minerals are crystal structures of several metal oxides which are associated with alumina in connection with water molecules such as magnesium or iron.

Figure 2-11: Model of the sedimentary process of deposition (Annenberg Foundation 2013). The alternation of layers is due to changes in the energy of the medium during the deposition.

2.2.2.2. Chemical rock

Biological and biochemical processes are essentially controlling the formation of these deposits, but in some cases purely physicochemical processes can be very important. In contrast to clastic rocks (usually allochthonous) carbonate rocks are autochthonous rocks, i.e. virtually no transportation is present, all processes are taking place within the sedimentation basin. Sediments are taken up in solution to lakes and seas where they precipitate as a result of physical processes (evaporites) or biochemical processes (limestone).

Carbonates are basically composed of fossilized skeletons and mineral grains of calcite; the two major types are limestone which is composed of polymorphous of $MgCO_3$ such as low magnesium calcite (LMC), high magnesium calcite (HMC) and aragonite; and dolostone is composed of the mineral dolomite $CaMg(CO_3)_2$.

Evaporites (salts) are sediments which are formed by the precipitation of mineral phases from concentrated brines. Pickles are natural solutions which have high concentrations of dissolved salts. The variety of evaporite minerals is very broad, including chlorides, sulphates and carbonates, among many other minerals. Evaporites are also an excellent seal for oil and gas.

2.2.3. Diagenesis

Diagenesis is the set of physical, chemical or biological processes which are affecting the sediments after deposition. Diagenesis can lead to destruction or enhancement of porosity and permeability which were initially controlled by the depositional environment. They become controlled by the diagenetic physicochemical processes during burial. Temperatures and pressures

are located between those of weathering environment and those of metamorphism. Normally it is considered that diagenesis occurs at temperature bellow 250^{o}C.

Temperature increases with depth; the heat flow of earth's crust is a product of the geothermal gradient and the thermal conductivity of the rocks. The global average geothermal gradient is taken as about 22^{o}C/km, but ranges from 10 to 50^{o}C/km in old shield areas and active zones of sea floor spreading. Different interleaved lithologies in stratigraphic sequences lead to slight changes in the gradient profile. Large anomalies are caused by igneous intrusions and meteoric cool water fluid. The importance of this is that the rate of diagenetic reactions is controlled by the temperature.

Pressure increases with depth. The lithostatic pressure is due to the pressure of the rock transmitted through grains contact and the fluid pressure is caused by the column of fluid within the pores of the sediment. Fluid pressure is related to the density of fluid and varies with temperature and salinity. The overpressure becomes relevant in the sediment diagenesis and petroleum generation and migration. Normally rock density increases with depth, while the porosity decreases; however there are two exceptions. First, overpressure clays, as already expounded, have anomalous high porosity; because fluid cannot escape and allow compaction to occur. And second, evaporites which do not change their density because they are not compacted during burial.

The chemistry of the fluid which infill the pores of sediment affects chemical reaction during burial process. There are three basic types of fluids, those are the following: Firstly, non-hydrocarbon gases; sediments above water table contain atmospheric gases infilling their pores, and gases which have been originated in volcanic emanation and the mantle. These gases affect the pH of the pore fluid.

Secondly, petroleum fluids; fluid hydrocarbons occur in both gaseous and liquid conditions, and they are controlled by their chemical composition in according to the pressure and temperature.

And finally, subsurface water: meteoric, connate and juvenile waters. Meteoric water derives from rain water and snow. It is normally oxidizing and acidic, making it a potential source of chemical reactions. Connate waters have evolved from the original water associated with deposition. Temperature, salinity and chemistry mark the difference with meteoric water. Fresh meteoric water is less dense than normally saline connate water and range of pH an, d Eh values is wide. Connate water is enriched in potassium, sodium, and chlorites from the seawater; but the calcium, sulphates and magnesium content is less. Juvenile or hydrothermal water has a deep magmatic origin and affects epigenetic mineralization.

2.2.3.1. Detrital rocks

Diagenesis in detrital rocks is developed following a series of stages: Eodiagenesis, Mesodiagenesis and Teodiagenesis (defined by Choquette and Pray in 1970). Eodiagenesis refers to the earliest stage which takes place at very shallow depth. Organic reworking or bioturbation leads to destruction of primary structures and formation of mottled bedding and other traces. Formation of pyrite (reduction environment) or iron oxides (oxidizing environment); and precipitation of quartz and feldspar, overgrowths carbonate cement, kaolinite, or chlorite are the results of cementation and replacement processes.

Mesodiagenesis is produced during deeper burial. Physical compaction heads to tighter packing, porosity reduction and bed thinning. Chemical compaction (pressure solution) regulates partial dissolution of silicate grain porosity reduction and bed thinning. Precipitation of carbonate (calcite) and silica (quartz) cements cause cementation accompanying porosity reduction. Dissolution caused by pore fluids triggers solution removal of carbonate cements and silicate framework grains, and creation of new (secondary) porosity by preferential destruction of less stable minerals. Mineral replacement of some silicate grains and clay matrix occur. Clay mineral authigenesis results in alteration of one kind of clay mineral to another.

Telodiagenesis refers to late stage of diagenesis which follows uplift of previously buried sediment into the regimen of meteoric water. Dissolution, replacement and oxidation lead solution of carbonate cement, alteration of feldspars to clay mineral, oxidation of iron carbonate mineral to iron oxides, oxidation of pyrite to gypsum, and solution of less stable minerals. (Boggs 2011)

2.2.3.2. Chemical rocks

After deposition, carbonate sediments are exposed to a variety of diagenetic processes which regulate changes in porosity, mineralogy, and chemistry. Carbonates are generally more susceptible to dissolution, recrystallization and replacement than silicates. Porosity of carbonate sediment may be reduced by compaction and cementation or enhanced by dissolution.

Diagenesis takes place in three major regimen or realms. The marine realm includes the sea floor and very shallow marine subsurface, characterized by seawater temperature and marine water with normal salinity. Meteoric realm comprises marine carbonate sediment brought from the seafloor realm, characterized by the presence of fresh water. And surface realm which is subjected to higher temperatures, increased pressures and changes pore fluids on the seafloor.

During diagenesis, processes and changes are produced. Biogenic alteration, organisms in carbonate depositional environment reworks sediment destroying primary structures. The cementation which takes place mainly in warm water areas within the pore space of grains-rich sediment or cavities destroys the porosity. Dissolution requires opposite condition to cementation.

Sediment	Lithology		Depositional Environment	Diagenetic processes	Rock situation		
	Type	Rock			Porosity	Strength	ROP
Sand	Detrital	Sandstones	Continental Shoreline Marine	Compactation Pressure-disolution Cementation	High	Low	High
Silt and Clay		Shales	Continental Shoreline Marine	Compactation Deshydration	Low	Medium	Medium
Organic debris Carbonate	Chemical	Limestone	Marine	Cementation Dolomitization Dedolomitizacion	Variable	Variable	Low
Salts		Evaporites	Marine Lake	Replacement	Null	High	Low

Table 2-1: Overview of engineering and geological concepts related to lithology in petroleum reservoir.

2.3. Petroleum

Petroleum reservoir fluids were formed million years ago and trapped in rocks when animal and plant matter were settled, and subsequently buried, into the seas together with sand, silt and rock. When the pressure caused by the burial and the temperature due to geothermal gradient occur at the right time; then organic matter becomes petroleum; and mud, silt and sand are converted to source rocks (Dandekar 2006).

Petroleum Geology deals with the study of how petroleum is formed and accumulated in the Earth's crust. Petroleum is a naturally occurring, chemically complex mixture of hydrocarbon molecules, sometimes with the addition of small quantities of nitrogen, sulphur and oxygen compounds (NSO). Petroleum is normally less dense than water. The type and size of the hydrocarbon molecules result in gaseous petroleum (dry gas, wet gas) or liquid petroleum (oil) through the thermogenic transformation of organic matter.

Petroleum is generated and accumulated in sedimentary rocks which are formed in sedimentary basins. A number of factors must be presented for a petroleum accumulation to occur, those are the following:

a. The existence of a sedimentary rock, **source rock**, which should be a sufficiently high amount of the appropriate type of organic matter in order to produce petroleum.

b. **Maturity** of the source rock is necessary to produce hydrocarbons which depend on both temperature and time. Temperature has exponential relationship to maturity making it the most important. For instance, increasing the temperature by 10^{o} doubles the maturity. While time maturity relationship is more linear. The longer a source rock is exposed to a given temperature, the more mature it is becoming.

c. **Migration** is the process by which petroleum moves from its place of origin to where it is accumulated, or for its destruction at the surface.

d. The existence of a large enough **reservoir** rock which accumulates petroleum. Reservoir rock should be with the permeability for the petroleum to be commercially workable.

e. A rock with low permeability acts as **seal** and prevents leakage of petroleum during its accumulation. Common seals are shales, evaporites or cemented limestones. The most effective seal is rock salt. Seals may also be developed along with faults by clay smear (gouge).

f. A **trap** is the petroleum bearing "container" which consists of a reservoir rock body overlain by a seal.

g. **Timing,** the generation of petroleum, migration and the formation of reservoir, seal and trap would occur in the correct sequence of events. (Lippard 2011)

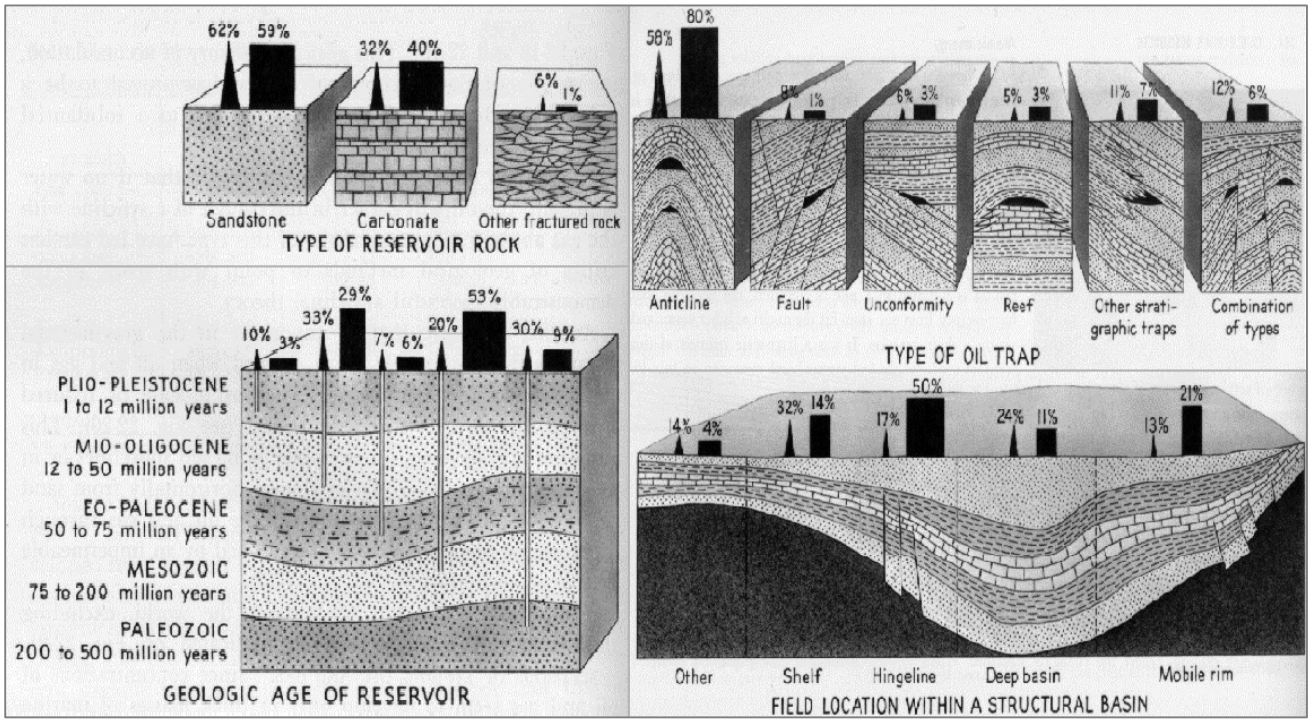

Figure 2-12: General situation of the petroleum reservoirs in different contexts presenting percentages for reservoir and its production. On the left, up on function of lithology current and down of the age of the reservoir; and on the right, up of the type of trap and down of the location in the basin. (Leet and Judson 1965)

Traps may be formed by regional tectonics (compression, extension, strike-slip); or local tectonics, such as compaction-drape and salt tectonics; or by sedimentary and diagenetic processes. The simplest traps are structural traps such as domes/anticlines or tilted fault blocks.

Stratigraphic traps are formed by primary stratigraphic processes which are often associated with unconformities.

2.3.1. Petroleum basins

The relative movements of tectonic plates generate basins which sediments are deposited in. A sedimentary basin is an area in which sediments have accumulated during a particular time period in significantly greater thickness than in surrounding areas. These basins contain sediments that range in thickness from less than 1 km to several 10's km.

There are six types of basin which are containing petroleum. About 90% of the funds accumulate is in continental rift basins, passive margin basins, and foreland basins.

Continental rift basins are relatively narrow and fault-controlled, often with a wider overlying post-rift "sag" basin. These are important for forming source rocks in poorly-circulated marine straits and lakes during the early stages of continental rifting (about 30% of the world's petroleum resources).

Passive margin basins form across passive continental margins and contain some of the world's largest sediment accumulations, often more than 20 km thick, especially where they are fed by large river systems (30% of the world's petroleum resources).

Foreland basins are formed at both continental collision margins and arc-continental collision margins. These are wedge-shaped basins thickening towards the deformed fold and thrust belt in the adjacent mountain areas (30% of the world's petroleum resources).

Intracratonic basins are relatively shallow, circulars occur in continental interiors containing a high proportion of gas compared to oil (5% of the world's petroleum resources). Forearc, interarc and backarc basins form at active continental margins in association with subduction and the development of island arcs. These basins are short lived and may be rapidly destroyed (1-2% of the world's petroleum resources). Strike-slip basins form in areas undergoing transform, strike-slip tectonics. These are narrow, deep basins that often show extremely fast subsidence (1-2% of the world's petroleum resources). (Lippard 2011)

2.3.2. Gullfaks

Gullfaks field is located in block 34/10 and is an oil producer from the Statfjord Fm. which is located in the Viking Graben in Norwegian sector of the North Sea. The formation can be divided into three members: Raude, Eiriksson, and Nansen in Gullfaks field area. Eiriksson and Raude members are alluvial and associated floodplain deposits, and the Nansen member is a shallow marine deposit. Figure 2-13 shows the Gullfaks location and Table 2-2 presents the lithology of formations penetrated during drilling.

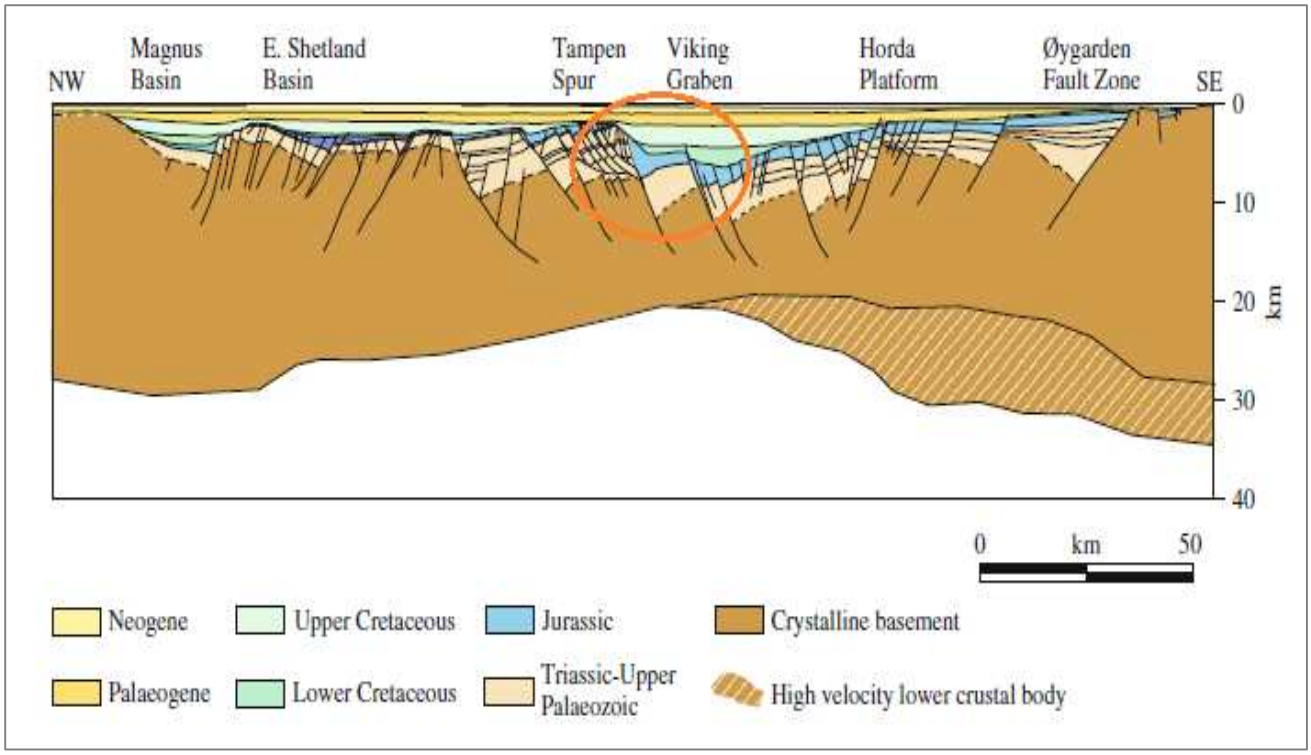

Figure 2-13: Interpreted regional deep seismic line and crustal transect across the northern North Sea (Faleide, Bjørlykke and Gabrielsen 2010) Gullfaks is marked in orange

Formation	Lithology
Utsira Fm.	Sandstones from very fine to fine and in places medium to very coarse grained separated by claystones and minor siltstones.
Hordaland Gp.	Claystones
Balder Fm.	Fissile shales with interbedded sandy tuffs and occasional stringers of limestone, dolomite and siderite. Sandstones are locally present.
Lista Fm.	Shales generally non-tuffaceous and poorly laminated with occasional stringers of limestone, dolomite and pyrite it contains. Less than 5 m thick sandstone layers are locally developed.
Shetland Gp.	Chalk facies of halky limestones, limestones, marls, and calcareous shales and mudstones with chert (flint). Siliciclastic facies of mudstones and shales, partly interbedded with limestones The shales and sandstones are from slightly to very calcareous.
Kyrre Fm.	Silty to calcareous mudstones with occasional limestone beds. Some Very fine to fine grained sandstone beds.
Krans Mb.	Sand
Statfjord Fm.	Shales interbedded with thin siltstones, sandstones and dolomitic limestones. Massive sandstone bodies interbedded with shales. The top consists of thick fossiliferous sandstones.

Table 2-2: Lithology of the drilled formation in C-47 (Norwegian Petroleum Directorate 2013)

The origin of Statfjord formation is from Early Jurassic to Rhaetian in the lower part. Three units are recognized on a sedimentological basis, the lowermost and thickest unit consisting of braided stream deposits and the upper two units comprising field-wide sheets of coastal barrier sands. The thickness varies in a range between 251 and 322 m. The formation is thinner on the crests of fault blocks and thicker on the downthrow sides of fault. Its completely development is located in the central part of the Viking Graben and can be recognized in the entire area between East Shetland Platform and the axis of the Viking Graben. (Deegan and Scull 1977)

Lithology of the formation exhibits a transition from continental to shallow marine sediments. At the base is a transitional coarsening upwards sequence consisting of grey, green and sometimes red shale interbedded with thin siltstones, sandstones and dolomitic limestones. Above this are massive white to grey sandstone bodies interbedded with greenish-grey to red-brown shales. At the top of the formation thick, white to grey, fossiliferous and glauconitic sandstones occur and these pass eastwards into dark grey calcareous siltstones and shales of the Dunlin Unit. (Deegan and Scull 1977)

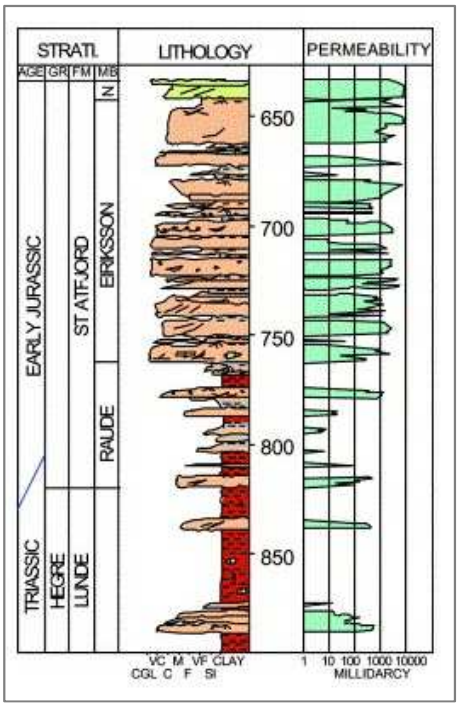

Figure 2-14: Statfiord lithostratigraphic column with permeability. Modified from (Hesthammer, Johansen and Watts 2000)

The boundaries are difficult to define. It is interpreted as the base of transitional unit which marks the passage from the shalier Cormorant Formation to the massive sandstones to the Statfjord Formation. The top of the formation is marked by the contact between medium to coarse-grained calcareous sandstones and micromicaceous shale or siltstone of the overlying Dunlin Unit. The top part of the calcareous sandstones in the UK sector passes laterally into calcareous shales and siltstones in the Norwegian sector.

The lower transitional unit appears to represent a passage from the purely continental deposits of the Cormorant Formation to the lower alluvial plain and braided stream deposits of the main part of the Statfjord Formation. Towards the top of the formation coarse sandstones with pebble beds, cross-bedding and channel structures appear to have been deposited in a coastal environment. The uppermost sandstones are relatively structureless but the presence of fossils and glauconite suggests a shallow marine environment.

3. Hardness interpreted from online drilling data.

This chapter presents the data obtained from Statoil and how it has been managed. The developed model is presented in order to obtain the parameters which are related to hardness of the formations. The interpretation of the data is based on the interactions between the different graphs is presented at the end of this chapter.

3.1. Data collection

The main Gullfaks field is located in block 34/10 in the northern part of the Norwegian North Sea. It has been developed with three large concrete production platforms. The Gullfaks A platform began its production on 22nd December 1986, with Gullfaks B following on 29th February 1988 and the C platform on 4th November 1989.(Statoil 2013)

3.1.1. General well data

The following information was extracted from *Final Well Report: Drilling and Completion 34/10-C-47* attached with the data.

- Drilling rig: Gullfaks C
- License number: PL 050
- Well name: 34/10-C-47
- Slot: 3
- Type of well: Oil Producer/ Water Injector, segment K2, K3
- Water depth/air gap: 216,9 m MSL/84,1 m MSL
- Wellhead deck: 43,5 m RKB
- Primary objective: Oil Producer
- Coordinates at Wellhead Level (UTM)
    - Structure Centre: 6787107,3 m; N 460990,8 m E
    - Slot Centre: 6787142,46 m; N 460998,20 m E

The well data available to us belongs to four sections NO 34/10-C-47 24”; NO 34/10-C-47 17½”; NO 34/10-C-47 12 ¼” MPD; and NO 34/10-C-47 8 ½”.

Section	Length (m)	Time		ROP (m/d)
		Hours	Days	
24”	1072	575,0	24,0	44,67
17 ½”	871	795,3	33,1	26,31
12 ¼” MPD	408	694,3	29,9	13,65
8 ½”	1612	303,5	12,6	127,94

Table 3-1: Overview of section (Christophersen 2007).

Run n°	Bit Size	Depth in (m)	Depth out (m)	Depth Drilled (m)	Time Drilled (h)	ROP (m/h)
1	24”	436	624	188	7,0	26,9
2	24”	624	1124	500	26,9	18,6
3	24”	1124	1508	384	49,4	7,8
4	17 ½”	1508	1511	3	3,5	0,9
5	17 ½”	1511	1514	3	0,6	5,0
6	17 ½”	1514	2070	556	38,2	14,6
7	17 ½”	2070	2116	46	1,8	25,6
8	17 ½”	2116	2379	263	22,7	11,6
9	12 ¼”	2379	2407	28	6,1	4,6
10	12 ¼”	2407	2787	380	30,0	12,7
11	8 ½”	2787	4399	1612	100,3	16,1

Table 3-2: Bit record (Christophersen 2007).

3.1.2. Formation evaluation by operating oil company

C-47 was planned as an oil producer from the Statfjord Fm. in segment K3 and K2. The primary target was to produce from S2/S1 on the eastern flank of the K2 segment, as shown in Figure 3-1. The secondary target was to produce an attic volume in a small horst at Top Statfjord (S10) and partly water flooded zones (S9-S3) below in the K3 segment. In addition, there was a possibility for production from Krans above the BCU.(Christophersen 2007)

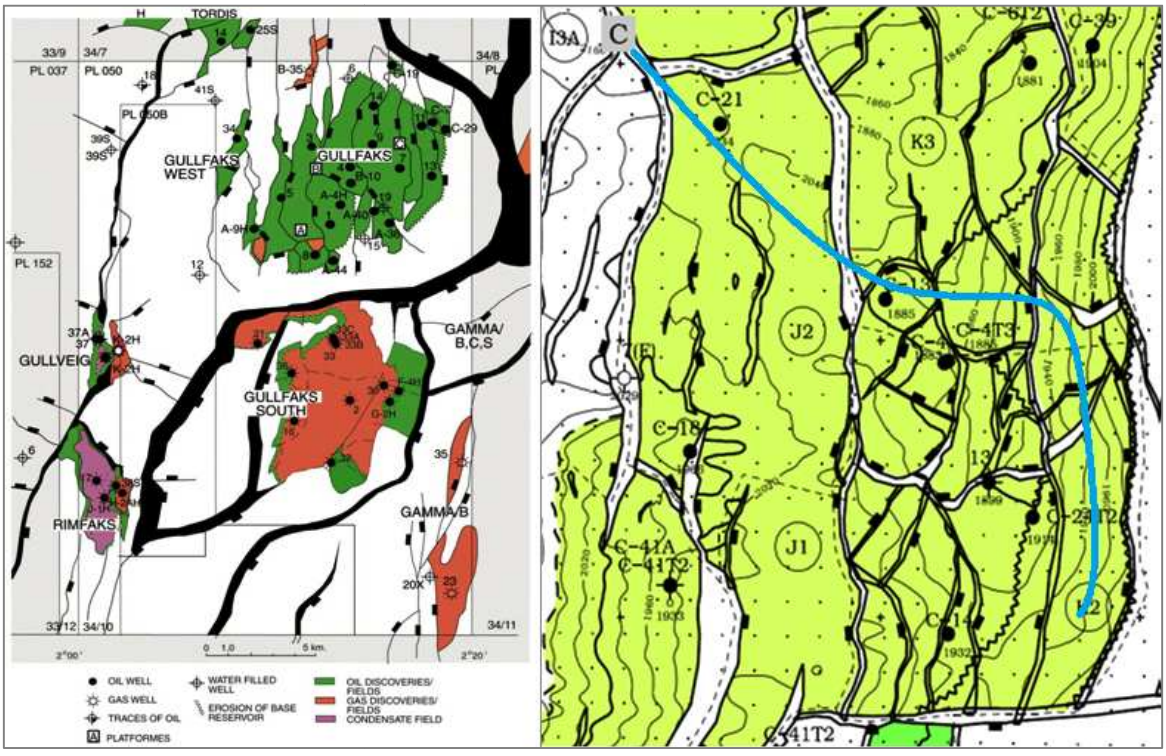

Figure 3-1: Gullfaks C general map (Hesthammer, Johansen and Watts 2000) and the planned well path going into the Statfjord Fm. east of C-13 in the K3 segment and then turning south along the east flank of the K2 segment (Christophersen 2007).

The sections in the data correspond to the following measured depth: Section 24” from 436-2116m; Section 17 ½” from 2116-2382m; Section 12 ¼” MPD from 2382-2787m, and Section 8 ½” from 2787 to 4399m.

The 24” section was drilled through two intervals which were containing shallow gas sands (1084m MD to 1090m MD and 1492m MD to 1508m MD). A few thin stringers of oil filled Krans sand were found at 2892 m MD (Section 8 1/2"). From S9-S3, partly flooded oil sands were drilled from 3028m MD to 3810m MD. The main target was found at 3810 m MD. The S2 sands had a SW of 0.7-0.9.

In the toe of the well, the Top S2/Base S3 came in at 4220 m MD/1994 m TD. This S3 sand had initial oil saturation and the vertical thickness was ~4 m.

The formation tops were drilled as shown in Table 3-3.

Formation	Measured Depth (m)	True Vertical Depth (m)	Section (Where start)
Top Utsira Fm.	995	882	24”
Top sandy Hordaland	1050	927	
Top sandfree Hordaland	1655	1282	17½”
Top Balder Fm.	2050	1486	
Top Lista Fm.	2200	1555	12 ¼”
Top Shetland Gp.	2411	1655	
Top Kyrre Fm	2833	1842	8 ½”
Top Krans Mb.	2892	1865	
Top S10	2929	1878	
Top S9	3028	1914	
Top S8	3047	1920	
Top S7	3058	1925	
Top S6	3075	1930	
Top S5	3150	1957	
Top S3	3202	1973	
Top S2	3810	2000	
Top S2/Base S3	4220	1994	
TD	4399	1982	

Table 3-3: Formation tops with depth (Christophersen 2007).

The faults listed in the Table 3-4 were crossed during drilling. These faults were interpreted on seismic data combined with dip data from density/neutron image data. The dip data indicated strongly that the layers have eastern dip of ~5-10^{o}, which were confirmed by the seismic signals. The eastern part of the K2 and K3 segments were reinterpreted as shown in figure 2, 3 and 4.

Fault / Formation	Measured Depth (m)	True Vertical Depth (m)	Section
1. Fault S3 (S5/S3)	3210	1975	
2. Fault S3	3425	1999	
3. Fault S3	3555	1998	
4. Fault S2 (S3/S2)	3810	2000	8 ½"
5. Fault S2	4080	2005	
6. Fault S2	4150	1999	
7. Fault S3	4350	1985	

Table 3-4: Faults interpreted from both well and seismic data (Christophersen 2007).

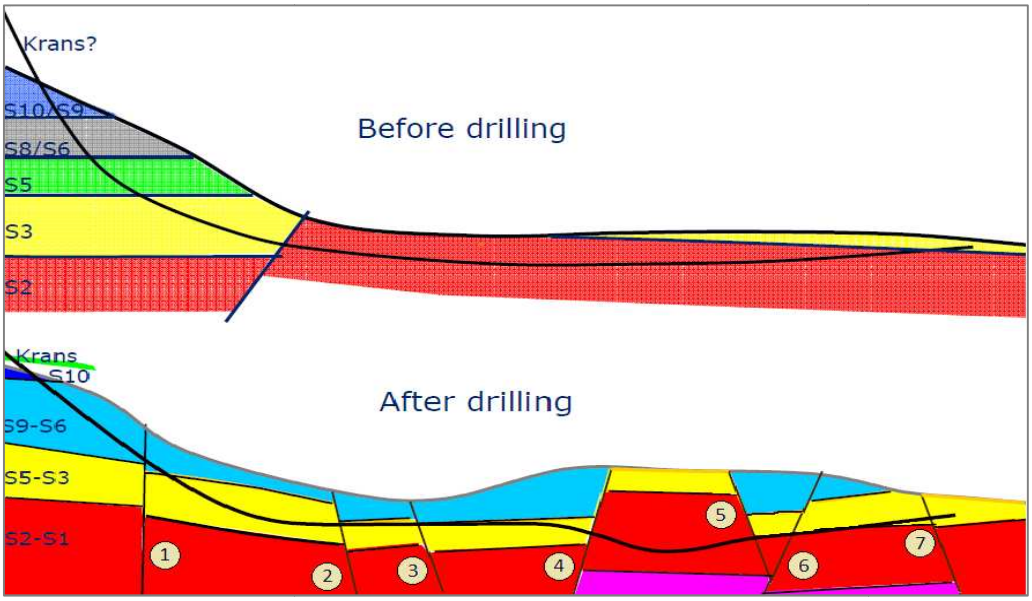

Figure 3-2: Well path and stratigraphy after and before drilling (Christophersen 2007). The numbers indicate shown faults in Table 3-4.

3.2. Hardness model development by present author

Model development based on the data from the different sections is performed in Excel. The data provided in Matlab is converted using the method which is described in the *Appendix A*. Export data to excel. The exported data is presented in 10 columns which are identified with the following items (in order of appearance): "Time, DBTM, DMEA, HKL, BPOS, SPP, MFI, WOB, RPMB, and TRQ". The columns Time, DBTM, DMEA, WOB, and RPMB are selected to the model.

The data had to be filtered in order to remove poor data input. The first filter criterion is the elimination of all data which has a difference between DMEA and DBTM greater than 0,1 m because drilling cannot occur with higher difference. Duplicate values are also removed. The first step in creating the model was to calculate the constant K based on the following equation:

$$\mathrm{ROP} = \mathrm{K} \cdot \mathrm{WOB} \cdot \mathrm{RPM}^{\mathrm{C}} \quad (16)$$

Where: K is the drillability constant. C is an exponent between 0,4 for very hard formations and 1,0 for soft formations

The instantaneous drilling rate at any point in time can be calculated using (16) and resulting from combination of the effort of the selected bit weight and the rotary speed. The use of this equation allows obtaining the drillability of formations which the developed model is based in

$$K = \frac{\mathrm{ROP}}{(\mathrm{WOB} \cdot \mathrm{RPM}^{\mathrm{C}})} \quad (17)$$

The coefficient C may be calculated as a simple extrapolation based on Average indentation hardness presented in the Table 3-5. Note that the calculation of C was made using the equation (18). The hardness of the ground depends largely on the degree of cementing which must be taken into account. The reason why the result needs the application of the coefficient C is graphically showed in Figure 3-3.

$$C_i = \frac{-0{,}6 \cdot AIH_i - AIH_{min}}{AIH_{min} - AIH_{max}} + 0{,}4 \quad (18)$$

Name of Rock	Average indentation hardness (MPa)	Average Compressive strength (MPa)	Ratio of inden. hardness to comp. strength	C
Sandstone	400	12,82	31,20	1,0
Mudstone	700	16,90	41,42	0,9
Argillite	1186	44,86	26,44	0,8
Siltite	1457	63,25	23,04	0,7
Granite	1843	68,00	27,10	0,6
Dacite	2143	N/A	N/A	0,5
Gneiss	2157	86,13	25,04	0,5
L. F. Quartzite	2300	103,02	22,33	0,4
C. F. Quartzite	2443	112,52	21,71	0,4

Table 3-5: Average indentation hardness (used to determine the hardness of a material to deformation), Average uniaxial compressive strength rocks (Jung, Prisbrey and Wu 1991) and the calculated coefficient C. The compressive stress is related to hardness as it was presented in subchapter 2.1.1.5

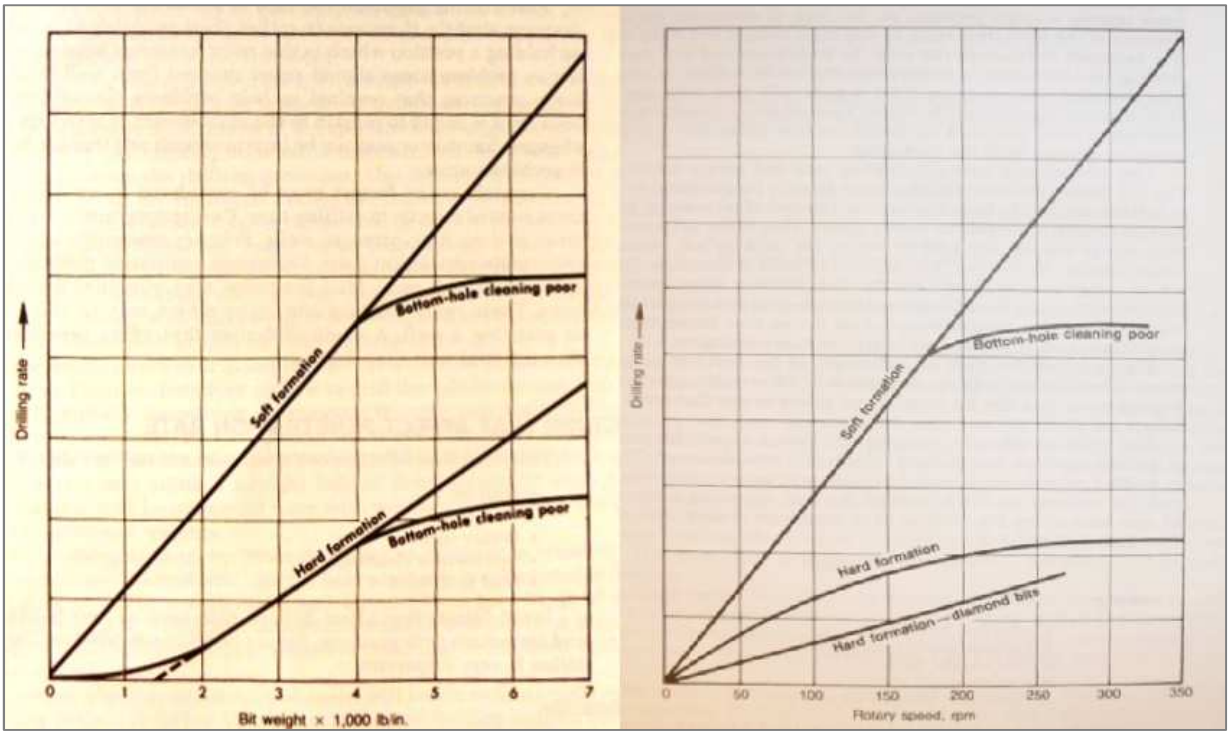

Figure 3-3: Bit weight and rotary speed have influence on drilling rate (Moore 1986). The increase of WOB and RPM is directly proportional to the increase ROP for soft formations when bottom hole is clean. In hard formations the WOB still directly proportional (less ratio) and the relation of RPM is showed as logarithm proportion. For this reason all the values that make zero the product WOB by RPM are deleted. Division of the depth variation by the time variation is required for the calculation of ROP.

The calculation of the constant drillability is performed using (17) and the grouped data (C value will be 0,9 based on then possessed information). The second filter criterion is the deletion of all data that makes zero the product WOB x RPM. The graphics are created of the different interactions of K with ROP, WOB and RPM as a function of both time and depth starting from this point.

In order to produce two different kinds of graphs, the data should be sorted in terms of both time and depth. The data is grouped into sets of 5 to 25 datapoints using the arithmetic average for this purpose. This has a twofold reason, on the one hand, reducing the large number of data which will be managed; and on the other hand, eliminating less significant local variations.

3.3. Hardness model result

The processing of data from the well 34/10-C-47 has resulted in parameter K for each valid value. Appendix B. Graphs presents the complete collection of resulted graphics with the interactions between the parameters chosen for this model.

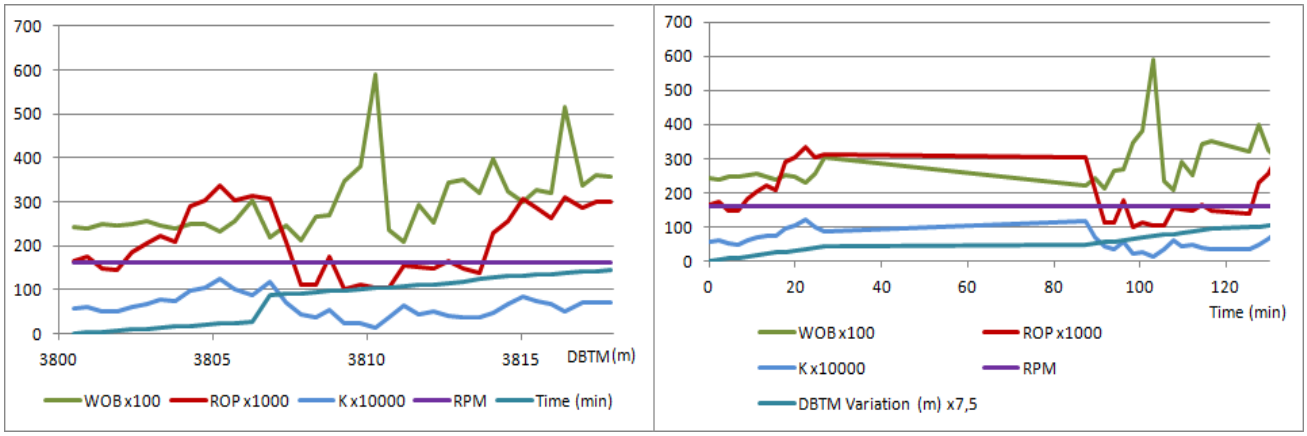

Figure 3-4: Example of output from the model. The following changes were achieved: unmodified DBTM (m); Δ DBTM (m) x 7,5; unmodified Time (min); WOB (t) x 100; unmodified RPM (rev/min); ROP (m/min) x 1.000; K (m/t·rev) x 10.000.

The values of the parameters were modified as set out in Figure 3-4 in order to improve the visual comparison on the same graph. Horizontal axis units are relative. Five different curves were made during the implementation for each of the sets (average of 5 and 25 datapoints), and for each of the two exposures (as a function on depth and time): ROP vs. WOB vs. RPM; ROP vs. K; WOB vs. K; RPM vs. K; and Time or DBTM vs. K.

3.4. Logging data interpretation

This section focuses on the interpretation of the graphs generated by the model. The detail of a relevant point such as the fault which separates the S2/S3 lithologies change is treated separately. The graphs depending on depth reflect the place where lithological changes occur (Figure 3-4, right). The plots depending on time show how the progress was carried out (Figure 3-4, left).

The data gap caused by its removal during filtration is visible in the graphs with respect to the depth. Deletions which correspond to data during the drilling periods are shown with straight lines from 20º to 70º slope. All these absences in the data were evident in the representations of all the parameters as abrupt changes in the general trend.

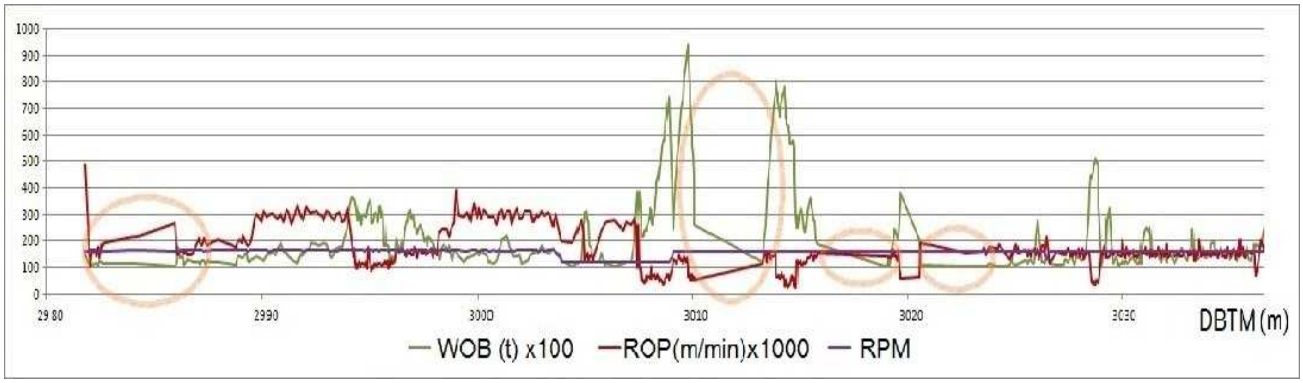

Figure 3-5: Representation of WOB, ROP and RPM vs. DBTM. The data gap corresponds to inputs deleted using filter criteria mentioned above during drilling time (areas marked with orange).

Periods of non-progress are visible in Figure 3-6 as stretches with vertical and horizontal straight lines with a slight slope due to the pooling of data. As the data sets are made in response to the average of the previous 5 or 25 datapoints, sets containing a stop generate the stroke deviation. In the graphs in Figure 3-6 there is a sharp jump in time to the same depth (top) and an increase in time without increasing the depth (bottom). Note that ellipses mark different areas in both Figure 3-5Figure 3-6.

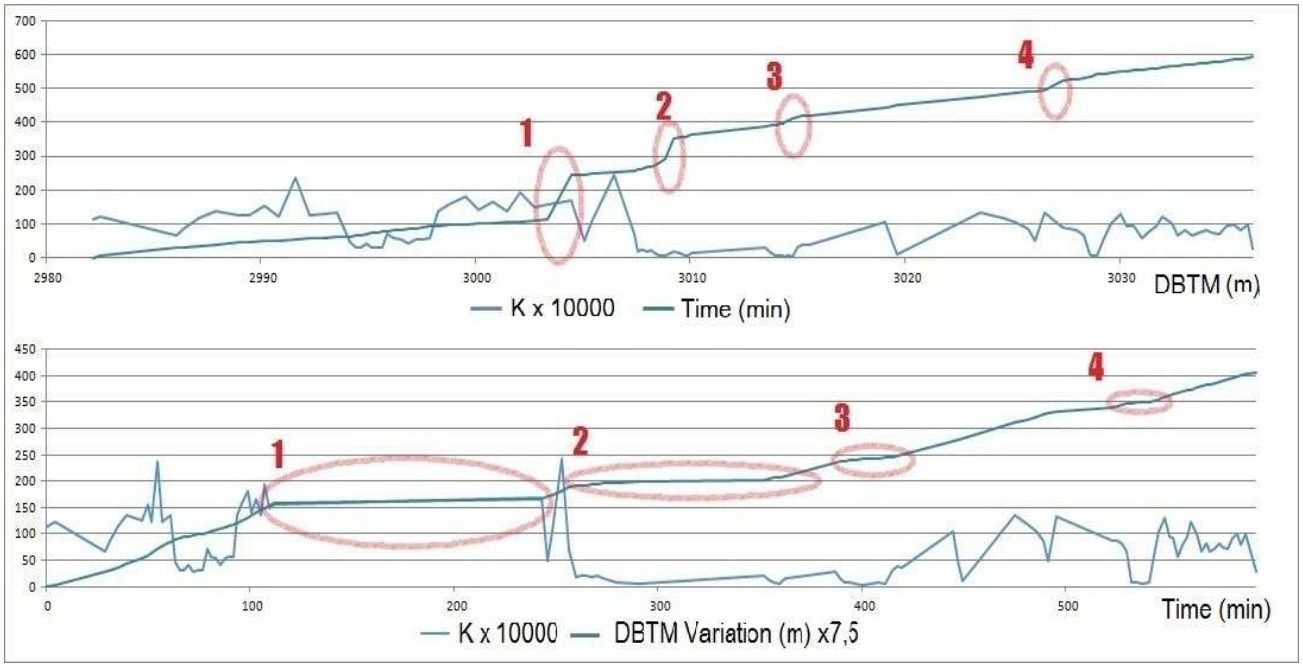

Figure 3-6: Representation of K and Time vs. DBTM (above) and, K and DBTM vs. time (below). The deleted data during no-drilling time are featured as straight line with horizontal and vertical trends (four red marked areas). The number of excluded data is larger when the length of the section is higher.

The focus on the graphs ROP vs. WOB vs. RPM shows that: the increase in WOB is accompanied by a decrease in ROP; the variation in WOB is the largest in relative terms; and the variation of the RPM is the least significant (Figure 3-7). The enlargement in the distance between

the WOB and ROP represents an increase in runtime when WOB is the one above and a decrease when the ROP is located above.

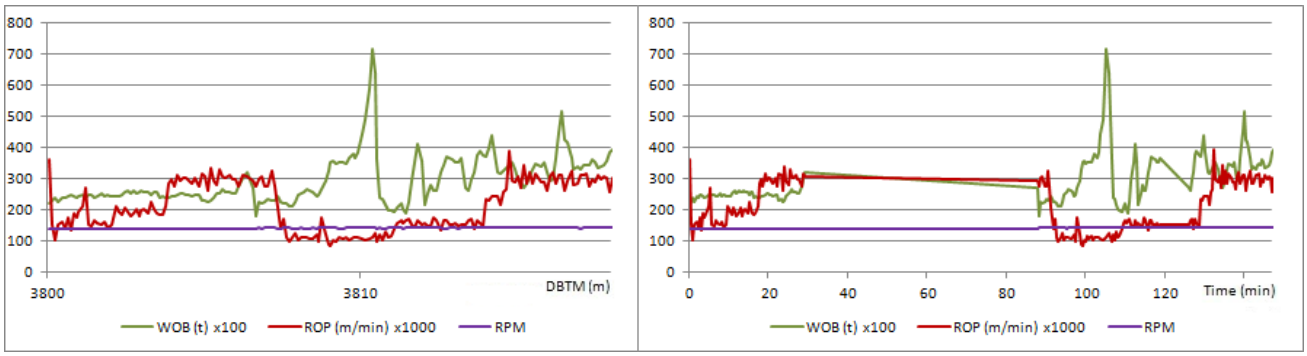

Figure 3-7: ROP vs. WOB vs. RPM comparison as a function of depth (left) and time (right).

The comparisons of K vs. ROP-WOB-RPM are the following: K and ROP lines succeed - as expected based on (16) - nearly parallel tendencies with smooth slope in case of K (Figure 9-4 and Figure 9-9). The decreasing of K involves the increasing of WOB. The separation between both of them entails increasing in runtime when K is decreasing. Finally, RPM does not vary considerably resulting in the less significant parameter in the analysis (Figure 9-6 andFigure 9-11).

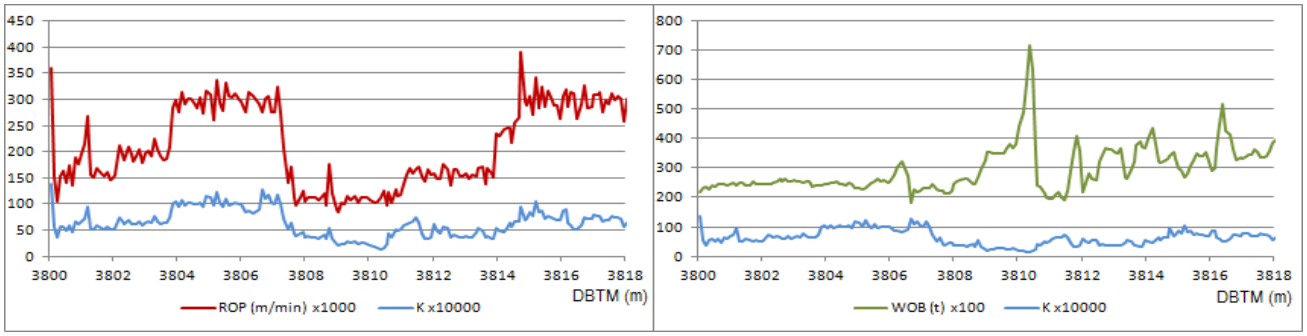

Figure 3-8: Representation of K vs. ROP and WOB-RPM as a function of depth.

The sets of 5 datapoints show clearly performance as a general rule. However, noise keeps being represented in a number of examples. The sets of 25 datapoints where is easier to notice general tendencies are utilized to eliminate it.

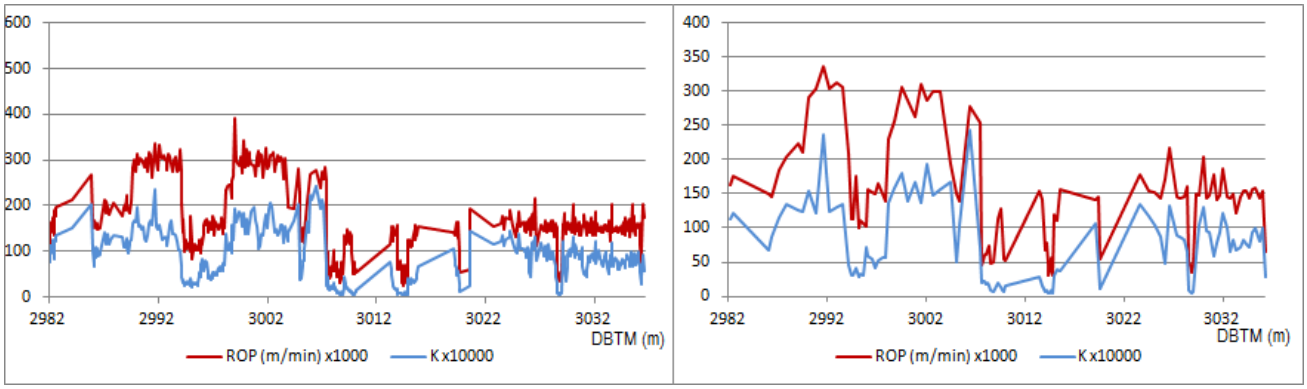

Figure 3-9: Comparison of short average (over 5 datapoints) and long average (over 25 datapoints).

3.4.1. Fault S2/S3

According to the Statoil report a fault which connects S2 and S3 formations is located at 3810 m Measure Depth. Figure 3-2 showed a large fault displacement (4) which makes it appropriate for a detailed analysis.

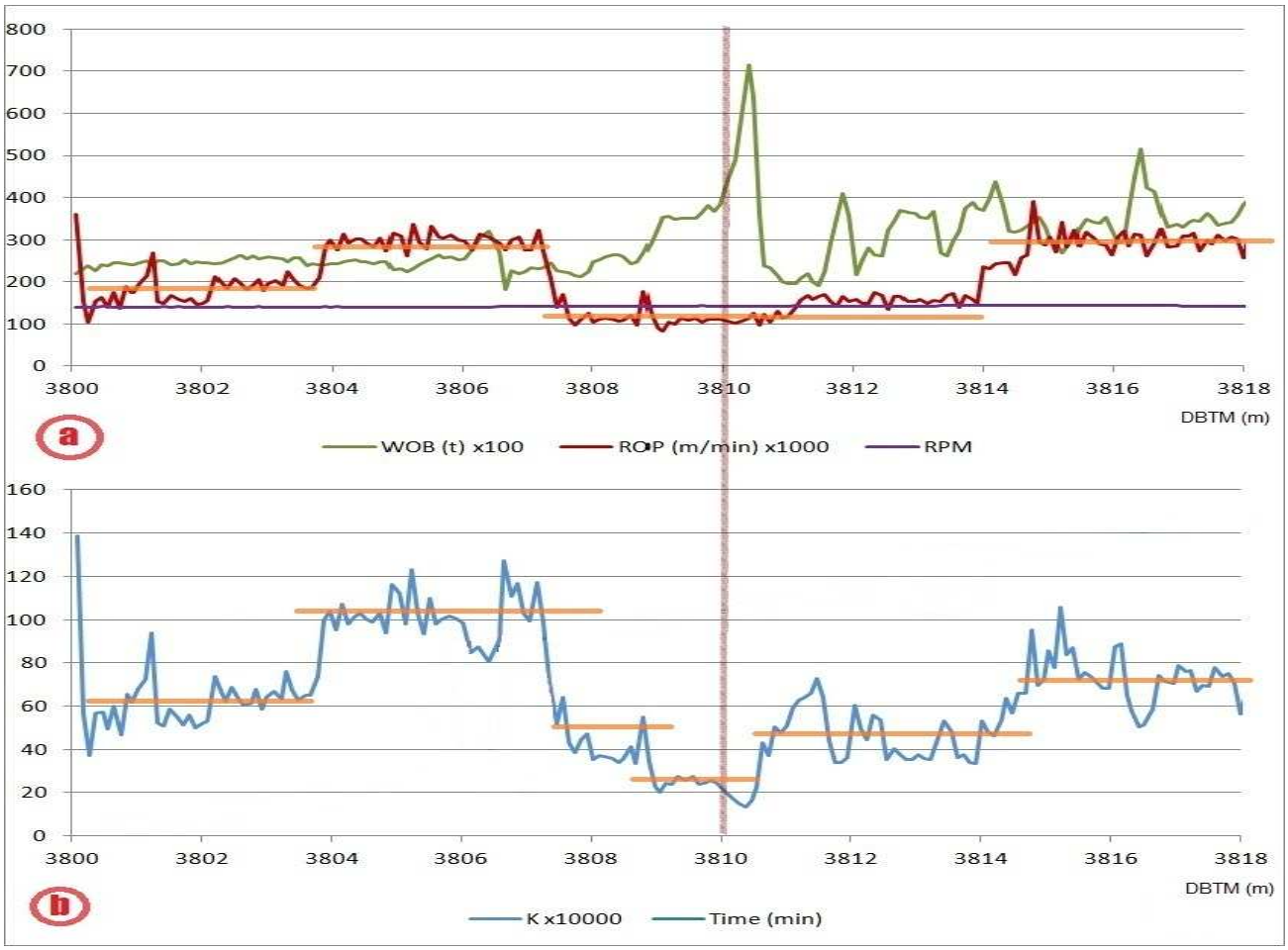

Figure 3-10: Comparison local behavior of the WOB vs. ROP vs. RPM, and K both as a function of depth in the environment of Fault S2/S3 (vertical line). **a** displays a punctual sharp rise on the WOB in the depth of the fault. The lower inclination and deviation on the left side is due to clustering process. The orange lines make visible different tendencies of the

ROP before, during and after the fault. ROP drop occurs in the area of the fault, the ROP before and after is maintained at the same height. b exhibits the same tendency lines for K which are shorter than these lines from ROP but still with a similar behavior. Three zones can be identified in the central region of the fault using K instead of the one that the ROP is showing.

The rise of WOB helps to detect the fault, and the change in the ROP to identify associated weakness zone (Figure 9-14 and Figure9-15). There is no apparent change in RPM (Figure 9-16). The graphics from the sets of 25 datapoints are useful only to indicate the area at this scale; in other respects they lose their functionality.

4. Discussion and evaluation.

This chapter presents the lithological interpretations from the model exposed in the previous section. The results are discussed and compared with previous works and interpretations. Furthermore, the method chosen to the realization of the model, its limitations, quality, and future improvements are also discussed.

Based on the general scheme presented in *Figure 2-13*, it is possible to have an idea of the situation in the well. The previous study of this and the information from the other exploration can help in its evaluation.

The interpretation is performed using the graphics of *WOB, RPM, ROP* and *K. WOB, RPM* and *ROP* support information that *K* transmits. The lithological interpretation is based on the relative changes in the drillability, which is not always consistent with the information of formations provided by the company. Note that the cuttings take time to reach surface while data are instantaneous. The information provided by the company is shown in "Comments" and “Lithology”, consisting of: cross formations, faults and changes of bit.

The interpreted lithologies are based on *Figure 2-9: ROP response in common rock types,* on *Figure 2-8: Simplification of ROP curve* and Table 2-2: Lithology of the drilled formation in C-47 . The secondary objective is to facilitate the identification of those points which may be conflicting in downhole.

First part of the section 24”, 17½” and 8 ½” sections and its lithological characterization are presented below. These sections cross mostly of formation and are a good base to interpret the variations of drillability in the well.

The different diameters in each section affect the value of K. The WOB which is employed in the sections is directly proportional to its diameter due to that reason the value of K is increased in smaller sections. The ROP is not apparently influenced by the size bit. The RPM is important in the larger sections. Lithologies are interpreted according to the following color code:

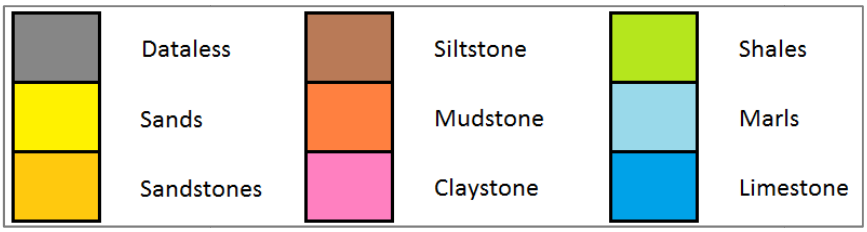

Figure 4-1: Key of colors.

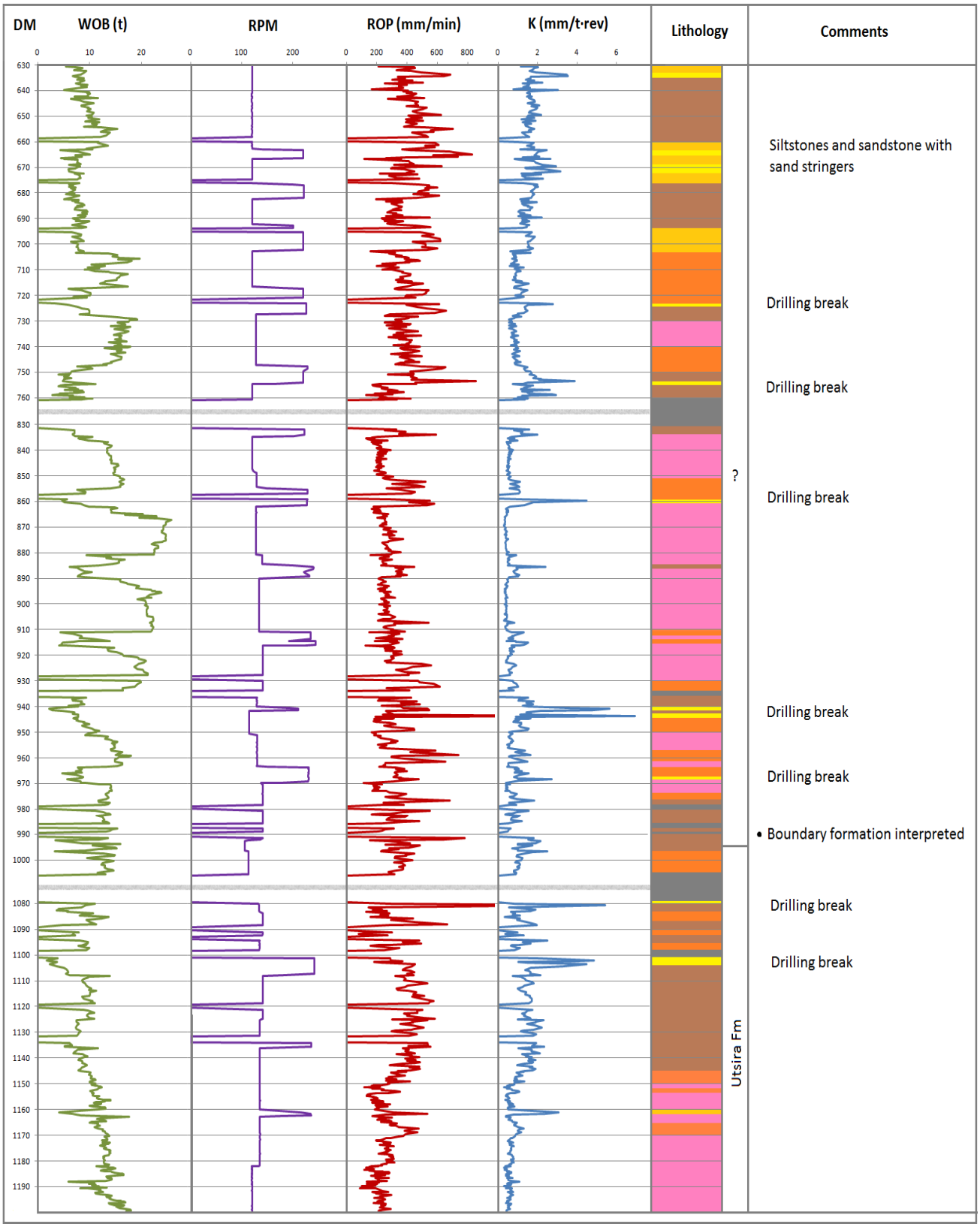

Figure 4-2: Interpretation from the first part of the section 24" Sandstones to Claystones with sand stringers. This section presents big grain-size in comparison with other ones. The interpreted lithology boundary is slightly higher than where the company fixed. Increase in the RPM line is coincided with higher grain-size.

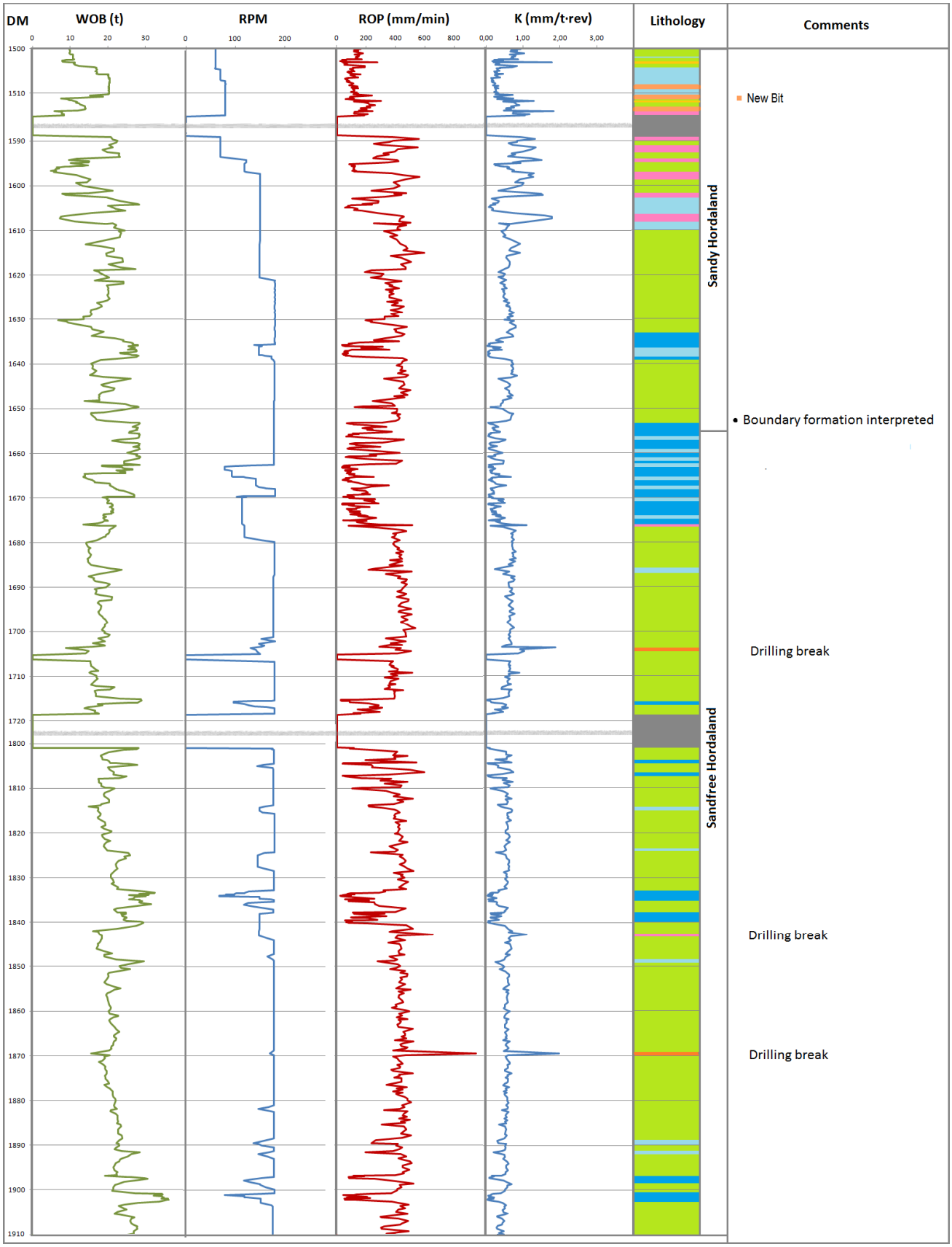

Figure 4-3: Interpretation from the section 17½" part a. Shales alternating with Limestones and Marls. The shales show regular line in ROP and K. When limestones occur, then RPM line decreases. The boundary formation is interpreted higher than the company.

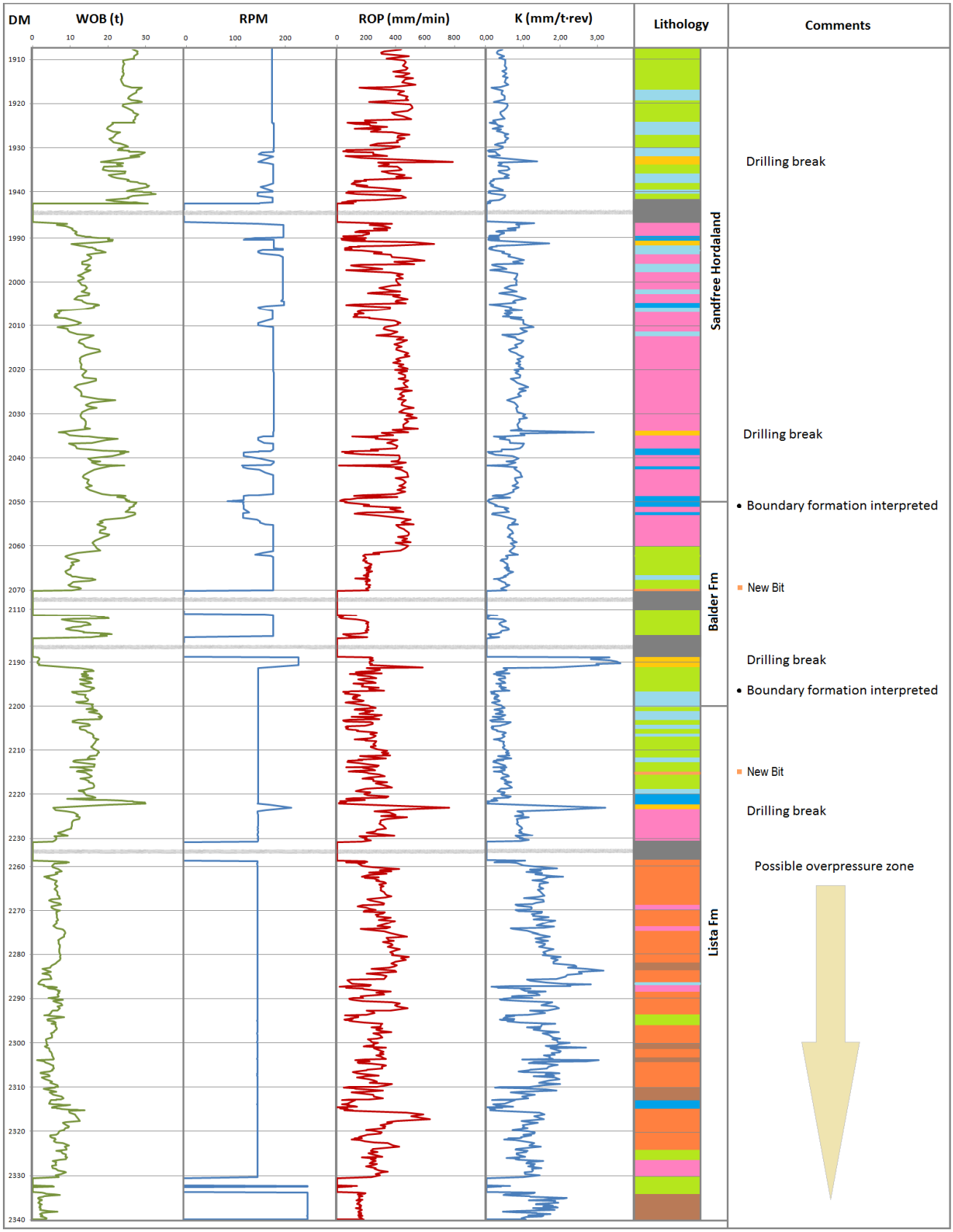

Figure 4-4: Interpretation from the section 17½" part b. Mudstones, Claystones and Shales with Limestones stringers. Sandfree Hordaland is formed basically by shales and claystones. Its boundary with Balder fm is interpreted at the same point as the company. The boundary Balder Fm- Lista Fm is interpreted slightly higher than the company. At the bottom of the representation we found possible overpressured area.

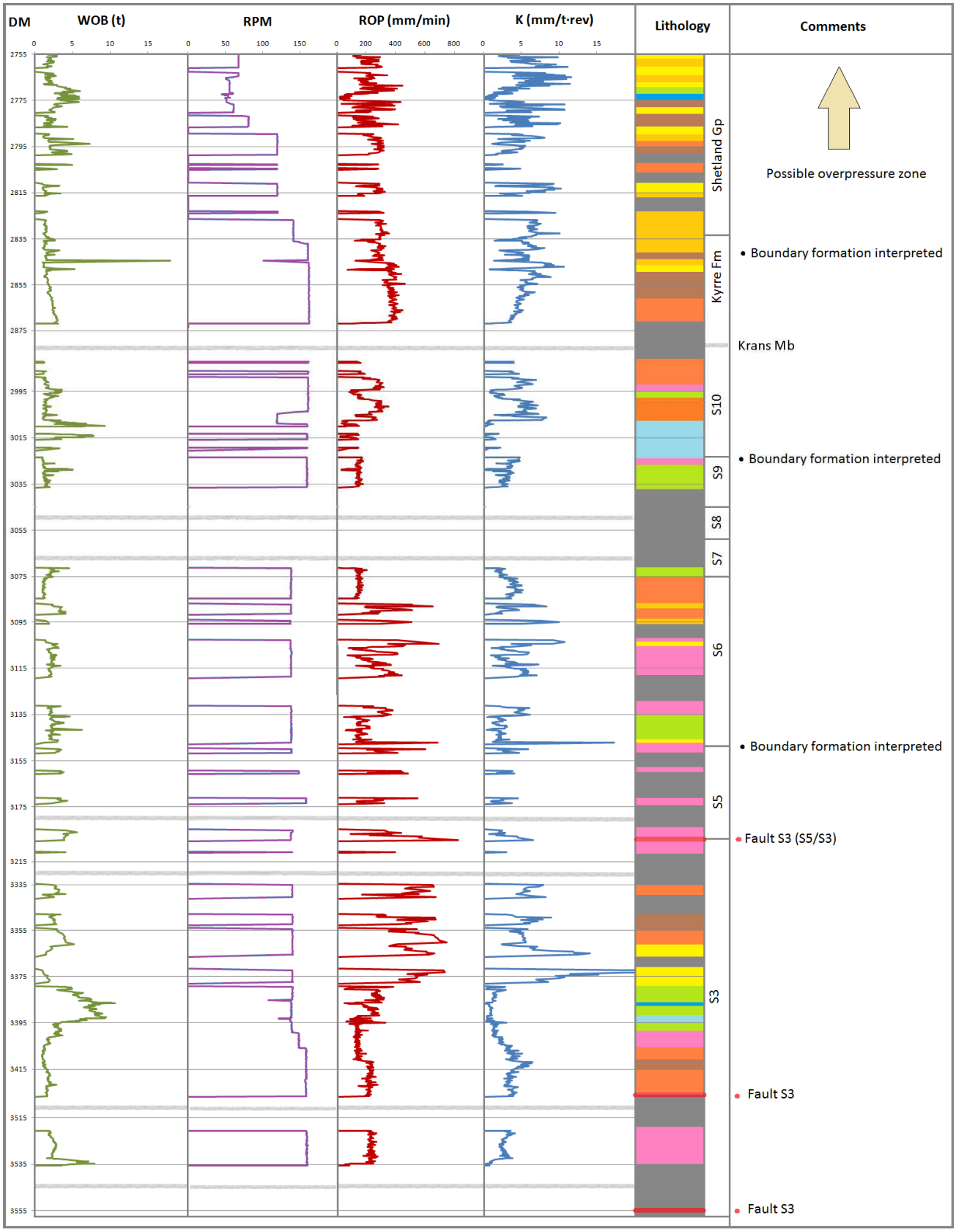

Figure 4-5: Interpretation from the section 8½" part a. Sandstones to Shales with layer of carbonates. This part of the section contains many data gaps which makes it difficult to interpret. Shetland Gp contains sandstones in possible overpressure. Fault S3 at 3400 DM can be observed only in K.

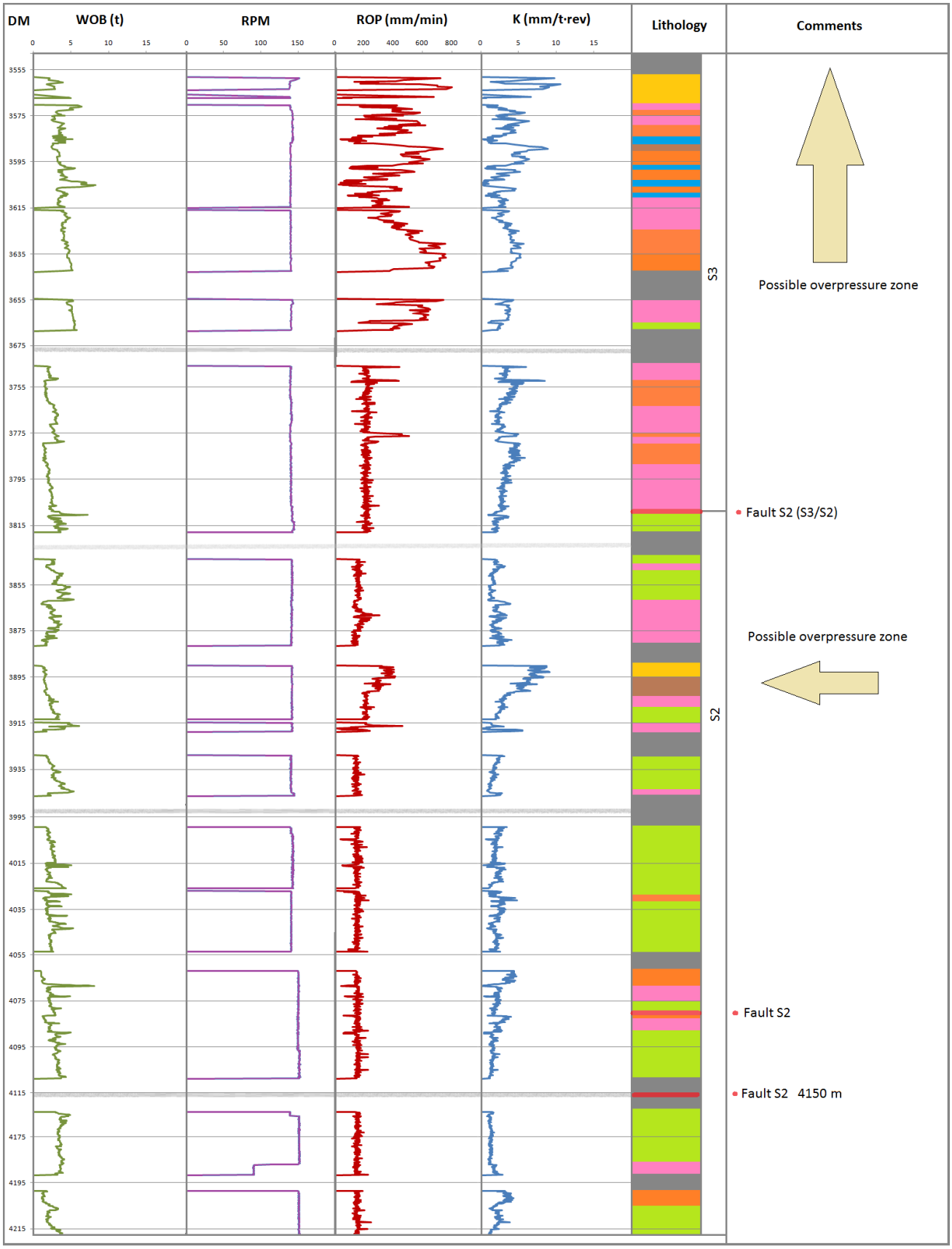

Figure 4-6: Interpretation from the section 8½" part b. Claystones and Shales, with Mudstones, and Limestones stringers. Most of the section is shales and claystones which appear as an uniform layer using ROP for interpretation, but the material changes are shown in K line. Two possible overpressured zones are identified.

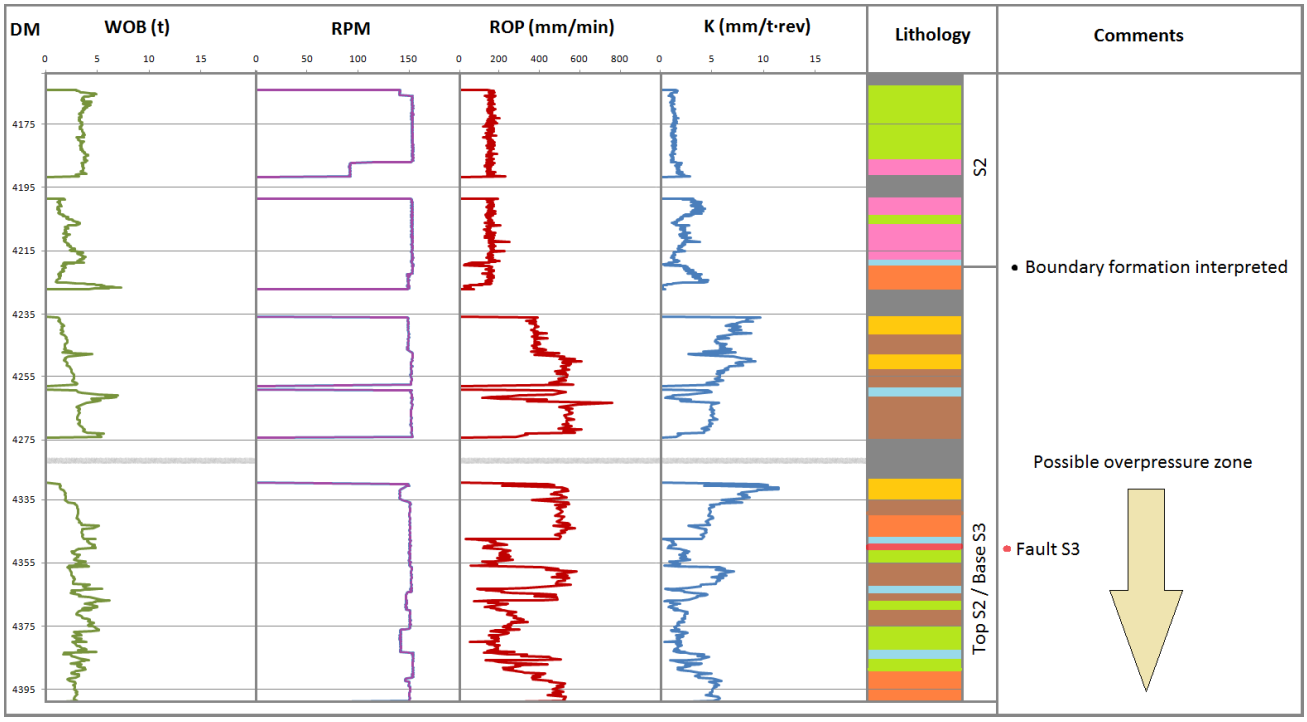

Figure 4-7: Interpretation from the section 8½" part c. Sandstones to Shales, with Limestones stringers. The interpretation of boundary coincide with the company information.

The curve which shows K is overall cleaner than the curve of the ROP. Lithologies with higher K values are more abrupt strokes, while those with lower values are more homogeneous strokes.

The behavior of WOB and RPM in different lithologies varies with K. Materials with higher K have a lower WOB and higher RPM. Lithologies with lower K have the opposite behavior. Note that there is a reduction in the WOB when reducing the size of the drill.

In areas with possible overpressure there is a reduction of WOB, which is incoherent with variation in ROP and RPM. The decrease in WOB, without the consequent decrease of ROP, and the occurrence of higher than normal fluctuations in the curve; are the warning track of the possible entry into one of these zones. Lithologies from these areas do not conform to the general trend and do not correspond to the prognosis of the literature.

The increase in pore pressure increases the value of K, but the traversed material is the same. Lithological interpretations are made strictly following the criteria set by the value of K causing them to be unreliable in overpressured zones. The value of K in these areas is overestimated and corresponds to materials with lower hardness of the real.

K values for each lithology may be calculated observing the generated plots (Table 4-1). Lithologies which are not present in one section are estimated based on their variation in each of the sections (Table 4-2).

Lithology Type	K_{24}	K_{17}	K_8
Limestones	0,1	**0,2**	0,4
Marls	0,3	**0,3**	**0,8**
Shales	0,4	**0,5**	**1,3**
Claystones	**0,7**	**1,0**	**2,5**
Mudstones	**1,0**	**1,4**	**3,5**
Siltstones	**1,5**	**1,9**	**5,0**
Sandstones	**2,0**	2,6	**6,5**
Sands	**2,5**	3,4	8,0

Table 4-1: Reference values of K for the identified lithologies in the three studied sections. Blue is the mean of values which are read from the graphic. Black values are a theoretical estimation of what would correspond to the lithology in that bit size.

Lithology Type	K_8 vs. K_{17}		K_8 vs. K_{24}		K_{17} vs. K_{24}	
	Ratio	Deviation	Ratio	Deviation	Ratio	Deviation
Limestones	2,3	-9,1	3,5	3,8	1,5	9,9
Marls	**2,7**	**3,9**	3,2	-5,1	1,2	-12,1
Shales	**2,6**	**1,3**	3,3	-3,6	1,3	-8,4
Claystones	**2,5**	**-2,6**	**3,6**	**5,9**	**1,4**	**4,7**
Mudstones	**2,5**	**-2,6**	**3,5**	**3,8**	**1,4**	**2,6**
Siltstones	**2,6**	**2,5**	**3,3**	**-1,1**	**1,3**	**-7,2**
Sandstones	**2,5**	**-2,6**	**3,3**	**-3,6**	1,3	-4,8
Sands	2,4	-8,3	3,2	-5,1	1,4	-0,4
Average	2,6	3,0	3,4	5,3	1,4	6,3

Table 4-2: Relation between k values of the three studied sections. Blue are the values which are able to compare with each other and which are considered as being deviations. Small deviation from the average occurs with a large number of coincidences.

Values of K have not a simple linear relation with the bit size, proportionality constant is required (Table 4-3).

Relation of bit size	17 ½" – 8 ½"	24" – 8 ½"	24" – 17 ½"
Ratio K	2,6	3,4	1,4
Ratio bit size	2,1	2,8	1,4
Ratio K - Bit size	1,2	1,2	1,0

Table 4-3: Relation between bit size and K.

4.1. Discussing results

Current interpretations of lithology use the ROP as a basis of interpretation (2.1.3.1 ROP). The obtained ROP in the estimation of K comes from real progress calculated from measurements in the well. The comparison of the K with ROP estimation verifies that the use of K is an improvement in the quality of interpretation.

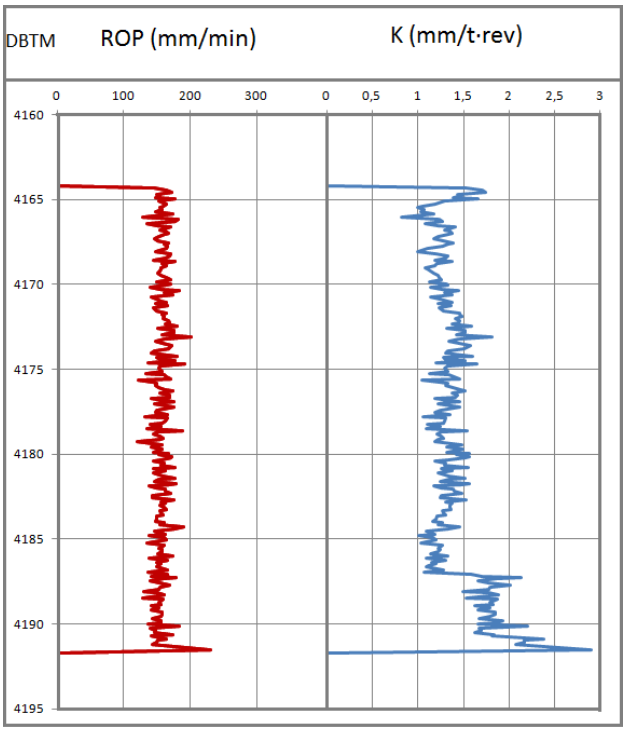

Figure 4-8: Comparison of ROP vs. K. This section corresponds to an area of shales interbedded with thin siltstones, according to the current interpretation methods and information on this stretch of the formation (Table 2-2). ROP line has an entirely straight line while the K line shows better the changes within the layer. The use of K allows the detection of two materials (shales and siltstones) instead of a single material that reflects ROP

The comparison between ROP and K values indicates that the use of K is an improvement in the lithological characterization of materials with medium-high hardness (shales and marls). Table 4-4 compares the lithological characterization using both interpretative bases ROP and K. Deviations of ROP-K ratio from the average in these materials confirm that the use of ROP has shortcomings. This relation is more or less linear except in the case of shales which have an average deviation of 30% in the three studied sections.

Lithology Type	ROP measured values	ROP vs. K_{24}			ROP vs. K_{17}			ROP vs. K_8		
		Ratio	Deviation inc. Shales	Deviation exc. Shales	Ratio	Deviation inc. Shales	Deviation exc. Shales	Ratio	Deviation inc. Shales	Deviation exc. Shales
Limestones	30	300	-0,9	0,3	**200**	**-14,6**	**-9,5**	86	-7,1	-3,4
Marls	70	280	-7,5	-6,4	**233**	**-0,3**	**5,6**	**88**	**-5,2**	**-1,4**
Shales	150	375	23,8	23,8	**300**	**28,2**	35,8	**115**	**25,0**	30,1
Claystones	220	**314**	**3,8**	**3,8**	**220**	**-6,0**	**-0,4**	**88**	**-4,7**	**-0,8**
Mudstones	300	**300**	**-0,9**	**-0,9**	**214**	**-8,5**	**-3,0**	**86**	**-7,1**	**-3,4**
Siltstones	450	**300**	**-0,9**	**-0,9**	**237**	**1,2**	**7,2**	**90**	**-2,5**	**1,5**
Sandstones	600	**300**	**-0,9**	**-0,9**	231	-1,4	4,5	**92**	**0,0**	**4,1**
Sands	750	**300**	**-0,9**	**-0,9**	221	-5,8	-0,1	94	1,6	5,7
Average		303			234			92		

Table 4-5: Comparison of the three sections with ROP showing the deviation from the average. Blue are the values which are used to calculate the average deviation from the ratio. Shales are those which cause more deviation from the average.

The relation K-ROP is more or less linear except in the case of shales. The difference between the lithologies suggested by K and ROP becomes most notable for shales in the interpretations. The use of K as interpretive basis exceeds clearly to ROP in these cases. Errors in the interpretation using K are caused by the lack of consideration of pore pressure in the model. This deficiency can be remedied by implementing the pore pressure in the model considering other wells with verified data.

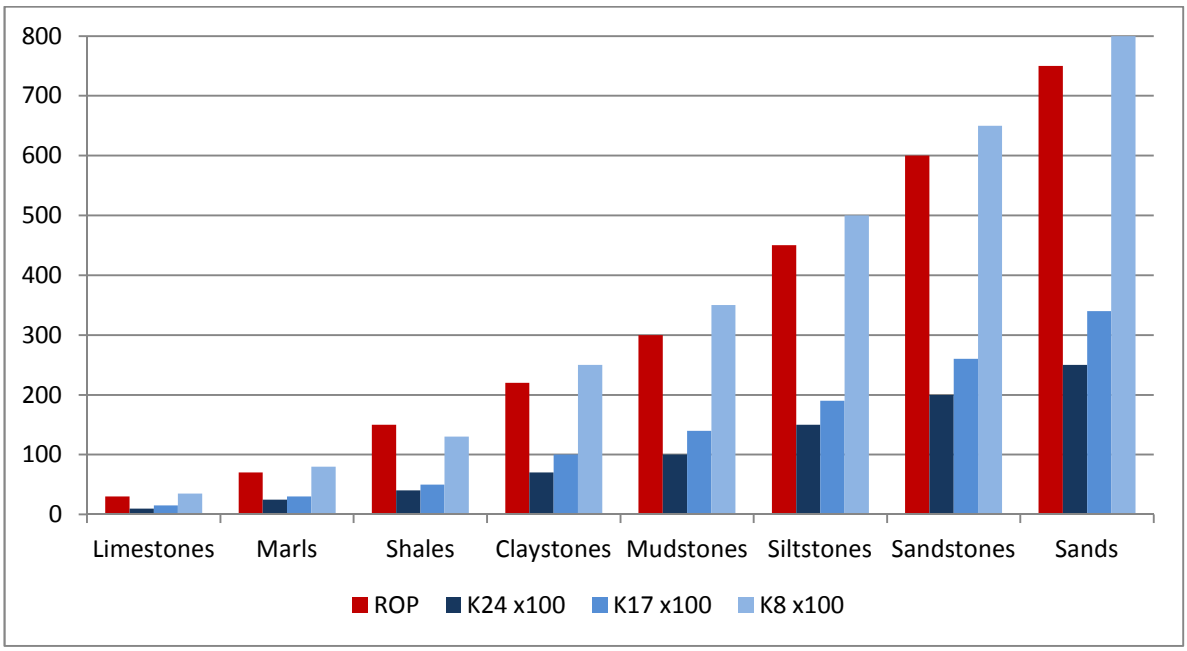

Figure 4-9: Graphic representation of the different values of K and ROP in the present lithologies of C-47.

4.2. Previous published work

A suitable reference to compare this model is the NROP model presented in Chapter 2. The NROP is similarly used for predicting lithology, and also has application for the pore pressure prediction. The curve is calculated by applying a filter to the parameters which affect ROP.

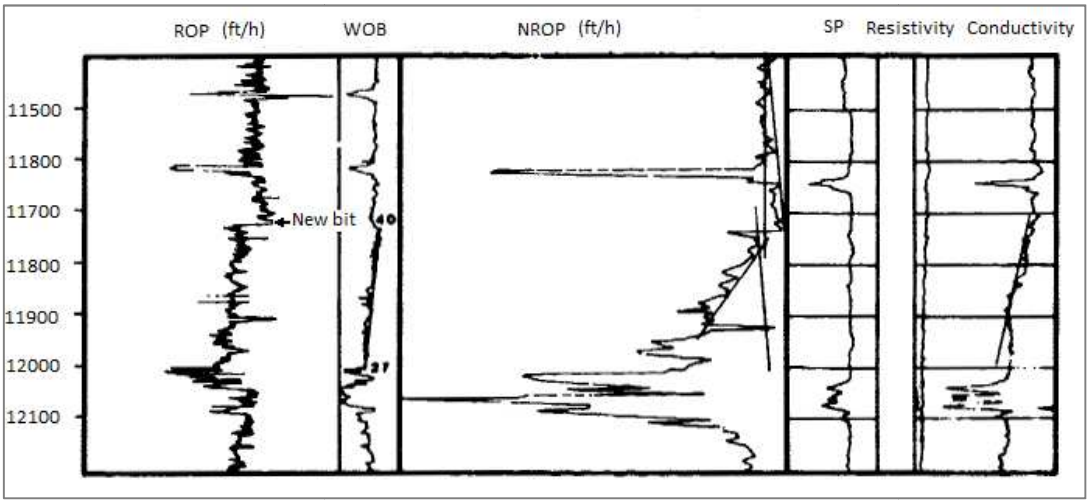

Figure 4-10: Comparison of ROP and WOB with NROP, SP, resistivity and conductivity (Provost Jr. 1987).

The trace of NROP presents more abrupt changes than simple ROP; analogously these changes appear in trace K. These changes allow a better comparison than using ROP.

Both methods shed more light than can be extracted using standard methods for predicting lithology. The model of NROP aided by geophysical logs also shows increases in pore pressure. The example studied here does not allow comparison with logs to verify if this relationship is possible. Moreover, it shows some marked differences that allow better lithological characterization.

4.3. Method

The method does not require complex mathematical operations which are depending on many factors. The inputs in obtaining K are simplified in order to minimize errors associated with the method. Using this simple equation for K, the use of parameters is reduced to ROP, WOB, RPM and C; having ROP and WOB as the most important in the calculation. RPM is almost always constant during most of the time of drilling; and in the well which is studied, there are no appreciable lithological differences so C is taken as constant according to the Table 3-5.

The calculation is performed from the equation (16) where all factors which affect the ROP are not taken into account. The drillstring configuration, the bit type, size and its conditions, bottom hole cleaning and hydraulic are left out. In addition, there are other factors which are beyond our control; such as compaction due to the depth, or the pressures which affect the

formation. Therefore, it has to be taken into account in the evaluation of the results the previous knowledge about the formation.

In the data provided by the company it was observed that three bits were used in only six meters. Poor condition or a bad configuration can lead to inadequate data, which carry interpretations, to the failure. These areas should be treated with extreme caution because the graph values are subjective.

The data selection processes is thought to eliminate those which were erroneous, for this reason it is applied the filter criteria which is listed above. Grouping has the main motivation to eliminate the very local conditions which lead to fail in interpretation (e.g. a punctual occurrence of quartz grains in an area of clays, without entailing any lithological change, can result in a peak in the curve). Moreover, when the area which is interpreted is large enough these variations are irrelevant.

The method results in achieving the curve K that is the reference for the interpretation of lithology. This analysis is performed by comparing K with current forms of estimation based on ROP.

4.4. Goal

The aim of this thesis is partly fulfilled due to the fact that a relationship between K and lithology which depends on the type and diameter of the drill is achieved, but the pore pressure is ignored. Changes in hardness of lithology affect the drilling process and obtaining K serves to help solve the problems encountered during drilling.

4.5. Restrictions or limitation

Comparisons which help to refine the model are not possible having only the data of one well. The lithological information provided by the company is too poor to establish a relationship with those obtained in the model leading to validation. The absence of logging forces to make interpretation without references which may endorse the results. Changes due to increases in pore pressure cannot be detected when lacking the necessary information.

The fact that it is a horizontal well at its final part, maintains drilling in the same formation. This suggests more lateral facies changes than changes between different lithologies. Similar materials are handled which do not allow the treatment of K in absolute terms, forcing to make relative comparisons.

Processing operations on data eliminate many different sections resulting in that there is no complete set of data from the well. The main sources of error are in the management of data that are lost by filtering, and Matlab import Excel to provide some inconsistent values.

The process of data pooling in set of 5 and 25 datapoints leads to clean the noise in data. But when the datapoints with which is calculated the average contain a gap; the value of these calculated points is wrong because they use values which are not in consecutive spaces.

Hardness estimation for the constant C is based on average values which do not take account of changes due to diagenetic processes. The compaction and cementation of the layers generates K decrease, and the dissolution causes its increase. The materials which show values with less variability such as quartzite or gneiss have no presence in oil wells. The wide range of values in which the hardness of the present formations varies, hinder to find the exact value for C.

The bit size varies the value of K for the same materials requiring standardization depending on the type and size of bit. The mechanical properties of the materials traversed depend, in some cases, on the angle of incidence of perforation (e.g. phyllosilicates have different properties depending if they are drilled from the top of the layer or from the inside, for that reason the direction of foliation can have influence on hardness).

The lack of references about pore pressure does not allow an adequate estimation of overpressured zones, causing K values higher than the actual material.

4.6. Quality and shortcomings of model

The model generates a drillability value associated with each drilling point based on real data which is a considerable help to detect trouble spots. On the one hand, the limitations of the available information, the fact that K has different values in relation to the size of the bit, and dismiss of pore pressure, causing an arbitrary interpretation at some points. On the other hand, the model maintains its utility to identify layers according to their relative hardness, despite the occasional difficulty of relating these layers to the lithology.

Whole model runs in Excel and therefore requires an informatics implementation in order to be used in real time. This is only a preliminary step; however no new equipments are required, so the costs of implementation are scarce.

Handling large amounts of data requires powerful computers which are capable of moving a lot of information making it difficult to the management of this data. The calculation of K in real time requires the use of parameters which are measured at the same time so that the filtering operations performed a posteriori in the model could not be performed. This leads to the occurrence of improper values for K and the need of evaluating the curve by qualified personnel.

4.7. Future improvements

Comparison of data from wells which penetrate formations of various kinds will be the next step to obtain a relationship between the value of K measured in drilled meters per ton of cargo

and revolution; and the different types of lithologies. The study of formations with well known lithologies is the base that the value K would be associated with this particular material. A range of lithologies including not only sedimentary rocks will enable its widespread use.

Other adjustments in connection with the drilling method, setting the drillstring, cleaning into the bottomhole, and hydraulic can be made from the detailed study of the drilling.

This discussion has established that size of the bit and pore pressure, have influence on K. This reason forces a correction in the calculation of K in order to compare K from different wellhole section. The formula can be improved as it is proposed below:

$$K = \frac{\mathrm{ROP}}{\mathrm{WOB} \cdot \mathrm{RPM}^{c_1}} \cdot \frac{e^{-wt}}{c_2 B_s} \cdot c_3 d \tag{19}$$

Where B_S refers to the bit size; c_2 is a proportionality constant which is depending on the type and configuration of bit; e^{-wt} is dependent from bit wear; c_3 is a correction factor; and d is the average fluid density and can be calculated from (7) as:

$$d = 10 \,.\, \frac{P_h}{h} \tag{20}$$

5. Conclusion.

The model shows a more efficient detection of lithologies than simply using the ROP. K is useful for detecting changes in hardness within the same layers. This is especially evident in the case of the shales. Where the use of ROP shows one uniform layer, K shows the variability of material within it.

Early detection of changes in lithology and hardness of the layers is an extra source of information. Its use helps to find the points which can cause problems within the bore.

The limitations of the model, such as different scales of values which K has as a function of the size and type of bit, or exaggeration of its value in overpressured zones; require careful interpretation to associate values of K to lithologies. The lithological identification is methodical after obtaining such association.

The development model is oriented to improve cost reduction with the help of the provided information. The bit election can be changed on the basis of these data. In horizontal drilling, such as this in its final part, faults and lateral changes of facies may change the expected circumstances.

A study completed later with geophysical data to frame the characterization of the perforated area can guide a future well construction.

6. Nomenclature.

A	Area
BPOS	Block Position
C	RPM Exponent
d	Average Fluid Density
DBTM	Measured depth of bit
DM or DMEA	Measured depth
F	Force
g	Gravity
h	Height
HKL	Hook Load
i	Hydraulic Gradient
k	Permeability
K	Drillability
K	Hydraulic Conductivity
L	Length
M	Formation threshold weight (lbs.)
MFI	Mud Flow In
MPD	Medium Density Particleboard
MWD	Measurement While Drilling
MWn	Normal mud weight (ppg)
Nn	Normal rotary speed (rpm)
No	Observed rotary speed
NROP	Normalized Rate of Penetration
NW	Observed mud weight
Pbn	Normal bit pressure drop (psi)
Pbo	Observed pressure drop
p_c	Capillary
P_h	Hydrostatic Pressure
P_p	Pore Pressure
Q	Volumetric Flow
Qn	Normal circulation rate (gpm)
Qo	Observed circulation rate
r	Rotary exponent (dimensionless)
ROP	Rate of Penetration
ROP	Observed rate of penetration (ft. /hr.)
RPM	Revolution per minute
RPMB	Revolution per minute in bit
S	Overburden Stress
SPP	Stand Pipe Pressure
TFAn	Normal bit nozzle area (in2)
TFAo	Observed bit nozzle area

TRQ	Torque
TVD	True Vertical Depth
Wn	Normal bit weight (lbs.)
Wo	Observed bit weight
WOB	Weight on bit
ε	Strain
μ	Viscosity
ρ	Density
ρ_b	Formation Average Bulk Density ($g \cdot cm^{-3}$)
ρ_f	Formation Fluid density (g·cm-3)
ρ_m	Matrix Density
σ	Stress
Φ	Porosity
Φ_{ef}	Effective Porosity
Φ_{nef}	Ineffective Porosity

7. Rosters

8.1. Figures

8.3. Tables

8. References.

Annenberg Foundation. *Earth & Space Science.* 2013. http://www.learner.org/courses/essential/earthspace/session2/closer1.html (accessed January 2013).

Bear, Jacob. *Dynamics of Fluids in Porous Media.* Ottawa: American Elsevier Pub. Co, 1972.

Bilgesu, H.I., L.T. Tetrick, U. Altmis, S. Mohaghegh, and S. Ameri. "A New Approach for the Prediction of Rate of Penetration (ROP) Values." *SPE Eastern Regional Meeting, 22-24 October 1997.* Lexington: Society of Petroleum Engineers , 1997.

Boggs, Sam Jr. *Principles of Sedimentology and Stratigraphy.* New Jersey: Pearson Education, Inc., 2011.

Christophersen, Lise. *Final Well Report: Drilling and Completion 34/10-C-47.* Statoil, 2007.

Dandekar, Abhijit Y. *Petroleum Reservoir Rock and Fluid Properties.* Boca Raton, FL, USA: Taylor & Francis, 2006.

Deegan, C. E., and B. J. Scull. *A standard lithostratigraphic nomenclature for the Central and Northern North Sea.* London: Institute of Geological Sciences, 1977.

Devereux, Steve. *Drilling Technology in nontechnical language.* Tulsa: Patterson, 1999.

Faleide, Jan Inge, Knut Bjørlykke, and Roy H. Gabrielsen. *Geology of the Norwegian Continental Shelf.* Heidelberg: Springer-Verlag , 2010.

FSU. *Florida State University. Geological Sciences.* 2013. http://www.gly.fsu.edu/~salters/GLY1000/11Seds_sedrocks/11Seds_sedrocks.htm.

G. Mensa-Wilmot, S. Southland, P. Mays, P. Dumrongthai, and D. Hawkins, Chevron, and P. Ilavia, Consultant. "Performance Drilling – Definition, Benchmarking, Performance Qualifiers, Efficiency and Value." *Drilling Conference and Exhibition.* Amsterdam: Society of Petroleum Engineers, 2009.

Gillis, Gretchen. *Oilfield Glossary.* 2013. http://www.glossary.oilfield.slb.com/en/Disciplines/Geology.aspx (accessed January 2013).

Hagoort, Jacques. *Fundamentals of Gas Reservoir Engineering.* Amsterdam: Elsevier Science Publishers, 1988.

Hannsen, T.H. “Rock Properties.” *Norwegian Tunnelling Today* (Norwegian Soil and Rock Engineering Association), no. 5 (1998): 41-44.

Herod, Matt. *GeoSphere.* 13 June 2011. http://globalgeology.blogspot.no/2011/06/back-to-basics-on-groundwater.html (accessed January 2013).

Hesthammer, J., T.E.S. Johansen, and L. Watts. “Spatial relationships within fault damage zones in sandstone.” Edited by Statoil. *Marine and Petroleum Geology, Volume 17, Issue 8*, September 2000: 873–893.

Hyne, Norman J. *Dictionary of Petroleum Exploration, Drilling & Production.* Tulsa: Pennwell Publishing Company, 1991.

J.Thomson, Ian, and Rohit Mathur. “The Use of Downhole Drilling Parameters Combined With Surface and Downhole Mechanical Specific Energy Data Helped Identify Underreamer Dysfunctions In GoM Deepwater Projects.” *SPE Deepwater Drilling and Completions Conference.* Galveston, Texas, USA: Society of Petroleum Engineers, 2010. 18.

Johnson, David E., and Kathrynne E. Pile. *Well Logging in Nontechnical Language.* Tulsa, Oklahoma: PennWell, 2002.

Jung, S J, Keith Prisbrey, and Guanglin Wu. *Prediction of rock hardness an drillabillity using acoustic emission.* Rotterdam: Rock Mechanics as a Multidisciplinary Science, Roegiers, 1991.

King, George E. *5000 Oilfield Terms: A Glossary of Petroleum Engineering Terms, Abbreviations and Acronyms.* George E. King Engineering Inc., 2010.

Leet, Lewis Don, and Sheldon Judson. *Physical Geology.* Englewood Cliffs: Prentice-Hall, 1965.

Lippard, Stephen John. *TGB4160 - Petroleum Geology - Lecture notes.* Trondheim: NTNU, 2011.

Miles, Jennifer A. *Illustrated Glossary of Petroleum Geochemistry.* New York: Oxford University Press, 1994.

Moore, Preston L. *Drilling practices manual.* Tulsa, Oklahoma: PennWell, 1986.

Mouchet, J P, and A Mitchell. *Abnormal Pressures While Drilling.* Boussens: Elf Aquitaine, 1989.

Nash, Katelyn M. *Shale Gas Development.* New York: Nova Science Publishers, Inc, 2010.

Nilsen, Bjørn, and Alf Thidemann. *Hydropower Development. Rock Engineering.* Trondheim: Norwegian Institute of Technology, 1993.

Norwegian Petroleum Directorate. *Norwegian Petroleum Directorate - FactPages.* 2013. http://factpages.npd.no/factpages/default.aspx (accessed February 2013).

Pawnee and Edwards Geology and Groundwater. "Kansas Geological Survey." June 2004. http://www.kgs.ku.edu/General/Geology/Pawnee/06_gw.html (accessed January 2013).

Provost Jr., C.E. "A Real-Time Normalized Rate of Penetration Aids in Lithology and Pore Pressure Prediction." *SPE/IADC Drilling Conference, 15-18 March 1987.* New Orleans: Society of Petroleum Engineers, 1987.

Ramm, Mogens, and Alf E. Ryseth. "Reservoir quality and burial diagenesis in the Statfjord Formation, North Sea." *Petroleum Geoscience*, 1996: v.2; p313-324.

Ramsey, Mark, and Texas Drilling Associates. *Oilfield Glossary.* 2013. http://www.glossary.oilfield.slb.com/en/Disciplines/Drilling.aspx (accessed January 2013).

Ryseth, Alf, and Mogens Ramm. "Alluvial architecture and differential subsidence in the Statfjord Formation, North Sea: prediction of reservoir potential." *Petroleum Geoscience*, 1996: v.2; p271-287.

Scott, Paul. *Wisegeek.com.* 2013. http://www.wisegeek.com/what-does-weight-on-bit-mean.htm (accessed January 2013).

Selley, Richard C. *Applied Sedimentology.* London: Academic Press, 2000.

Shanmugam, G., and J. B. Higgins. "Porosity Enhancement from Chert Dissolution Beneath Neocomian Unconformity: Ivishak Formation, North Slope, Alaska." *AAPG Bulletin*, May 1988: 523-535.

Singer, Julian. *Schlumberger Oilfield Glossary.* 2013. http://www.glossary.oilfield.slb.com/en/Disciplines/Drilling-Fluids.aspx (accessed January 2013).

Statoil. "Statoil.com." 2013. http://www.statoil.com/en/OurOperations/ExplorationProd/ncs/Gullfaks/Pages/default.aspx (accessed January 2013).

Stuck Pipe Course. Interpretado por Statoil. 1992.

Tarbuck, Edward J., y Frederick K. Lutgens. *Earth. An Introduction to Physical Geology.* New Jersey: Pearson, 1993.

Tucker, Maurice E. *Sedimentary Petrology.* Oxford: Blackwell Scientific Publications, 1981.

Zarza, Ana M. Alonso. «Petrología sedimentaria. Notas de teoría.» *Reduca (Geología)*, 2010: Vol.2. Nº3.

Ziaja, M.B., and J.C. Roegiers. *Lithology Diagnosis Based on the Measurements of Drilling Forces and Moments at the Bit.* Jakarta: Society of Petroleum Engineers , 1998.

9. Appendices.

A. Export data to excel

This appendix sets out the procedure to export data from Matlab to Excel and what is needed to generate the graphics. The first part of the process, export, requires to operate several files in Matlab. The process is the following:

a) Open all given files and run runConfig.m in order to fix Matlab current directory. This directory is different for each section and refers to the folder where the files are.

```
op_system = 'windows';
screenx = 1024;
screeny = 768;

mat_dir = 'E:\Usuario\Tesis\RTDD_uduak\C-47-all sections\8_5_inch';
```

b) Run and close viewedge.m to prepare the file to be exported and get its preview.

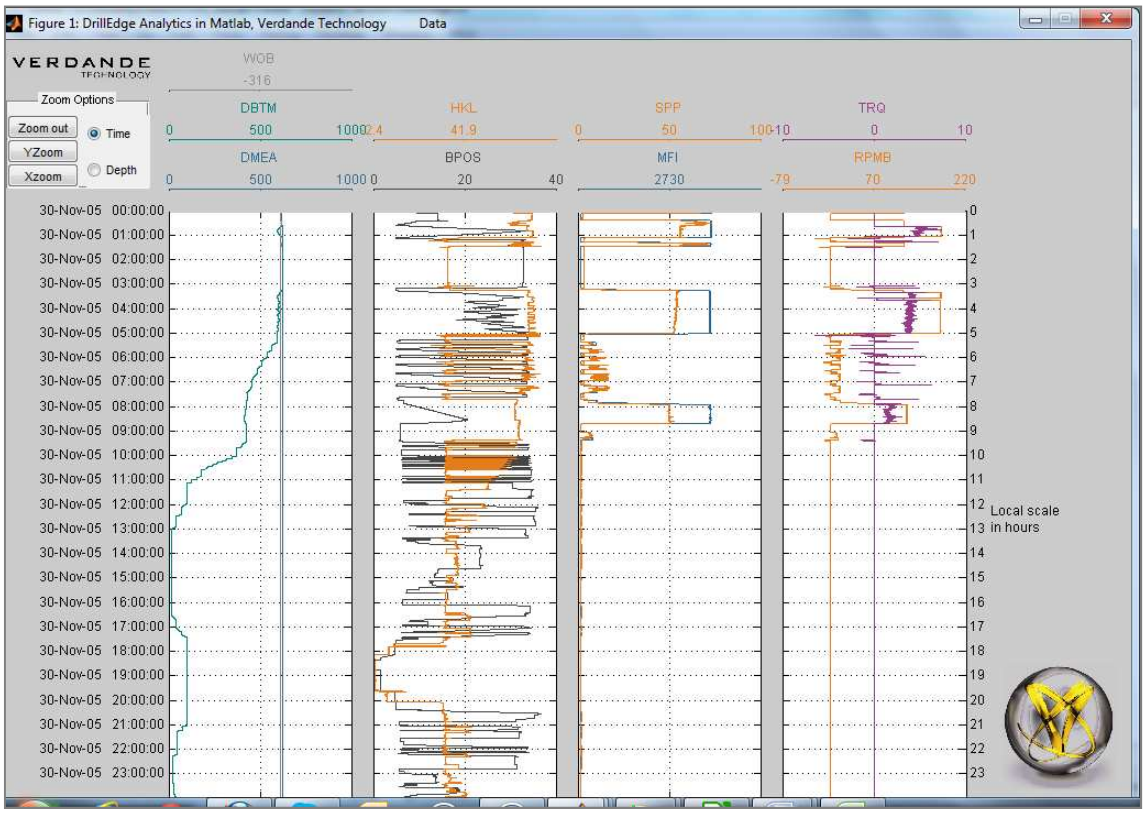

Figure 9-1: Preview of the data in Matlab

```
runConfig;

a = dir(mat_dir);

% file_name = a(3).name;
```

```
file_name = a(4).name;

 X = importH5(fullfile(mat_dir,file_name));

tagged = [];
recognized = [];

viewgui(screenx,screeny,op_system,[],[],'Time',...
   X,'DMEA','DBTM','WOB','BPOS','HKL',[],'MFI','SPP',[],...
   'RPMB','TRQ',[],...
   [1 0 0 0],recognized,tagged);
```

c) In order to write the data into 'tab delimited.txt' file run LT030706_write_POOH_data.m where it is necessary to change the name of the file which we want to export each time (six different positions).

```
file2 = 'LT120405.ASC.h5';

if file2 == file_name

% POOH start: 07-March-06 06:00:00
% POOH stop: 07-March-06 00:00:00
hours_to_POOH_start = 6;
hours_to_POOH_stop = 24;
POOH_start_index = hours_to_index(hours_to_POOH_start);
POOH_stop_index = hours_to_index(hours_to_POOH_stop);

%write trip data
LT120405_ASC_h5_data = fopen('24LT120405_ASC_h5_data.xls','w');
for i = POOH_start_index:POOH_stop_index
    fprintf(LT120405_ASC_h5_data,'%f\t %f\t %f\t %f\t %f\t %f\t %f\t %f\t %f\t
%f\n', ...
    X.Time(i),X.DBTM(i),X.DMEA(i),X.HKL(i), X.BPOS(i), X.SPP(i), X.MFI(i),
X.WOB(i), X.RPMB(i), X.TRQ(i)); % 10 columns will appear on the excel sheet:
Time, DBTM, etc
end
fclose(LT120405_ASC_h5_data);

% read POOH data
fid2 = fopen('24LT120405_ASC_h5_data.xls');
POOH2 = fscanf(fid2, '%f', [10 inf]);
fclose(fid2);
POOH2 = POOH2';

else
    disp('FILE MIX UP')
end
```

The second part is the management of data in Excel and it includes filtering and obtaining all plots.

d) Open the new .xls-file and transform it into .xlsx.

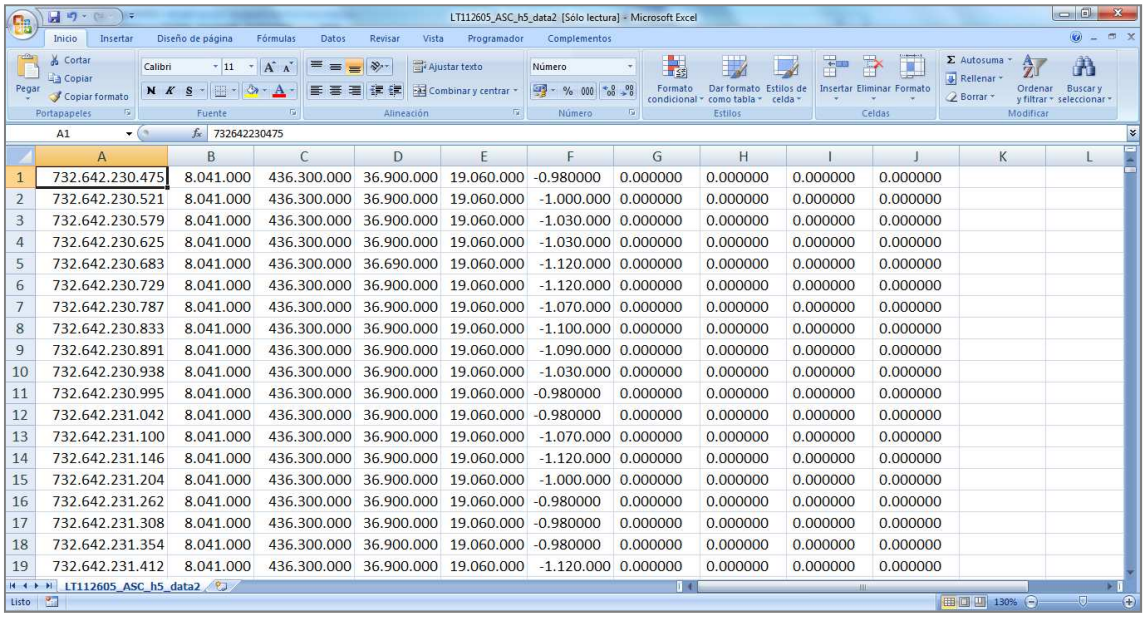

	A	B	C	D	E	F	G	H	I	J	K	L
1	732.642.230.475	8.041.000	436.300.000	36.900.000	19.060.000	-0.980000	0.000000	0.000000	0.000000	0.000000		
2	732.642.230.521	8.041.000	436.300.000	36.900.000	19.060.000	-1.000.000	0.000000	0.000000	0.000000	0.000000		
3	732.642.230.579	8.041.000	436.300.000	36.900.000	19.060.000	-1.030.000	0.000000	0.000000	0.000000	0.000000		
4	732.642.230.625	8.041.000	436.300.000	36.900.000	19.060.000	-1.030.000	0.000000	0.000000	0.000000	0.000000		
5	732.642.230.683	8.041.000	436.300.000	36.690.000	19.060.000	-1.120.000	0.000000	0.000000	0.000000	0.000000		
6	732.642.230.729	8.041.000	436.300.000	36.900.000	19.060.000	-1.120.000	0.000000	0.000000	0.000000	0.000000		
7	732.642.230.787	8.041.000	436.300.000	36.900.000	19.060.000	-1.070.000	0.000000	0.000000	0.000000	0.000000		
8	732.642.230.833	8.041.000	436.300.000	36.900.000	19.060.000	-1.100.000	0.000000	0.000000	0.000000	0.000000		
9	732.642.230.891	8.041.000	436.300.000	36.900.000	19.060.000	-1.090.000	0.000000	0.000000	0.000000	0.000000		
10	732.642.230.938	8.041.000	436.300.000	36.900.000	19.060.000	-1.030.000	0.000000	0.000000	0.000000	0.000000		
11	732.642.230.995	8.041.000	436.300.000	36.900.000	19.060.000	-0.980000	0.000000	0.000000	0.000000	0.000000		
12	732.642.231.042	8.041.000	436.300.000	36.900.000	19.060.000	-0.980000	0.000000	0.000000	0.000000	0.000000		
13	732.642.231.100	8.041.000	436.300.000	36.900.000	19.060.000	-1.070.000	0.000000	0.000000	0.000000	0.000000		
14	732.642.231.146	8.041.000	436.300.000	36.900.000	19.060.000	-1.120.000	0.000000	0.000000	0.000000	0.000000		
15	732.642.231.204	8.041.000	436.300.000	36.900.000	19.060.000	-1.000.000	0.000000	0.000000	0.000000	0.000000		
16	732.642.231.262	8.041.000	436.300.000	36.900.000	19.060.000	-0.980000	0.000000	0.000000	0.000000	0.000000		
17	732.642.231.308	8.041.000	436.300.000	36.900.000	19.060.000	-0.980000	0.000000	0.000000	0.000000	0.000000		
18	732.642.231.354	8.041.000	436.300.000	36.900.000	19.060.000	-0.980000	0.000000	0.000000	0.000000	0.000000		
19	732.642.231.412	8.041.000	436.300.000	36.900.000	19.060.000	-1.120.000	0.000000	0.000000	0.000000	0.000000		

Figure 9-2: Data in Excel. Columns resulting are Time, DBTM, DMEA, HKL, BPOS, SPP, MFI, WOB, RPMB, and TRQ.

e) Select columns Time, DBTM, DMEA, WOB, and RPMB and delete all the rest.
f) Generate a column subtraction DBTM-DMEA. Apply a filter number in this column to show only the values between zero and 1000. Columns WOB and RPM are also filter showing the values bigger than 1000. Copy the result of filtering to other sheet
g) Convert values from columns to suitable unit:
    a. 'Time' to minutes divided by 600
    b. 'DBTM' and 'DMEA' to meter dividing by 1.000.000
    c. 'WOB' to tonne dividing by 1.000.000
    d. 'RPM' to revolution per minute dividing by 1.000.000
h) Calculate ROP column: $DBTM_x$-$DBTM_{x-1}$/$TIME_x$-$TIME_{x-1}$
i) Get columns with the average of 5 and 25 values: (value x_1:value x_5)/5 and (value x_1:value x_{25})/25 for ROP, WOB and RPM.
j) Export to other sheet one of each 5 or 25 values: '=INDIRECT("sheet2!A"&5*ROW(A2)-4;1)' Where '"sheet2!A"' refers to the column which is imported; and '5*ROW(A2)-4;1' , refers to the interval of values to import and to the row where it starts.

k) Calculate the K column: '=ROP/(WOB*RPM^0,9)'
l) Create the graph collection

B. Graphs

This appendix lists the catalog of graphics obtained during the performance of the model. The graphics are presented showing the parameters plotted against DBTM (m). The vertical axes have relative values which are based on the explanation in section *3.3.* Hardness model result.

The graphics belong to two different areas of drilling; the first ten plots represent a working day for section 8 ½" and the ten following plots represent the nearby of the fault S2/S3. There are presented two groups of graphs for each of these areas, the first with sets of 5 datapoints and the second set of 25 datapoints. The colors of the lines are maintained in all graphs to help interpretation.

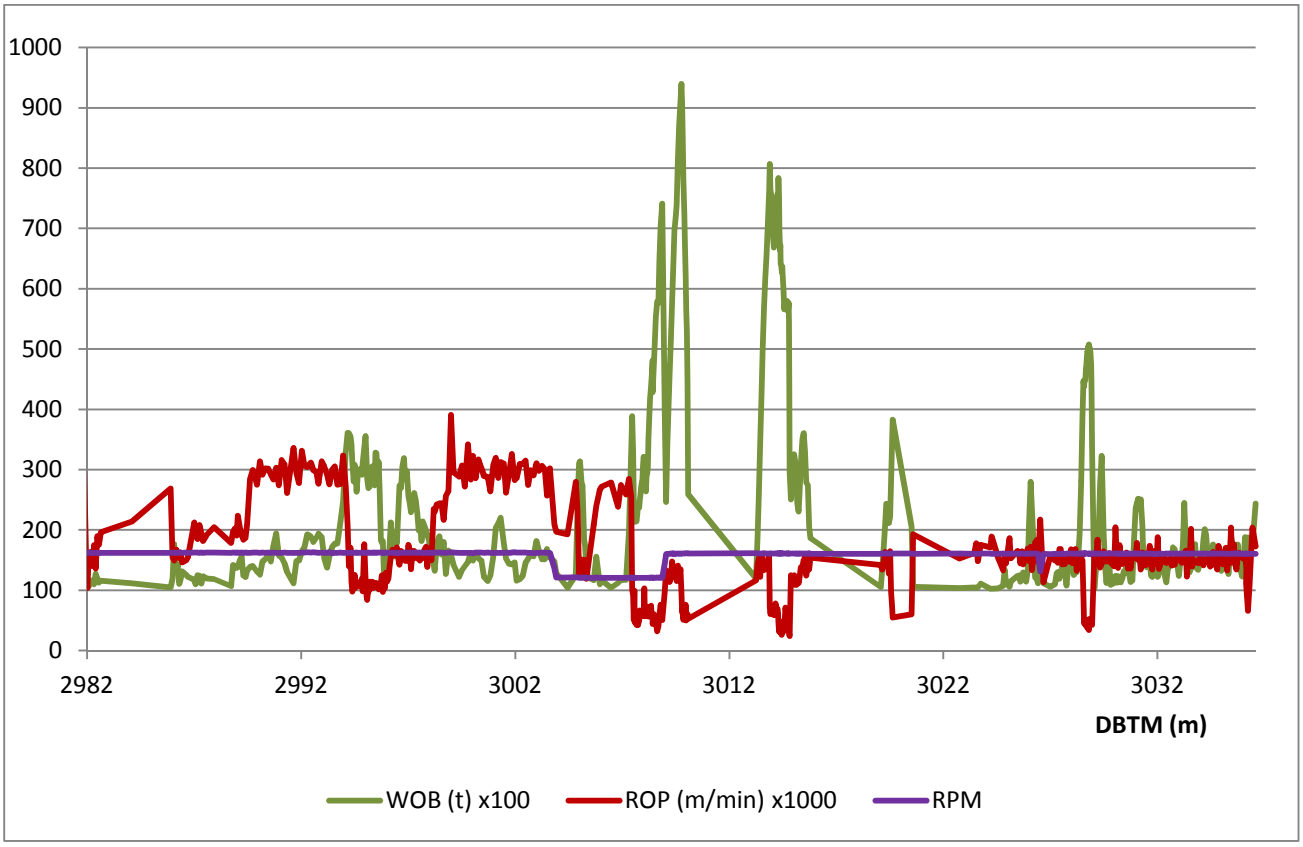

Figure 9-3: Comparison of ROP, WOB and RPM function of Depth (5 average)

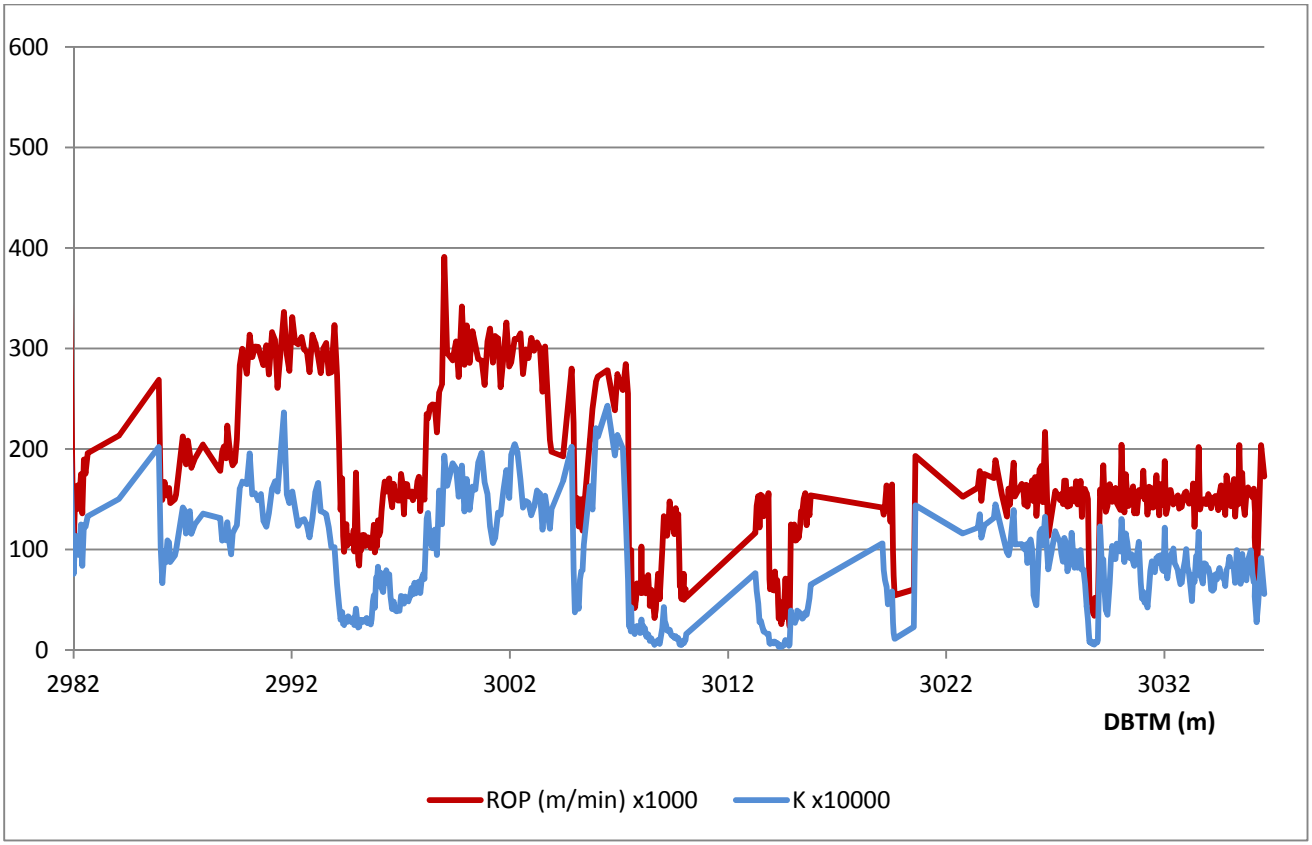

Figure 9-4: Comparison of ROP and K function of Depth (5 average)

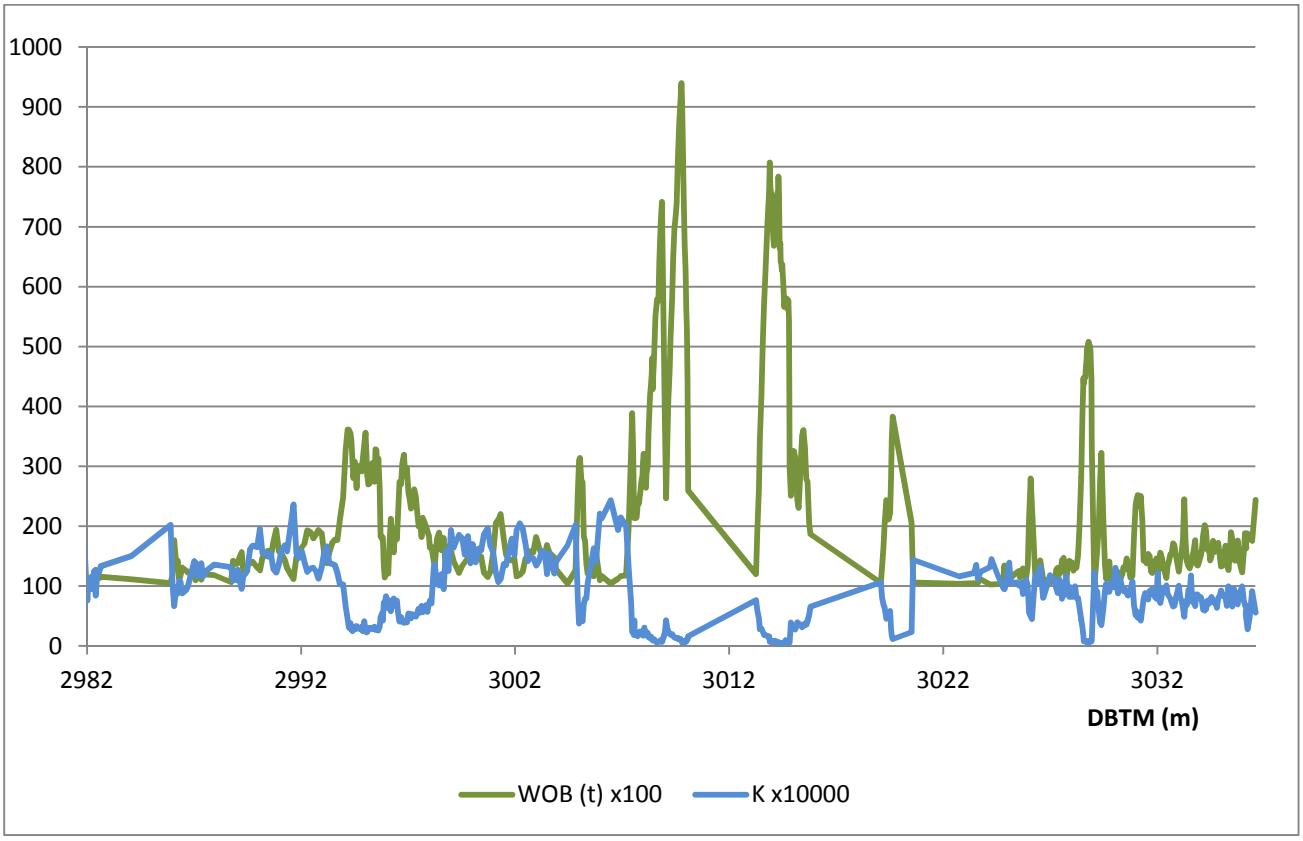

Figure 9-5: Comparison of WOB and K function of Depth (5 average)

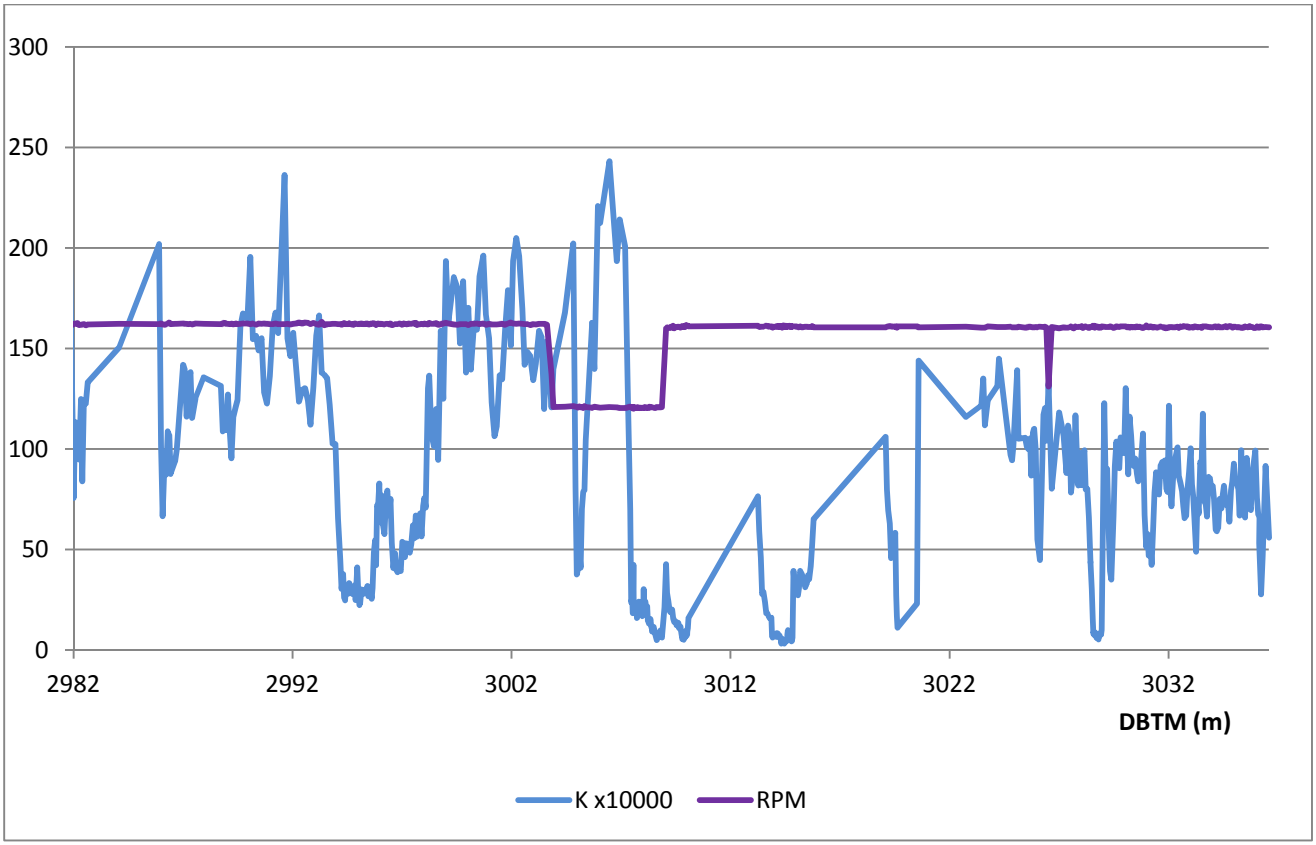

Figure 9-6: Comparison of RPM and K function of Depth (5 average)

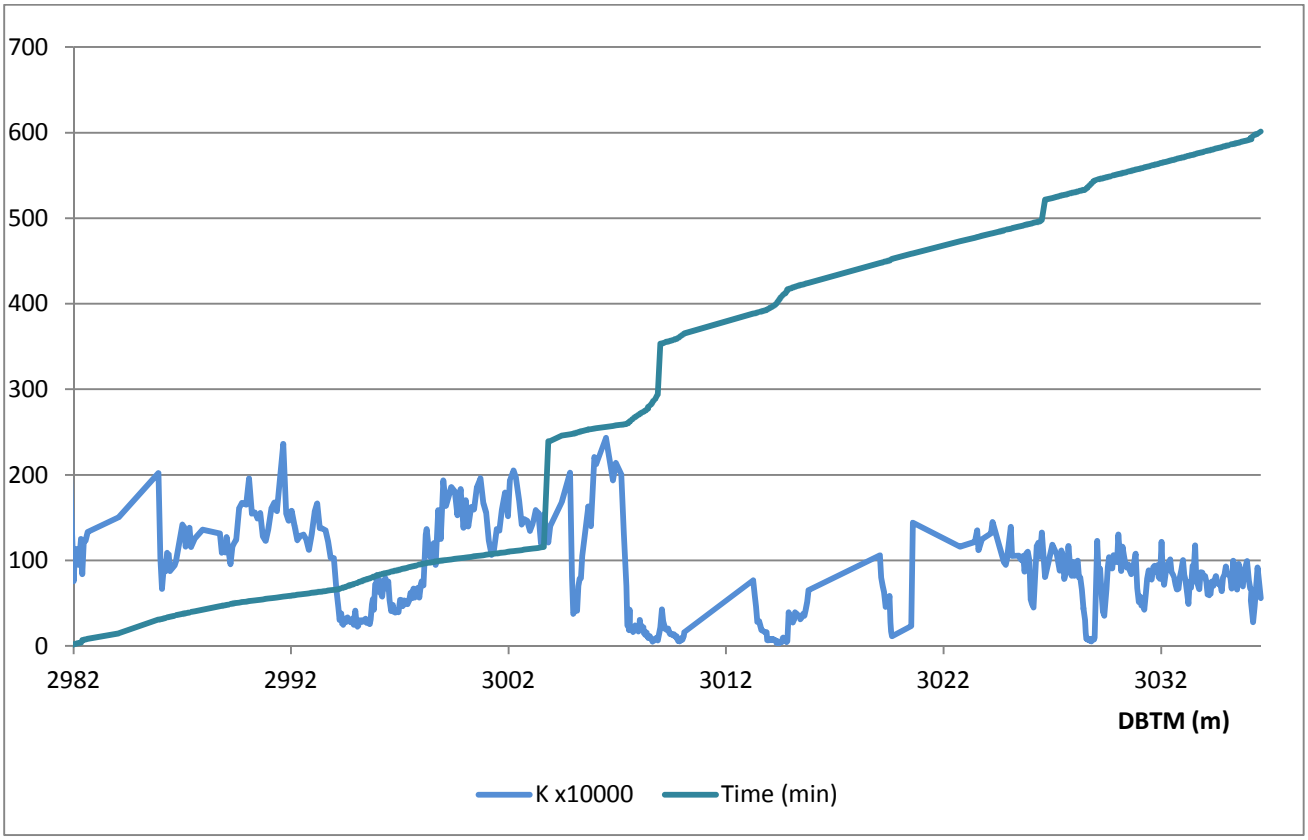

Figure 9-7: Comparison of K and Time function of Depth (5 average)

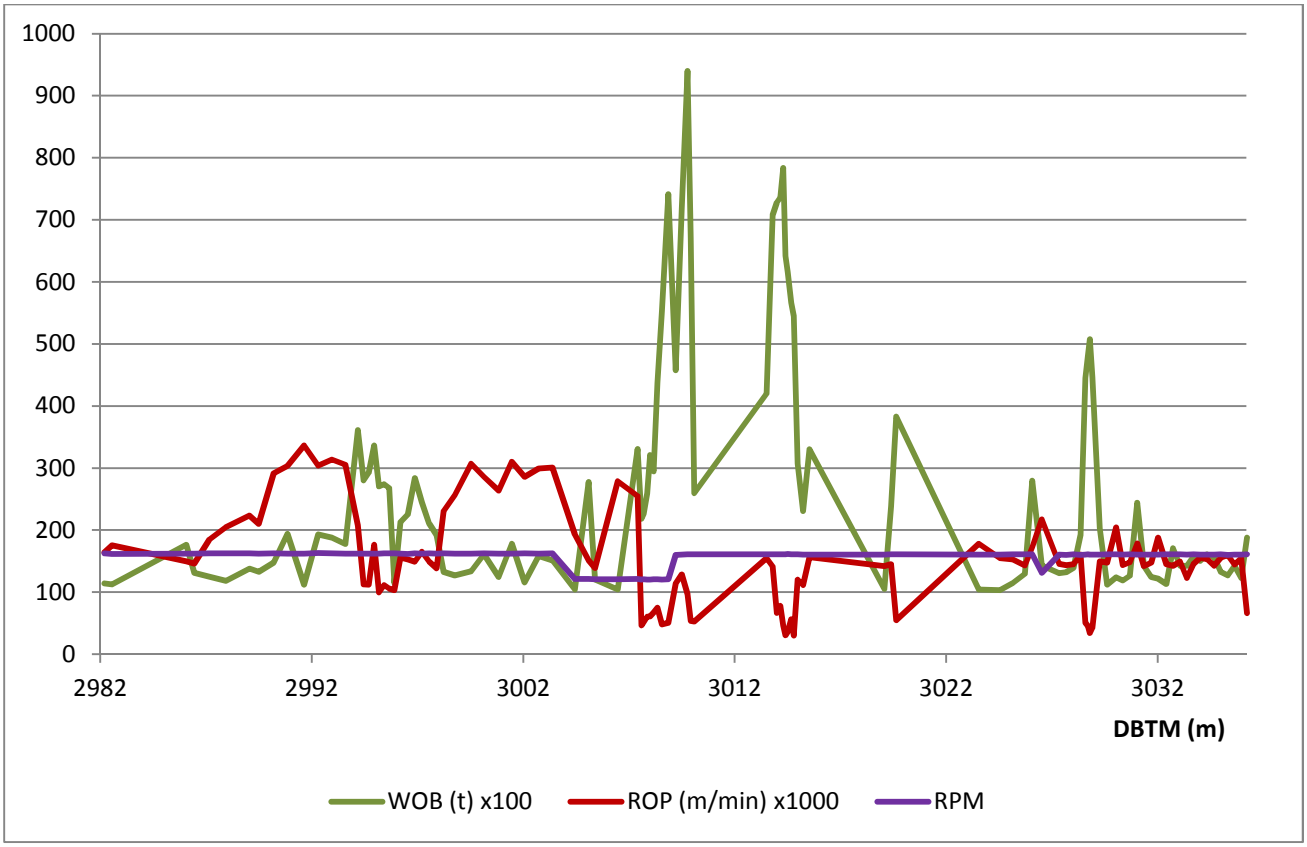

Figure 9-8: Comparison of ROP, WOB and RPM function of Depth (25 average)

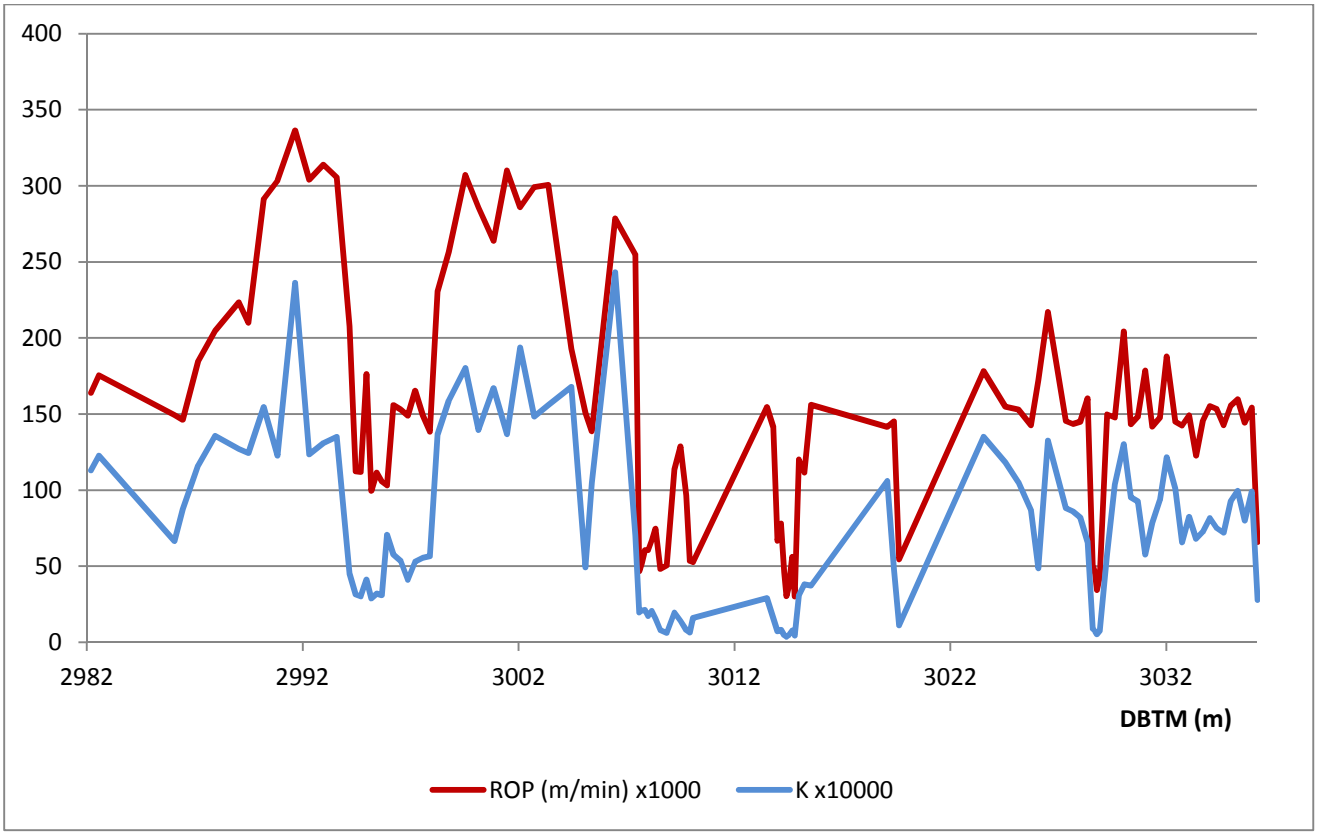

Figure 9-9: Comparison of ROP and K function of Depth (25 average)

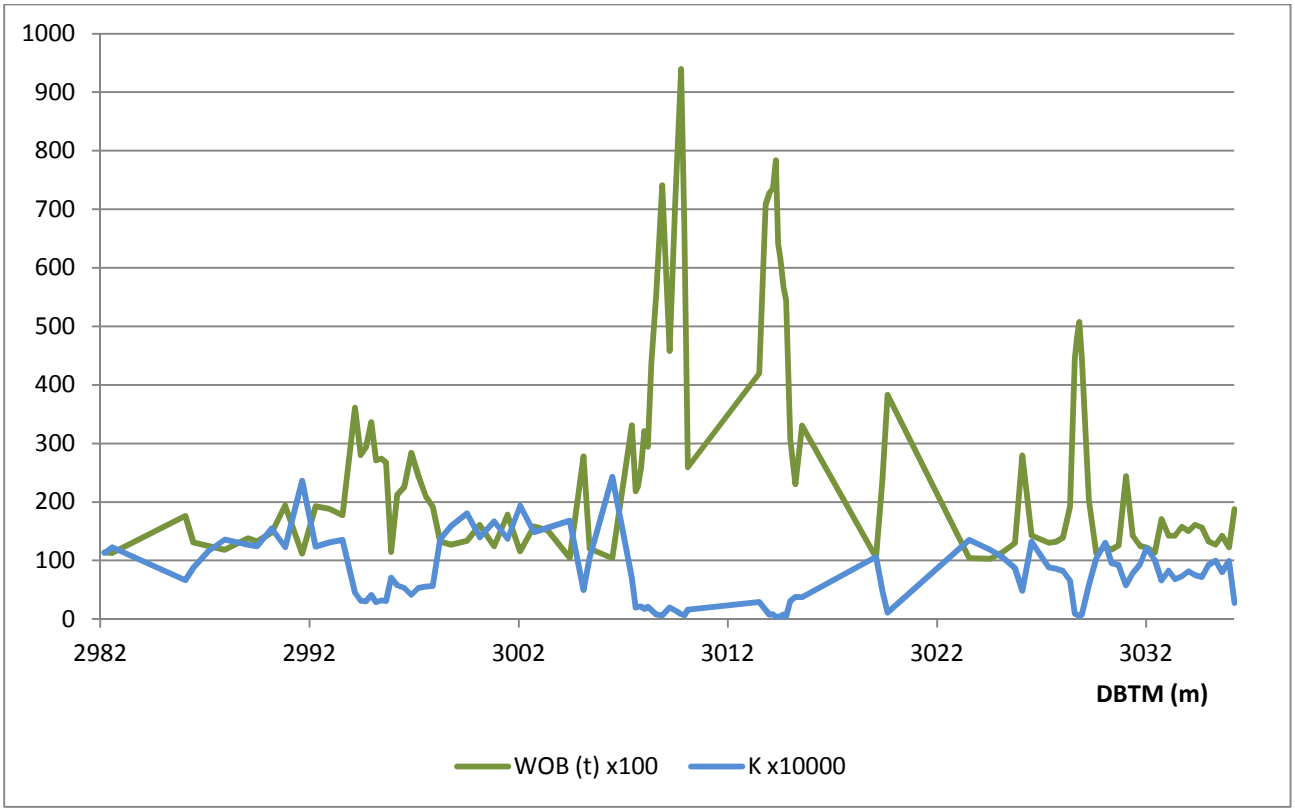

Figure 9-10: Comparison of WOB and K function of Depth (25 average)

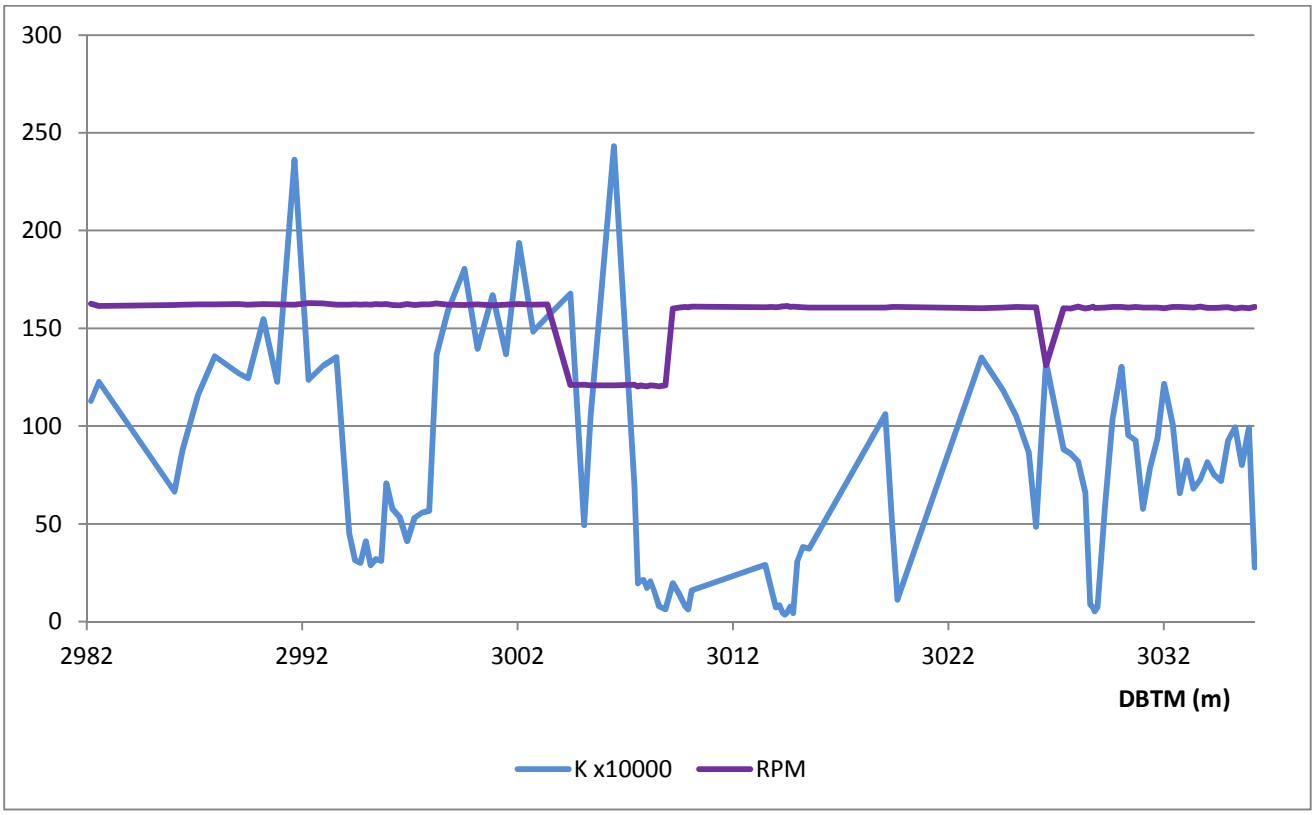

Figure 9-11: Comparison of RPM and K function of Depth (25 average)

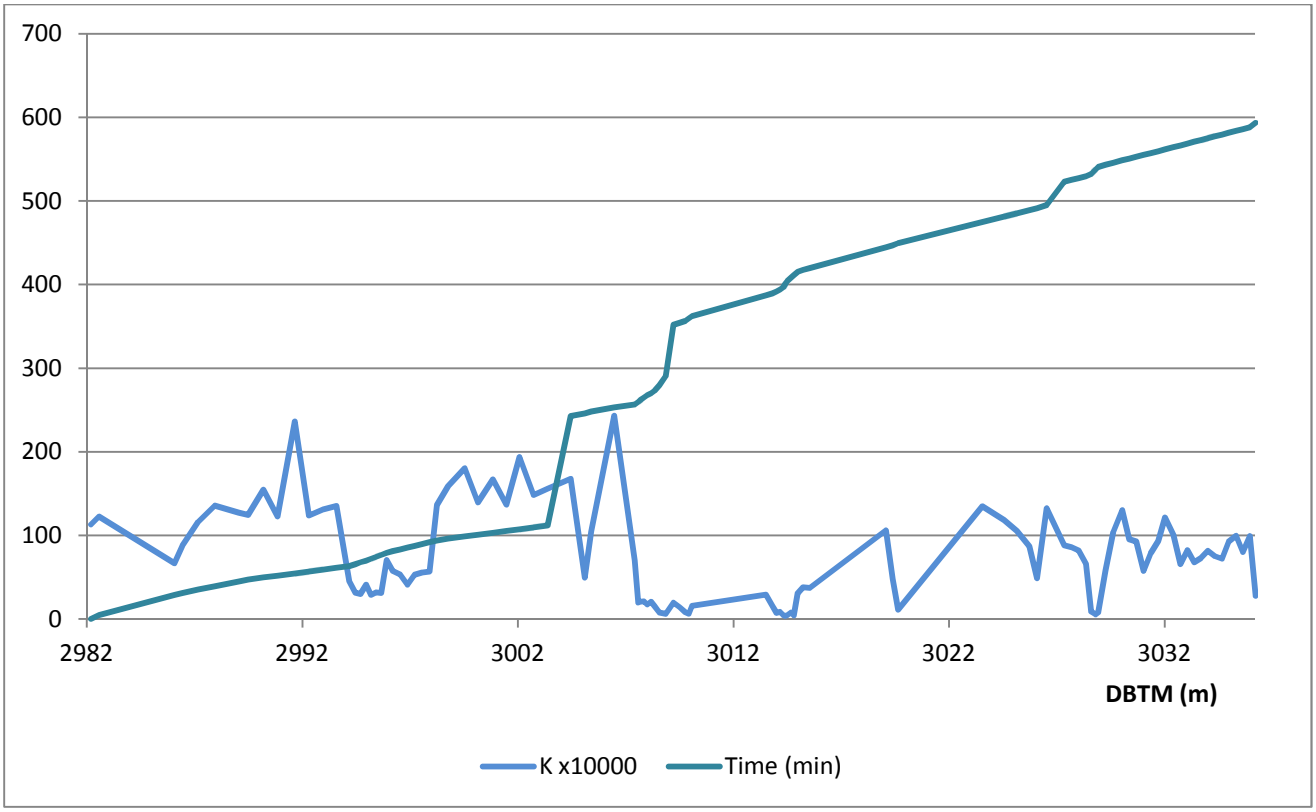

Figure 9-12: Comparison of K and Time function of Depth (25 average)

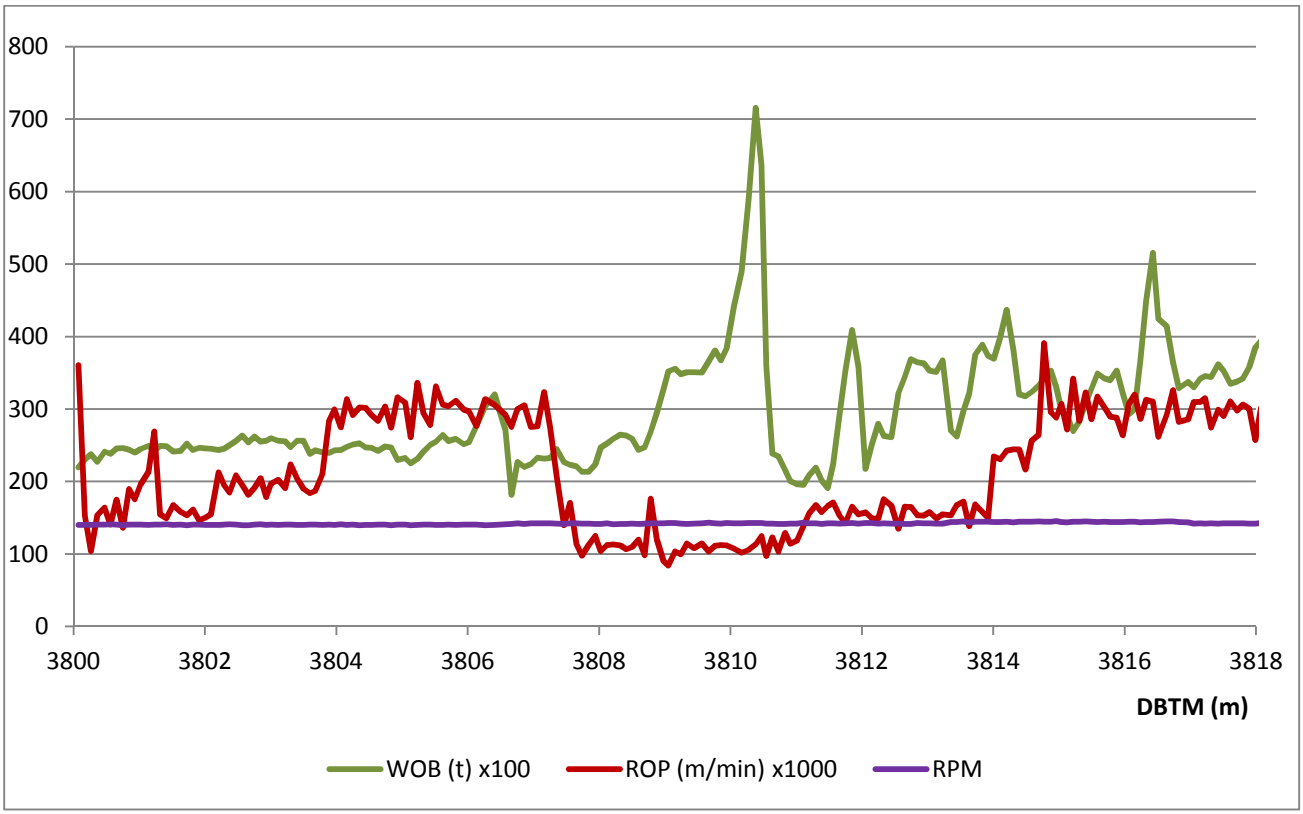

Figure 9-13: Comparison of ROP, WOB and RPM function of Depth section fault S2/S3 (5 average)

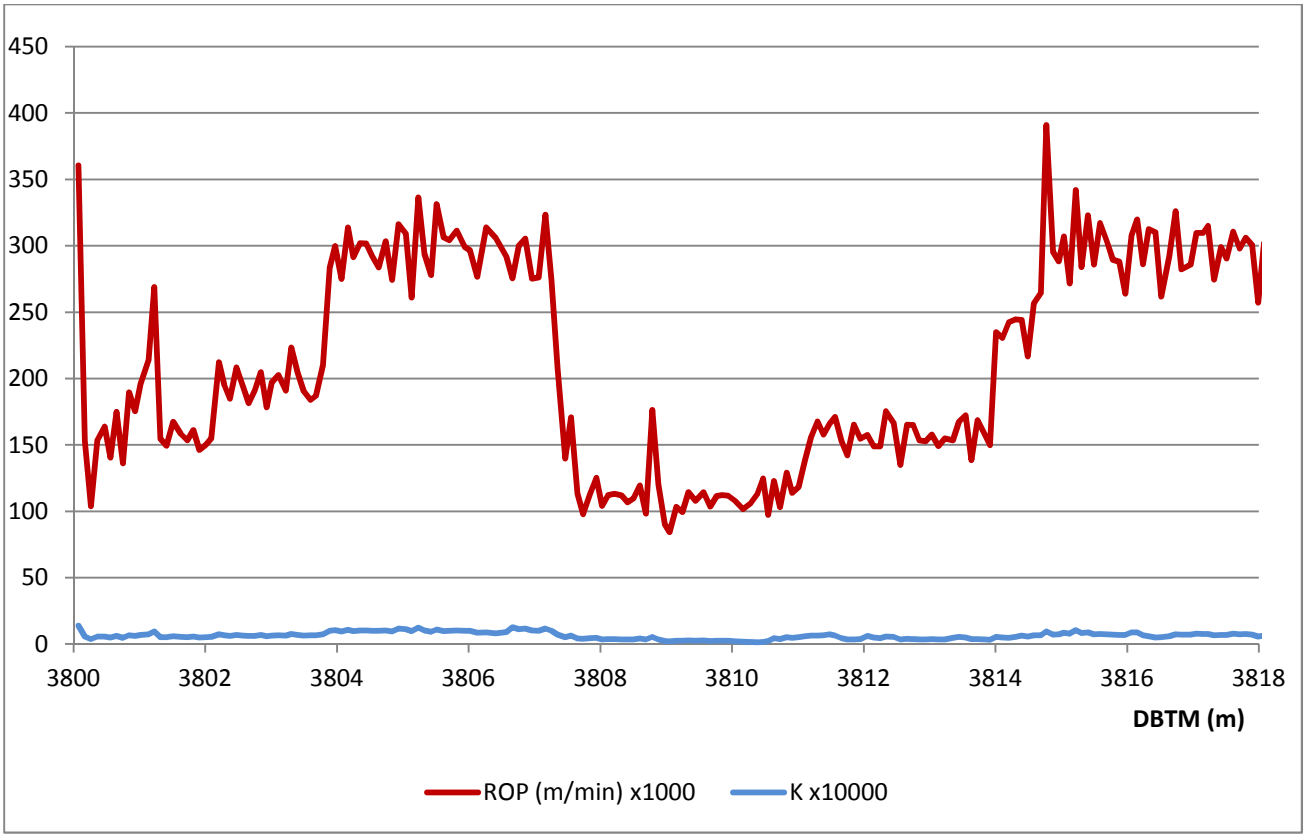

Figure 9-14: Comparison of ROP and K function of Depth section fault S2/S3 (5 average)

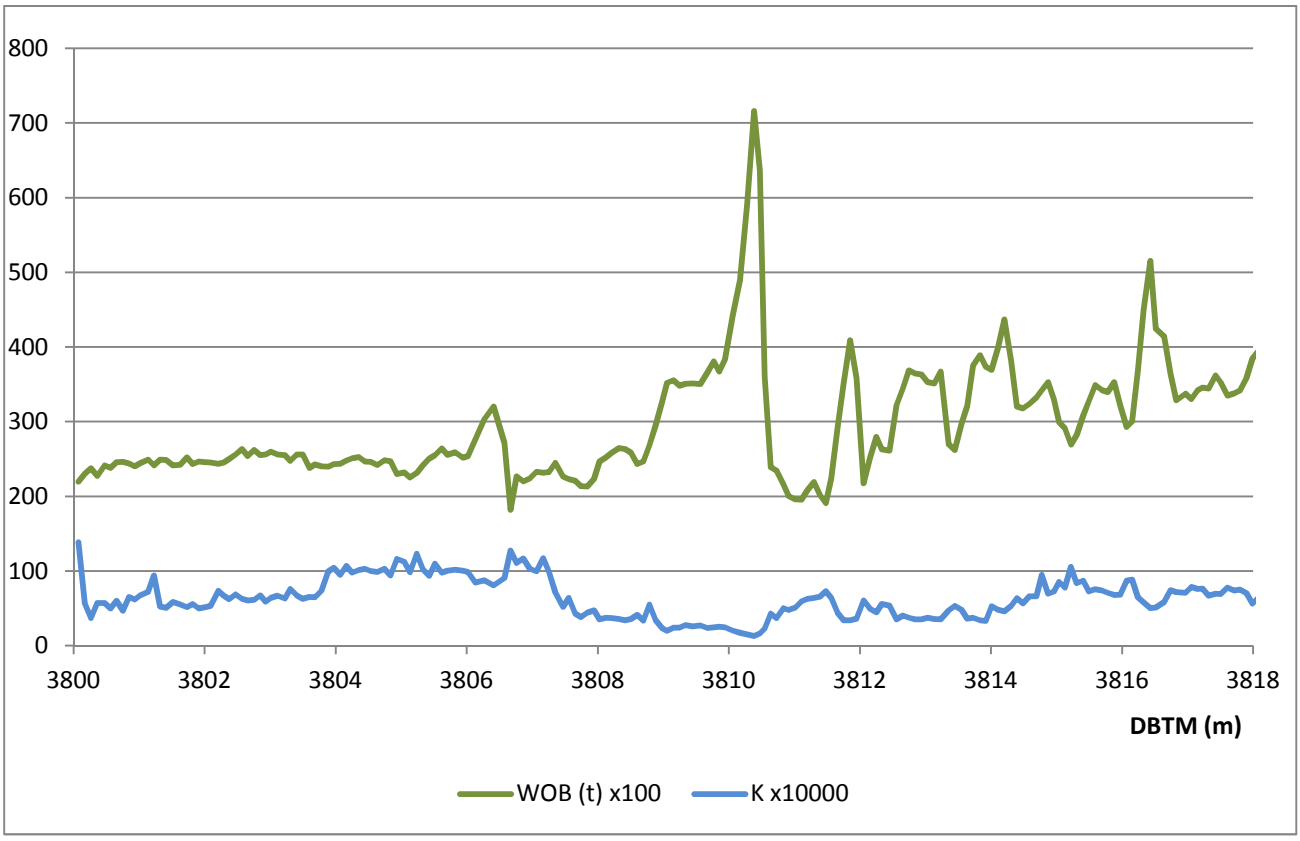

Figure9-15: Comparison of WOB and K function of Depth section fault S2/S3 (5 average)

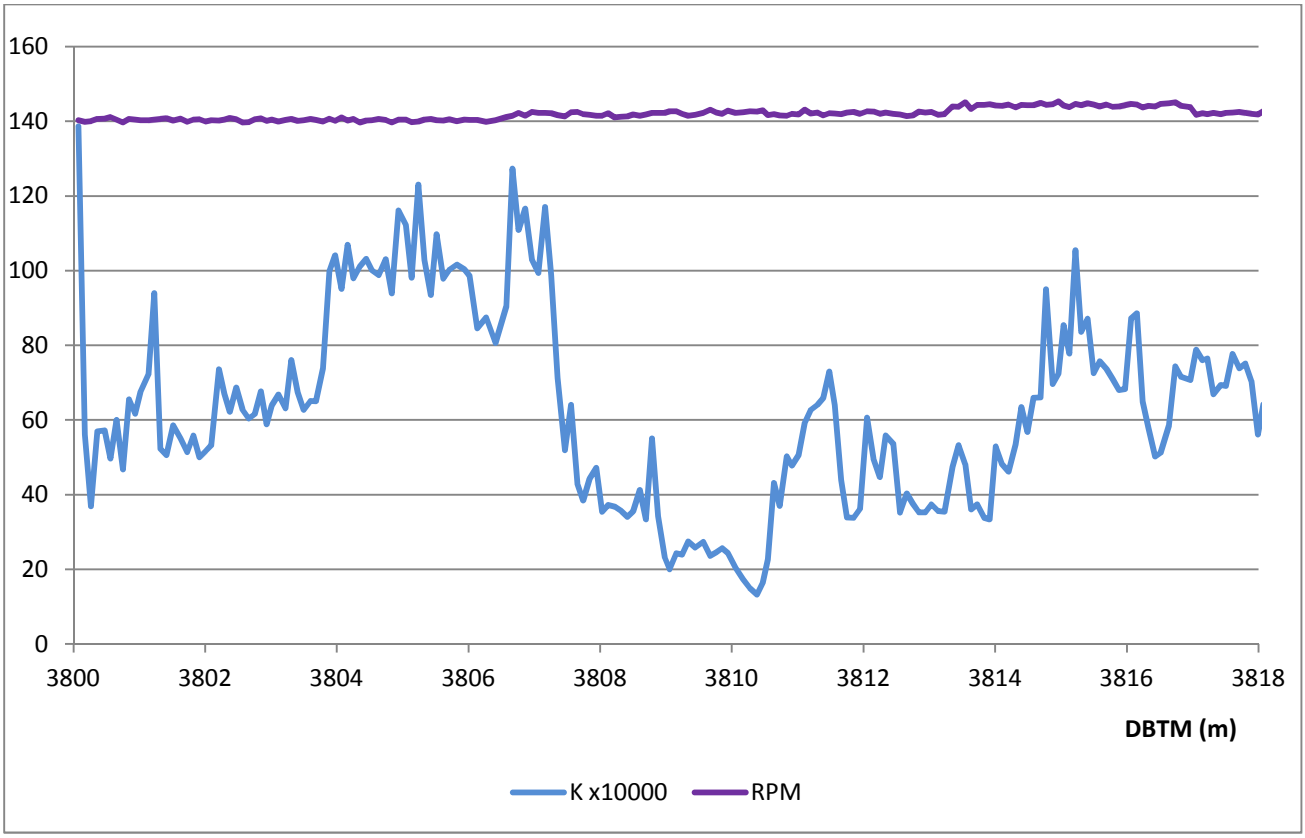

Figure 9-16: Comparison of RPM and K function of Depth section fault S2/S3 (5 average)

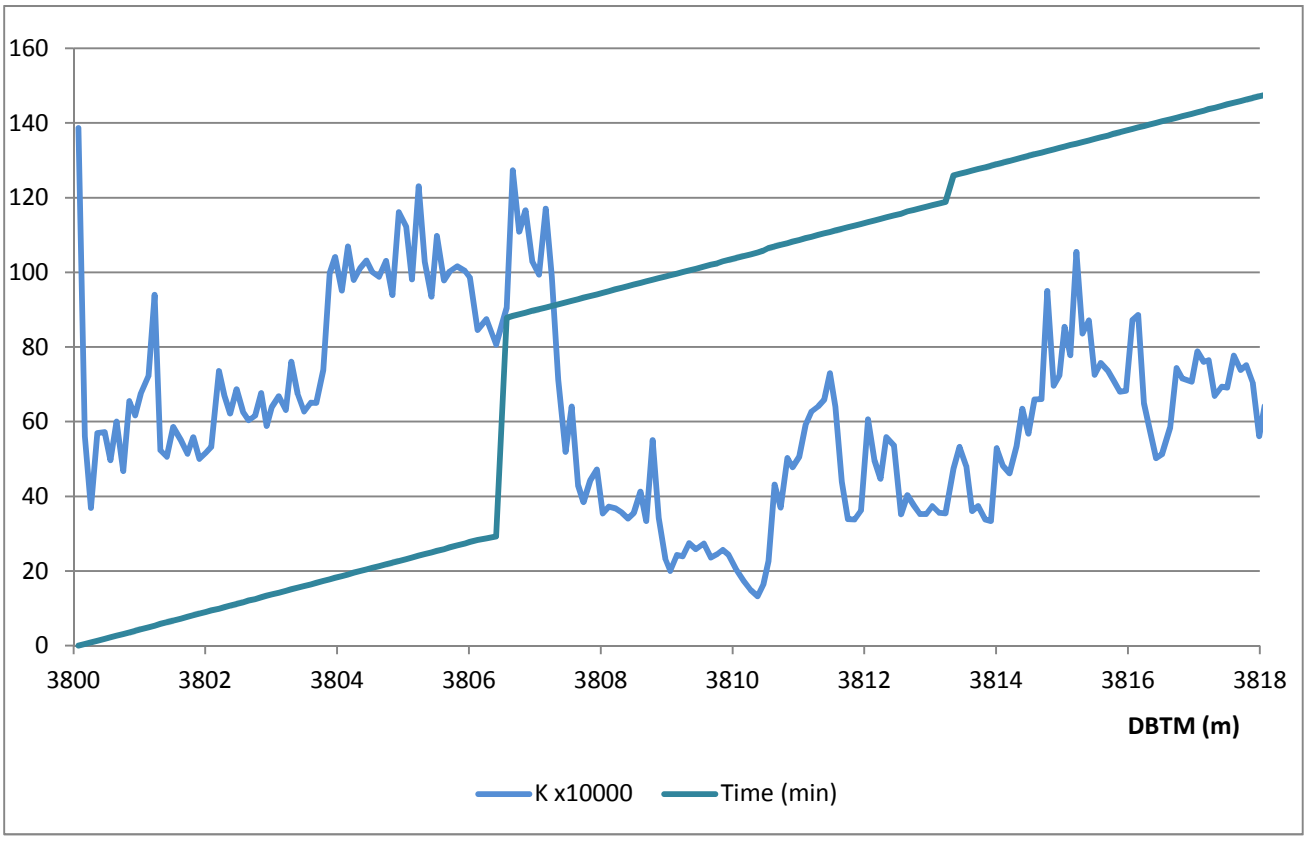

Figure 9-17: Comparison of K and Time function of Depth section fault S2/S3 (5 average)

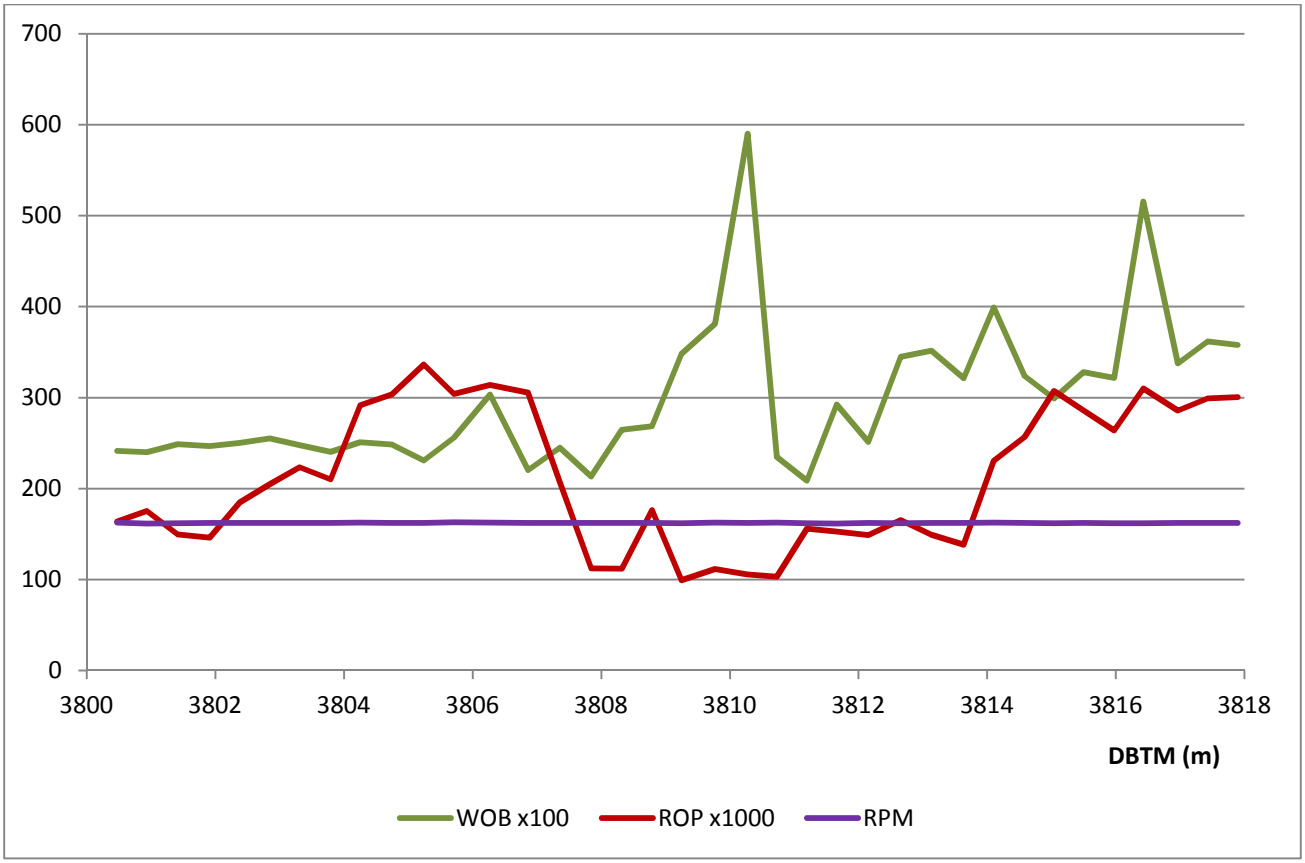

Figure 9-18: Comparison of ROP, WOB and RPM function of Depth section fault S2/S3 (25 average)

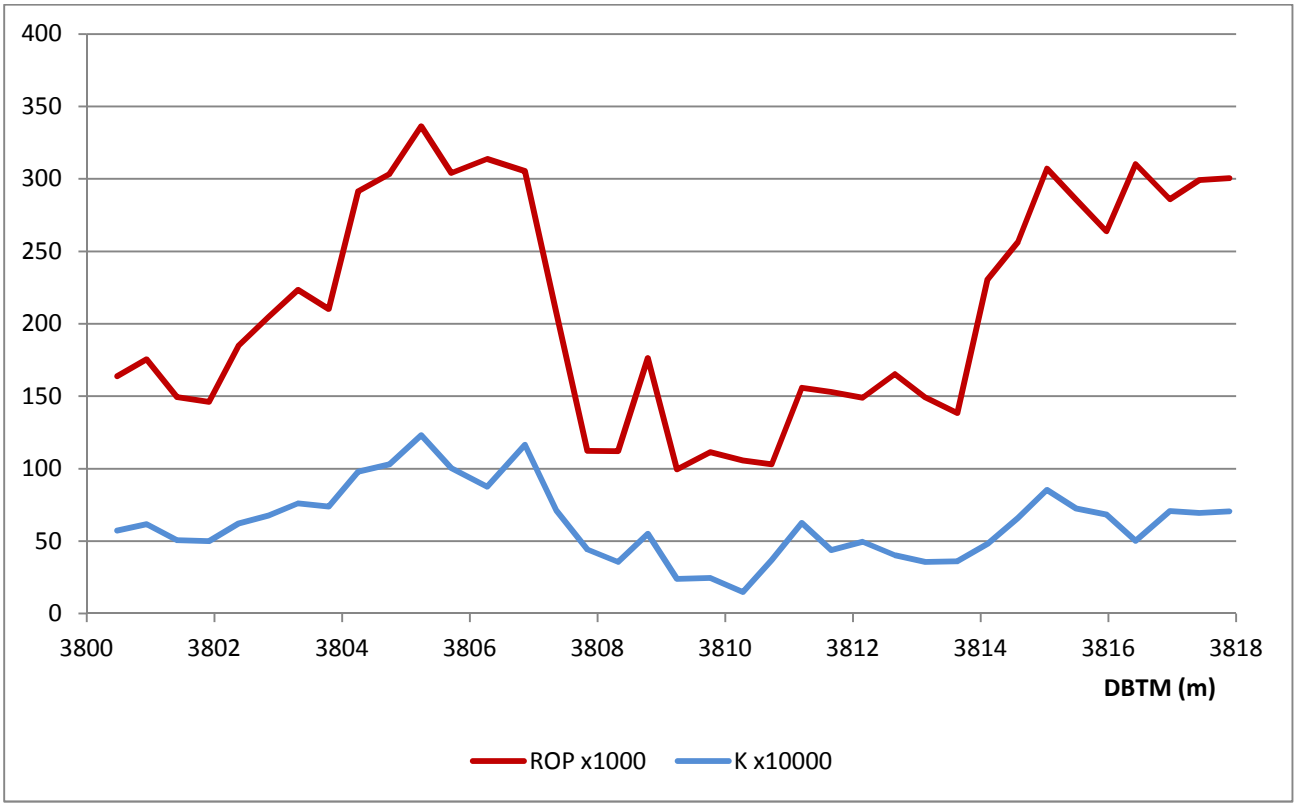

Figure 9-19: Comparison of ROP and K function of Depth section fault S2/S3 (25 average)

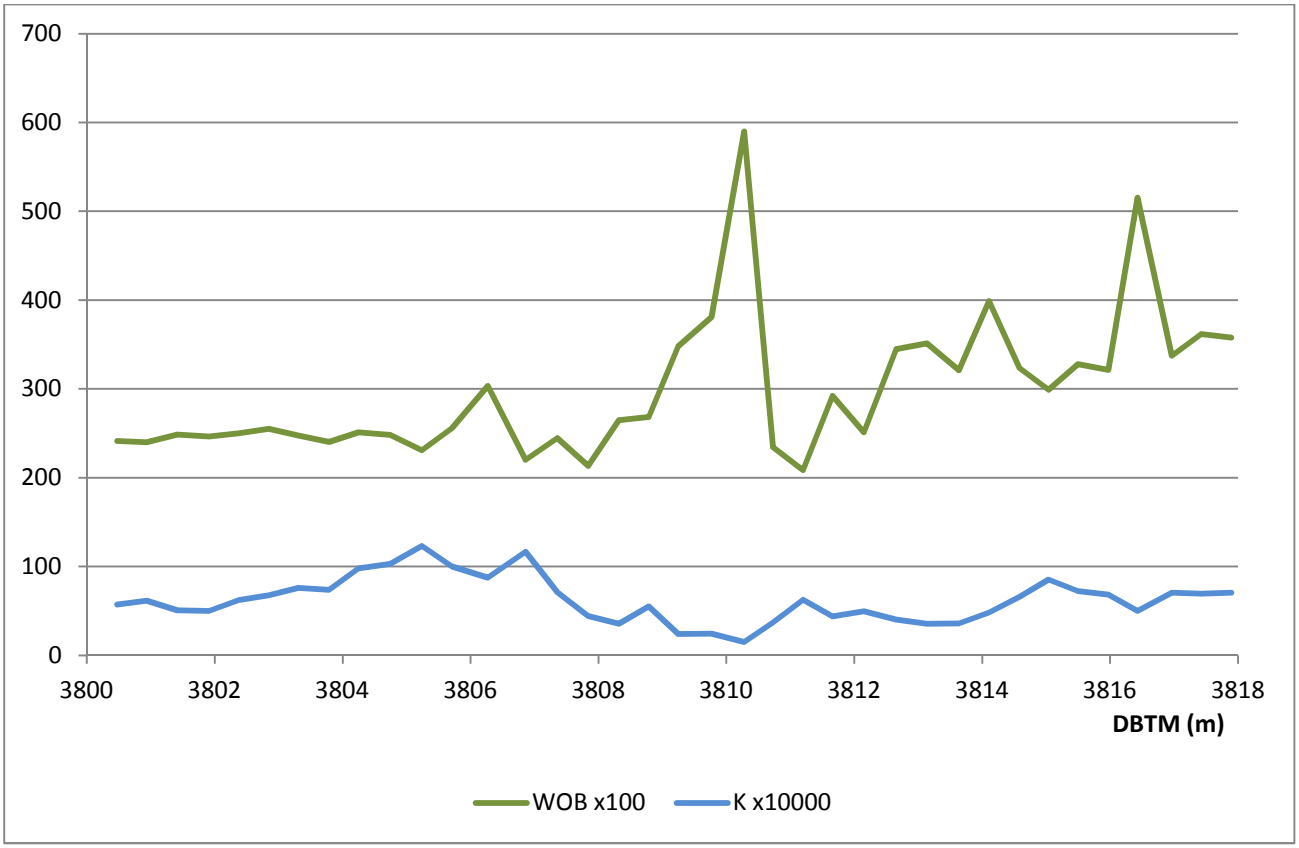

Figure 9-20: Comparison of WOB and K function of Depth section fault S2/S3 (25 average)

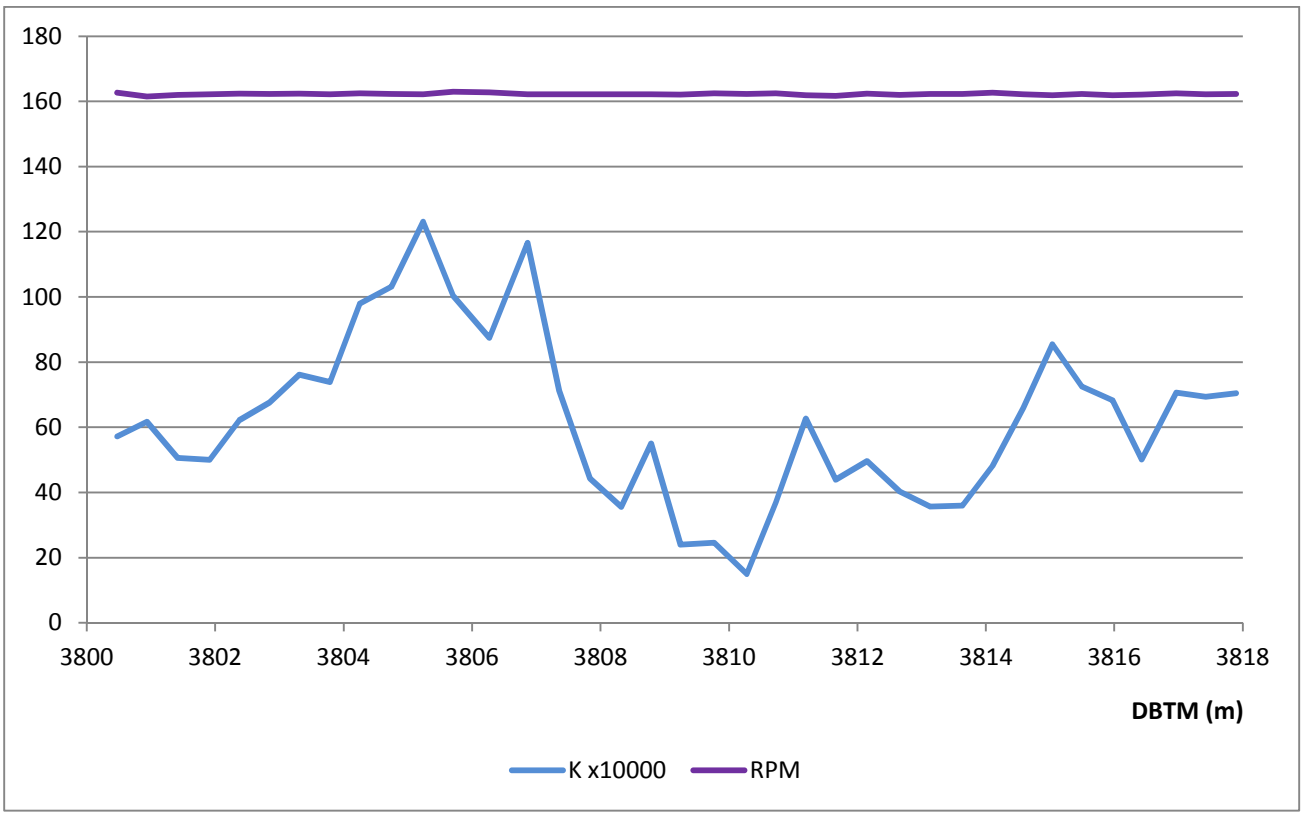

Figure 9-21: Comparison of RPM and K function of Depth section fault S2/S3 (25 average

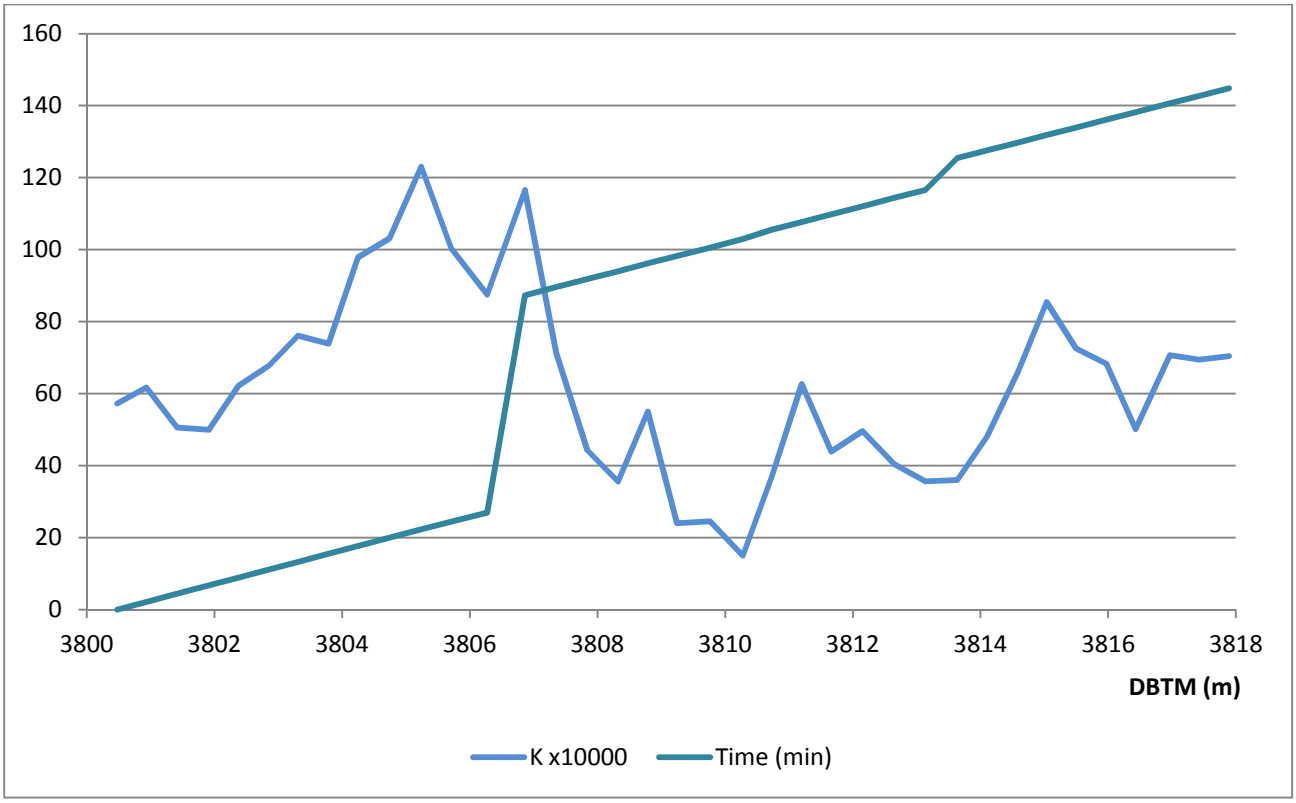

Figure9-22: Comparison of K and Time function of Depth section fault S2/S3 (25 average)